Time-Optimal Paths for a Dubins Car and Dubins Airplane with a Unidirectional Turning Constraint

by

Heejun Choi

A dissertation submitted in partial fulfillment
of the requirements for the degree of
Doctor of Philosophy
(Aerospace Engineering)
in The University of Michigan
2014

Doctoral Committee:

Professor Ella M. Atkins, Chair
Emeritus Professor Elmer G. Gilbert
Professor Ilya Kolmanovsky
Professor Dawn Tilbury

ACKNOWLEDGEMENTS

This dissertation would not have been possible without the guidance and support of many people. First and foremost, my heartfelt gratitude goes out to my advisor, Professor Ella M. Atkins, for her unfaltering guidance, instruction, generosity, and enthusiasm throughout my years at the University of Michigan as a doctoral student. I also thank Professor Elmer Gilbert for his insightful comments and suggestions at a critical juncture in formulation of this project, as well as Professors Ilya Kolmanovsky and Dawn Tilbury for their valuable feedback, without which I would have not been able to fine-tune this project for its final submission. I was also fortunate to work in the company of friendly, intelligent colleagues during my time as a member of Professor Atkins laboratory.

I would also like to thank my family for their moral support and continued encouragement throughout my graduate school experience. My parents and my sisters Jungwon and Hye-eui provided me with their unconditional love and support throughout this whole process. Finally, I am also grateful to Shin Young Hwang for her love and support throughout the often long-winded writing process of this dissertation.

The research and writing of this dissertation were made possible with the generous support of NASA.

TABLE OF CONTENTS

LIST OF FIGURES

Figure

LIST OF TABLES

Table

LIST OF SYMBOLS

$\mathcal{A}$	reference arc
$\mathcal{H}$	Hamiltonian for the optimal problem
H	Hamiltonian for the time-optimal problem
J	cost to be minimized
L	switching line
n	number of basic pairs
n_m	minimum number of basic pairs
P	center of the initial circular arc
Q	center of the final circular arc
r	minimum radius of curvature
$r_{\mathcal{A}}$	radius of reference arc
T	final time
t	time
$\mathbf{U}$	control region
U	control region for turn rate
u	turn rate
$\mathbf{u}$	control vector
V	control region for vertical rate
v	vertical (or climb/descent) rate
x	x coordinate of vehicle
$\mathbf{x}$	state vector
y	y coordinate of vehicle
z	z coordinate of vehicle
θ	arctangent of the y position adjoint divided by the x position adjoint
λ	square root of the sum of the squares of the x and y position adjoints
ϕ	orientation of vehicle in the plane with respect to the x axis
ψ	adjoint vector

Subscript

min	minimum value
T	final value
0	initial value

ABSTRACT

Time-Optimal Paths for a Dubins Car and Dubins Airplane with a Unidirectional Turning Constraint

by

Heejun Choi

Chair: Ella M. Atkins

The primary goal of an aircraft emergency landing planner is to safely and efficiently land on a runway. One commonly used tool is the solution of Dubins problem, which defines minimal-time paths for vehicles moving in a plane with constraints on turn rate. The Dubins solution presumes that vehicles can follow straight paths and turn in both directions. A vehicle, however, can be constrained to unidirectional (i.e., either clockwise or counterclockwise) turning motions after experiencing severe structural damage and/or control failure. A unidirectional turning constraint specifies lower and upper bounds on turn rate, both of the same sign. This dissertation addresses, for the first time, the problem of finding time-optimal paths for Dubins vehicles constrained to unidirectional turning motions.

This dissertation initially considers a Dubins vehicle in a plane, called Dubins car, with unidirectional turning constraints for which the optimal paths are characterized by employing Pontryagin's minimum principle. A geometric interpretation of the identified extremal paths enables direct identification of the optimal path. To extend these planar results to aircraft emergency landing planning, it is necessary to consider the unidirectional Dubins airplane where the planar motions of this unidirectional

Dubins car are supplemented by allowing changes in altitude. Optimal paths for the unidirectional Dubins airplane have one of two transition times: the shortest time for the unidirectional Dubins car or the time equal to the absolute altitude difference required to descend divided by the maximum vertical rate. In some instances of the latter case, a suboptimal path must be constructed to guarantee a feasible solution.

Both the unidirectional Dubins car and airplane algorithms developed in this dissertation can be implemented in real-time, thus integrated easily into embedded vehicle management systems. Moreover, these algorithms are complete, thus can be guaranteed to find a feasible solution which in most cases is also time-optimal. Throughout the dissertation, the proposed algorithms are validated through a series of test cases. The dissertation applies the unidirectional Dubins airplane algorithm to aircraft emergency landing at LaGuardia airport to demonstrate its ability to rapidly identify and present a full suite of landing options to the pilot and automation.

CHAPTER I

Introduction

1.1 Motivation

On May 1, 1983, an F-15 aircraft was flying on a training exercise over the Negev desert, Israel. After colliding with an A-4 Skyhawk, the F-15 lost its right wing, resulting in a descending spiral flight. The A-4 pilot ejected immediately, but the F-15 pilot was miraculously able to regain control of the F-15. Eventually, the F-15 made an emergency landing on a runway at the nearest base despite the structural damage.

Aviation is safe but accidents still occur. Most accidents occur due to multiple contributing factors. Degradation in performance such as the asymmetric lift experienced by the F-15 pilot remains a particularly difficult challenge to handle. To conduct experiments to assess automation aids that may reduce the likelihood of loss-of-control (LOC) in off-nominal flight conditions, NASA Langley Research Center has developed the Airborne Subscale Transport Aircraft Research (AirSTAR) testbed (Jordan et al. (2004); Bailey et al. (2005)). The AirSTAR aircraft is a 5.5% dynamically scaled model of a twin-engine transport aircraft called a Generic Transport Model (GTM). This platform has been modeled, simulated, and flight-tested to characterize the in-flight effect of damage and failure conditions, providing a modeling and simulation environment for which researchers have evaluated and validated

technologies for Integrated Resilient Aircraft Control (IRAC) (Krishnakumar et al. (2010)).

NASA's IRAC program has evolved to focus on loss-of-control (LOC) more generally. Models and control strategies continue to be developed to enable an aircraft experiencing damage or failure conditions to operate safely and efficiently. Adaptive control has long been studied to handle stability and control problems resulting from damage or failure such as structural damage or a control surface jam (Rysdyk and Calise (1998); Bosworth and Williams-Hayes (2007); Nguyen et al. (2008)). The goal of adaptive control is to regain or maintain control of the aircraft despite reduced performance such that an aircraft can safely land.

Automation aids to promote safe landing in emergency situations have been developed. Chen and Pritchett (2001) proposed an Emergency Fight Planner to compute and display emergency landing trajectories to a flight crew. Such trajectories are defined by a series of pilot-centric actions (e.g., fly to waypoint, descend at a given rate). Atkins et al. (2006) proposed the Adaptive Flight Planner (AFP) to generate landing plans by first selecting a destination runway then building a trajectory to that runway that met flight envelope constraints. Meuleau et al. (2009) developed the Emergency Landing Planner to optimize landing plans with respect to risk. Their planner lists possible landing trajectories with different runways by measuring risk to the aircraft based on performance and en-route environment constraints (e.g., weather) as well as approach and runway properties (e.g., runway length).

Balachandran and Atkins (2013) proposed the Envelope-Aware Flight Management System (EA-FMS) including the AFP to prevent LOC, as shown in Figure 1.1. The notion of the EA-FMS is similar to that of Aircraft Integrated Resilient Safety Assurance and Failsafe Enhancement (AIRSAFE) proposed by Belcastro and Jacobson (2010). The EA-FMS consists of the following six main modules: (1) Flight Safety Assessment and Management, (2) Sensor Diagnostics, (3) System Identifica-

tion, (4) Envelope Estimation, (5) Adaptive Control, and (6) Adaptive Planning and Guidance. These modules interact in real-time to prevent or recover from LOC

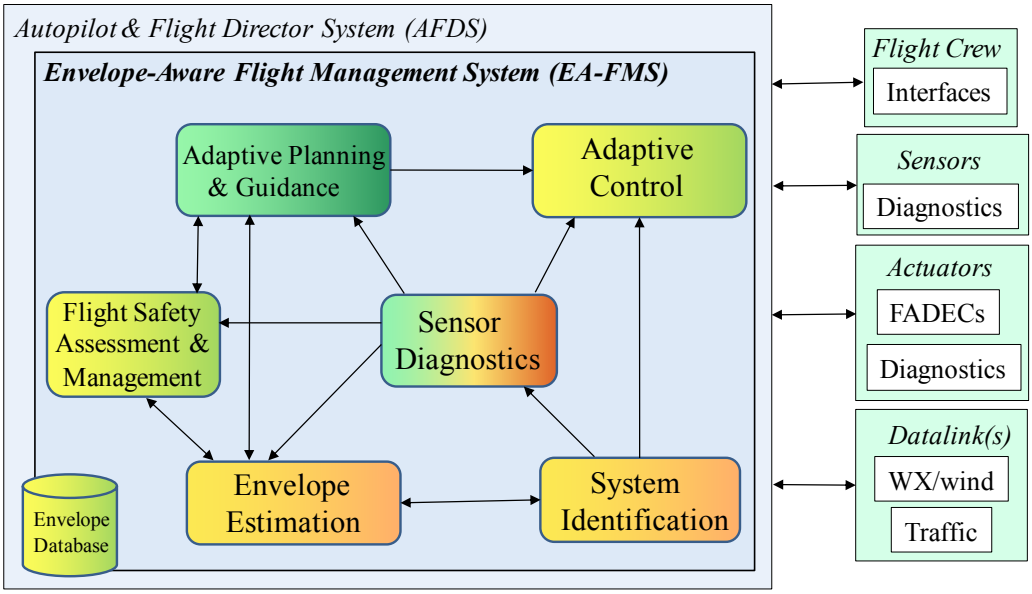

Figure 1.1: Envelope-Aware Flight Management System (Balachandran and Atkins (2013)).

The Flight Safety Assessment and Management module continuously monitors and evaluates airplane health and flight safety. In case of a LOC accident, this module gives the flight crew a LOC warning based on data from the Sensor Diagnostics module. The System Identification module (Zhong et al. (2013)) estimates the degraded dynamic model based on measurements of system inputs and outputs. The Envelope Estimation module (McDonough et al. (2014)) evaluates the achievable flight envelope resulting from the LOC accident. The Adaptive Control module regains or maintains stability and maneuverability employing the updated dynamic model from the System Identification module.

To continue the flight or land the airplane, safe trajectories are computed by the Adaptive Planning and Guidance module. Solutions must respect envelope and other constraints such as remaining fuel available or local terrain. Flight envelope constraints are specified in terms of climb/descent rate, turn rate, and airspeed as a

function of air density (altitude). This dissertation concentrates on path planning, and thus assumes modules (1) through (5) in the EA-FMS are available.

Safely landing following an in-flight emergency is time-critical because continued flight under emergency conditions may induce secondary damage or system failures. Therefore, it is important that length-optimal or time-optimal paths are computed in real-time, i.e., quickly enough so they are effective in the EA-FMS. Perhaps even more important is employing a path planner that is capable of always finding a solution (i.e., a complete algorithm) in real-time. Given an initial state, final state, and turning constraints, the Dubins path planner (Dubins (1957)) offers an optimal geometric path construction algorithm that is guaranteed to be minimum-length and that is complete. The Dubins planner defines length-optimal paths for a vehicle that moves forward in a plane with constant speed and constraints on turn rate.

Dubins solutions have been frequently applied to aircraft path planning problems (Yang and Kapila (2002); Atkins et al. (2006); Techy and Woolsey (2009)) and are comprised of three segments, typically with a "turn-fly (straight)-turn" construction. The Dubins car problem was extended to the Dubins airplane problem by Chitsaz and LaValle (2007), which defines time-optimal paths for an airplane moving forward in a space with constant horizontal speed and constraint on turn and climb rates. Turn and climb rates are typically assumed to be independent of each other. Figure 1.2 illustrates an example path, generated by the AFP in Atkins et al. (2006). They considered a loss-of-thrust emergency and extended the solution of the Dubins car problem to reach the chosen runway by adding an intermediate turn or final approach straight segment. To follow a Dubins-based landing path (e.g., Figure 1.2), the aircraft must have the ability to maintain straight flight and turn in both directions.

Although rare, a damaged aircraft may lose the ability to fly straight and/or turn in both directions. An aircraft with damage to a wing, aileron, or rudder, for example, can exhibit asymmetric turning constraints (Nguyen et al. (2006)). Figure 1.3 illus-

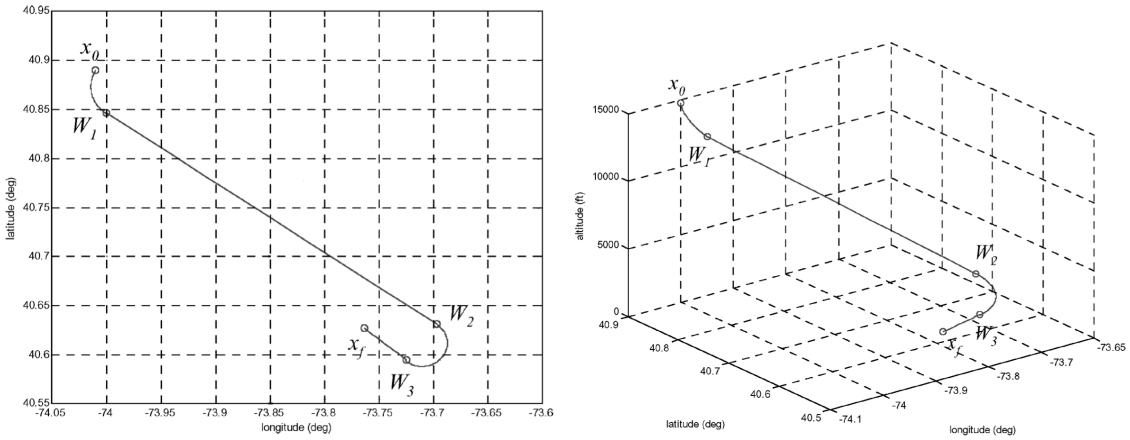

(a) Horizontal plane.

(b) Three-dimensional space.

Figure 1.2: A Dubins path with final approach leg for a loss-of-thrust case study with landing on JFK 31L (Atkins et al. (2006)).

trates the Generic Transport Model (GTM) with such damage as modeled in Nguyen et al. (2006). Nguyen et al. suggest that maintaining steady-state flight requires bank angle constraints that place straight flight near or potentially beyond envelope constraints. Tang et al. (2007) computed the full steady-state flight database for the damaged GTM with a missing left wingtip. Figure 1.4 shows flight envelopes of the GTM with a missing left wingtip at different altitudes from 10 ft to 30,010 ft, in increments of 10,000 ft. In this figure, a green point indicates a stable and controllable steady-state flight condition, while a blue point indicates a naturally unstable but stabilizable flight condition. The damaged GTM allows a narrow range of clockwise turn rates at lower altitudes and few to no clockwise turn rates at higher altitudes. A wider range of counterclockwise turn rate options are available at all altitudes. This means turning left is easier than turning right. As indicated in the analysis by Tang et al. (2007) introduction even a modest safety margin, e.g., to account for wind disturbances, renders the aircraft unable to maintain straight flight and clockwise turns. Such an aircraft thus has a unidirectional turning constraint.

Strube et al. (2004, 2005) present another of an aircraft constrained to unidirectional turns. Strube et al. computed the steady-state flight database for an F-16

Figure 1.3: Damaged GTM (Nguyen et al. (2006)).

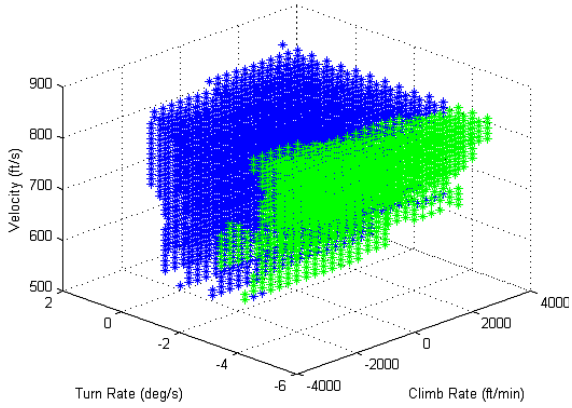

(a) An altitude of 10 ft.

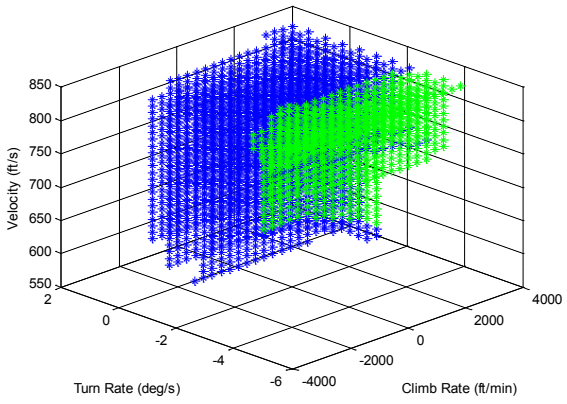

(b) An altitude of 10,010 ft.

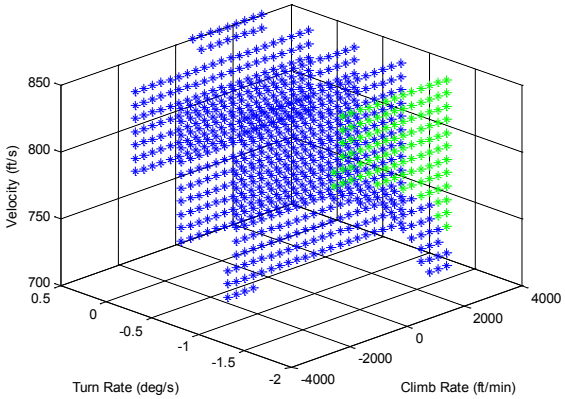

(c) An altitude of 20,010 ft.

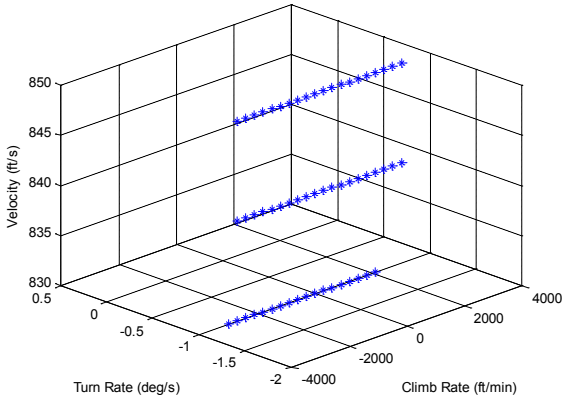

(d) An altitude of 30,010 ft.

Figure 1.4: Flight envelopes of the GTM with left wing damage at different altitudes (Tang et al. (2007)).

aircraft with rudder or aileron jammed at different deflection angles. Figure 1.5 illustrates the flight envelope for an F-16 aircraft with an aileron jammed at +14 degrees at an altitude of 10,000 ft. In this case, the disabled F-16 aircraft can hold a straight flight condition for an airspeed less than or equal to 225 ft/sec, but the aircraft may encounter stall before it reaches a nominal stall airspeed of 200 ft/sec. This follows from the fact that the stall speed for turning flight is higher than that for straight and level flight, and with asymmetric lift the stall speed in the preferred turning direction is lower than it in the non-preferred turning direction. Therefore, the disabled F-16 aircraft can fly in control but cannot fly straight for an airspeed above 225 ft/sec at 10,000 ft or above.

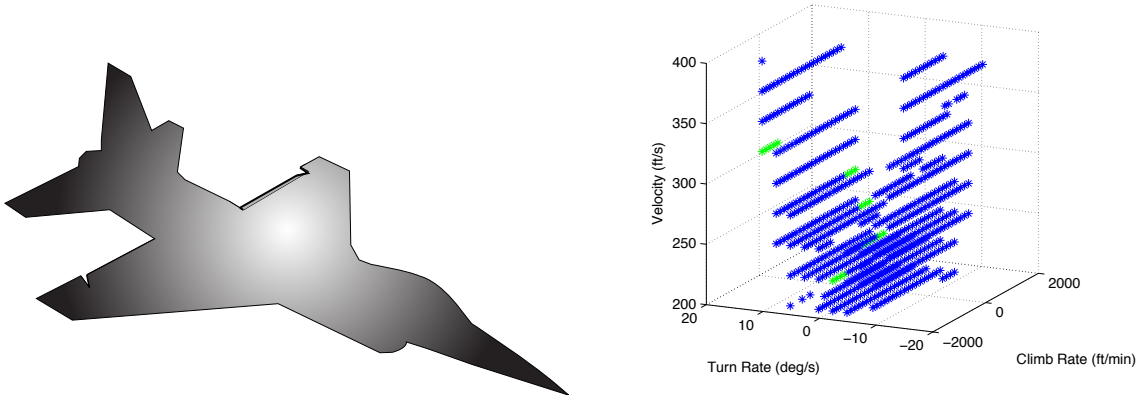

(a) The F-16 aircraft with jammed aileron.

(b) Damaged F-16 flight envelope at an altitude of 10,000 ft.

Figure 1.5: Flight envelope for an F-16 aircraft with an aileron jammed at 14 degrees (Strube et al. (2004)).

1.2 Problem Statement

This dissertation addresses the problem of finding time-optimal paths for vehicles constrained to forward motion and unidirectional (clockwise or counterclockwise) turns to transfer from a given initial oriented point to a given final oriented point. In two-dimensional Euclidean space, this optimal path-finding problem is a variant of

the classical Dubins car problem first solved by L. E. Dubins (1957). Dubins considered a car moving forward at constant speed with a given minimum turning radius but no maximum radius. Unlike the Dubins problem, this dissertation studies motion planning with constraints on both maximum and minimum turning radii corresponding to lower and upper bounds on turn rate that are of the same sign. We generate paths for vehicles constrained to forward and unidirectional turning motions which has not yet been carefully considered in the literature.

The planar (or two-dimensional) solution to the time-optimal path planning problem is applicable without modification to an aircraft that maintains a constant altitude (or cruise condition). To support the descent required for an emergency landing, we adapt the Dubins car with unidirectional turning constraints to consider altitude. Chitsaz and LaValle (2007) formulated a variant of the Dubins car problem to find time-optimal paths in three-dimensional Euclidean space. They considered an airplane, called the *Dubins airplane*, moving forward with given maximum turn and climb (or descent) rates that are independent of each other. In a similar manner, we extend the unidirectional Dubins car to the Dubins airplane with unidirectional turning constraints. Thus, this dissertation proposes a complete solution to the unidirectional Dubins airplane problem to provide time-optimal emergency landing paths in conditions where straight flight is not possible.

In this dissertation, we make the following assumptions:

1. The Earth is flat and not rotating.

2. The vehicle is modeled as a particle at its center of gravity. The simple kinematic models for the particle are adopted from the unidirectional Dubins car (Boissonnat et al. (1994)) and airplane (Chitsaz and LaValle (2007)). These models can be regarded as reference models even given damage and failure conditions since envelope constraints associated with the degraded condition are incorporated. The simple kinematic models used in the dissertation are pre-

sumed valid and an (inner-loop) adaptive controller is also presumed able to follow geometric paths that respect specified kinematic constraints.

3. The vehicle can only move forward and turn unidirectionally (clockwise or counterclockwise). The rate of turn is allowed to vary within given lower and upper bounds that are of the same sign. These bounds are determined from the extremes of the current flight envelope updated by the envelope estimation module. Such bounds are presumed applicable throughout landing since achievable flight conditions at high altitude are typically contained in the flight envelope available at low altitude, as illustrated in Figure 1.4 (see Tang et al. (2007)).

1.3 Approach

To find optimal paths for the unidirectional Dubins vehicle, we first show that such optimal paths always exist. Proof of existence involves two steps. We construct piecewise continuous controls bounded on a control region (called *admissible controls*). Then, we employ Filippov's theorem in Cesari (1983) to demonstrate the existence of optimal paths connecting given initial and final oriented points.

Even though we can construct admissible paths, this construction alone does not provide a means of fully computing optimal paths for the unidirectional Dubins car and airplane. To construct these optimal paths, we determine their structure using Pontryagin's minimum principle, which was formulated in Pontryagin et al. (1962). A path or control satisfying necessary conditions from the minimum principle is said to be *extremal*. Since this principle provides only necessary conditions for optimality, further conditions on the identified extremal paths are established to enable the generation of optimal paths.

For the Dubins car with unidirectional turning constraints, the identified extremal paths are concatenations of alternating arcs of two tangent circles with minimum and

maximum turning radii or subpaths of these concatenations. These concatenations are specified as four combinations of initial arc and final arc, based on their respective turning radii. For each combination, we derive the geometric interpretation of extremal paths to provide further necessary conditions for optimality. We then develop an algorithm for finding optimal paths for the unidirectional Dubins car.

For the Dubins airplane with unidirectional turning constraints, optimal paths must have one of two transition times to reach a given final oriented point. One of these times equals the shortest time for the unidirectional Dubins car, and the other is determined by the difference between the initial and final altitudes. Thus, the algorithm to find optimal paths for the Dubins airplane with unidirectional turning constraints will consist of two parts. In the former case, the algorithm for finding optimal planar paths can be used to compute optimal paths in three-dimensional Euclidean space. In the latter case, we extend optimal planar paths to pass through the final oriented point at the greater time required to descend safely. This follows from the assumption that turn and vertical rates are independent of each other.

This dissertation develops a real-time algorithm for finding optimal paths for the unidirectional Dubins airplane and evaluates its completeness, optimal path's existence (optimality), and applicability to an emergency landing case study. In this dissertation, "real-time" means "fast enough so that a pilot or autopilot can execute planned paths." This implies the computation time for finding optimal paths is sufficient for the pilot to receive the plan as an advisory by the time he/she recognizes the need for such a plan. Real-time performance is achieved if the algorithm has a worst-case execution time less than a maximum time constant, e.g. 1 second, given available onboard processing resources.

1.4 Contributions and Innovations

The main contributions of this dissertation are as follows:

1. This dissertation provides a real-time algorithm to compute time-optimal paths for vehicles under unidirectional turning constraints imposed by damage and/or failure conditions.

2. This algorithm solves a problem that is rare but almost impossible for a human pilot to handle: quickly computing a precise geometric path to place an aircraft on a runway (or final approach) with only turning trajectory segments.

3. This dissertation proposes complete algorithms for two-dimensional and three-dimensional spaces. These algorithms can readily be transitioned to a ground vehicle or an aircraft cockpit.

4. Because the time-optimal metric in this study is derived independently of planners and/or controllers, it can be used as an effecitive benchmark to compare the performance of different planners and/or controllers.

The main innovations of this dissertation are summarized as follows:

1. Previous studies in the field of motion planning have extensively dealt with finding the optimal path for vehicles able to travel along straight paths because vehicles are usually assumed capable of driving or flying straight. This study for the first time finds time-optimal paths for vehicles unable to travel straight due to extreme kinematic constraints imposed by damage and/or failure conditions.

2. Through a combination of the minimum principle of Pontryagin and geometric considerations, this research enables a complete characterization of optimal paths for the unidirectional Dubins car.

1.5 Thesis structure

The dissertation is organized as follows. Chapter II is devoted to reviewing relevant background material. In particular, we present a brief summary of Dubins

vehicles, Filippov's theorem, and Pontryagin's minimum principle, and also review the literature related to these concepts. In Chapter III, we present an initial exploration into admissible but potentially suboptimal controls which yield paths of the Dubins car and airplane given a unidirectional turning constraint to reach a given final oriented point. Filippov's theorem is used to demonstrate the existence of optimal paths for unidirectional Dubins vehicles. Chapters IV and V begin by applying the minimum principle of Pontryagin to our optimal path-finding problems in two- and three-dimensional spaces, respectively.

In Chapter IV, we determine the structure of shortest paths (i.e. minimal-time paths presuming constant speed) for the unidirectional Dubins car based on Pontryagin's minimum principle. We then derive geometric properties of the identified extremal paths. Using these properties, we present algorithms to find the optimal path for the unidirectional Dubins car and analyze their ability to rapidly and consistently identify solutions.

Chapter V addresses the problem of finding time-optimal paths for the unidirectional Dubins airplane. Using a similar approach to that employed in Chapter IV for the unidirectional Dubins car, we derive necessary conditions for time-optimal paths using the minimum principle. We then extend time-optimal planar paths to reach a given final oriented point at a time greater than that of optimal planar paths based on the requirement to extend the path for the descent. We develop an algorithm to find the optimal path in three-dimensional Euclidean space using the algorithm for the unidirectional Dubins car and the extended optimal planar paths. A case study applies the unidirectional Dubins airplane algorithm to an aircraft experiencing a failure constraining the system to clockwise turns near LaGuardia airport.

CHAPTER II

Background and Related Work

2.1 Introduction

The Dubins problem refers to finding minimum-length (or minimum-time) paths for vehicles that move forward in a plane with constant speed and a given minimum turning radius subject to specified initial and final conditions. Dubins (1957) characterized the optimal paths carefully by proving geometric arguments. This problem was approached again by Boissonnat et al. (1994) and Sussmann and Tang (1991) using optimal control theory known as the minimum principle of Pontryagin, which resulted in simpler and easier solution derivations.

The advent of modern high-speed digital computers led to a renewed interest in optimal control theory and gave rise to a whole new discipline, computational optimal control. The survey in Betts (1998) gives a comprehensive overview of computational optimal control, distinguishing direct and indirect methods. The direct method applies nonlinear programming (Betts (2010)) to a finite dimensional optimization problem derived from the optimal control problem. The indirect method is a process for solving the multiple-point boundary value problem resulting from the necessary conditions for optimality which are given by optimal control theory (Pontryagin et al. (1962)).

Computational optimal control has been widely used to solve complex problems.

In general, such problems have no analytical solution. However, even the modern techniques of computational optimal control face challenges with computational efficiency, convergence, and solution accuracy given a space with numerous local minima.

The computational issues that arise in numerical optimal control may not enable its real-time implementation. Such real-time issues are not present for solutions that can be computed analytically. The most common method of finding an analytic solution to path planning problems is founded upon the necessary conditions for optimality. Two research teams, Bellman and Kalaba (1965) and Pontryagin et al. (1962), independently developed optimality conditions. Specifically, Bellman and Kalaba (1965) introduced a necessary and sufficient condition for optimality that is expressed by a first-order nonlinear partial differential equation system called the Hamilton-Jacobi-Bellman (HJB) equation. This equation provides a rule for defining optimal controls of continuous-time systems directly and easily from the solution of the equation. However, the HJB equation is not easy to solve.

Pontryagin et al. (1962) introduced a necessary condition for optimality called Pontryagin's minimum principle. This principle can also be derived from the Hamilton-Jacobi-Bellman equation only under very strong conditions. However, the statement of Pontryagin's minimum principle directly provides necessary conditions for optimal control. This set of necessary conditions is used widely to characterize in certain ways analytic solutions to optimal control problems. This thesis also uses Pontryagin's minimum principle to characterize time-optimal paths.

This chapter is organized in two primary parts. The first, consisting of Sections 2.2 and 2.3, discusses existence of optimal solutions and the Pontryagin's minimum principle. The second introduces the Dubins car and airplane problems in the context of optimal path characterization.

2.2 Optimal Path Existence

Pontryagin's minimum principle provides necessary conditions for optimal paths assuming they exist. The existence of optimal paths was proved by Filippov (1962), Cesari (1965) and many others including Cesari (1966). The Filippov-Cesari existence theorem has multiple formulations for different optimal problems. Since problems presented in this dissertation are time-optimal, the Filippov-Cesari existence theorem for the time-optimal problem (Filippov (1962)) ensures the existence of optimal paths. This theorem will be presented here without proof.

To state this theorem, we first define some terminology. The set of all real numbers is denoted $\mathbb{R}$. $\mathbb{R}^n$ denotes *Euclidean n-space* which is defines as the set of all n-tuples $(x_1, x_2, \cdots, x_n)$ of real numbers $x_i \in \mathbb{R}$, $1 \leq i \leq n$. A control is a function given by $\mathbf{u} : [0, T] \to \mathbf{U} \subset \mathbb{R}^r$ where $\mathbf{U}$ is called the *control region*. Note that the control region U depends on t and $\mathbf{x}$ in Filippov (1962), but not in this dissertation. The control $u(t)$, $0 \leq t \leq T$, is said to be *measurable* if for every open subset O of $\mathbb{R}^r$, the set of all t for which $u(t) \in O$ is Lebesgue measurable in the interval $[0, T]$. The control $u(t)$, $0 \leq t \leq T$, transfers an object from a given oriented point $\mathbf{x}_0 \in \mathbb{R}^n$ to a given oriented point $\mathbf{x}_T \in \mathbb{R}^n$. The path $\mathbf{x} = (x_1, x_2, \cdots, x_n)$ of the controlled object is a solution of the system of differential equations

$$\dot{\mathbf{x}}(t) = f(t, \mathbf{x}(t), \mathbf{u}(t)), \tag{2.1}$$

where $f : \mathbb{R}^{n+r+1} \to \mathbb{R}^n$ is a vector-valued function given by

$$f(t, \mathbf{x}, \mathbf{u}) = (f_1(t, \mathbf{x}, \mathbf{u}), f_2(t, \mathbf{x}, \mathbf{u}), \cdots, f_n(t, \mathbf{x}, \mathbf{u}))$$

for $(t, \mathbf{x}, \mathbf{u}) \in \mathbb{R}^{n+r+1}$.

The time-optimal control problem is to find the control $u(t)$ such that $\mathbf{x}(t)$ from

$\mathbf{x}(0) = \mathbf{x}_0$ passes through $\mathbf{x}_T$ at minimum time. With these definitions, the Filippov-Cesari existence theorem for the time-optimal problem with a fixed set U takes the following form:

Theorem II.1. *(Filippov (1962)) There exists a time-optimal path $\mathbf{x}(t)$ from $\mathbf{x}_0$ that passes through $\mathbf{x}_T$ at minimum time T if the following conditions hold:*

(1) f is a continuous function of t, $\mathbf{u}$, $\mathbf{x}$ and a continuously differentiable function of $\mathbf{x}$.

(2) There exists a constant C such that for all t, $\mathbf{x}$ and all $\mathbf{u} \in U$,

$$\langle \mathbf{x}, f(t, \mathbf{x}, \mathbf{u}) \rangle \leq C\left(1 + \|\mathbf{x}\|^2\right).$$

(3) The control region $\mathbf{U}$ is compact. Furthermore, when $\mathbf{u}$ varies in $\mathbf{U}$, the image set described by $f(t, \mathbf{x}, \mathbf{u})$ is convex for all t and $\mathbf{x}$.

(4) There exists an admissible path from $\mathbf{x}_0$ to $\mathbf{x}_T$.

2.3 The Minimum Principle

Filippov's theorem guarantees the existence of time-optimal paths, but it does not provide a formula for such paths. Such a formula can be obtained using the minimum principle of Pontryagin. In this section, we will briefly review this principle formulated in Pontryagin et al. (1962). The principle is first given in the more general situations considered in Pontryagin et al. (1962), and then the principle for time-optimal problems is derived. We want to find a control $\mathbf{u}$ minimizing the functional

$$J = \int_0^T f_0(\mathbf{x}(t), \mathbf{u}(t))\, dt$$

such that $\mathbf{x}(t)$ satisfies the boundary conditions

$$\mathbf{x}(0) = (x_1(0), \cdots, x_n(0)) \triangleq \mathbf{x}_0 \text{ and } \mathbf{x}(T) = (x_1(T), \cdots, x_n(T)) \triangleq \mathbf{x}_T.$$

To formulate the minimum principle of Pontryagin, we introduce additional variables $\psi = (\psi_0, \psi_1, \cdots, \psi_n)$ that are solutions of a system of the following differential equations

$$\frac{d\psi_i}{dt} = -\sum_{j=0}^{n} \frac{\partial f_j(\mathbf{x}, \mathbf{u})}{\partial x_i} \psi_j, \quad i = 0, 1, \cdots, n. \tag{2.2}$$

Let $\mathcal{H} : \mathbb{R}^{2n+2+r} \to \mathbb{R}$ be a function defined by

$$\mathcal{H}(\psi, \mathbf{x}, \mathbf{u}) = \sum_{i=0}^{n} \psi_i f_i(\mathbf{x}, \mathbf{u}).$$

The function $\mathcal{H}$ is the inner product of ψ and $\dot{x}$ and is called the *Hamiltonian.* It follows that systems (2.1) and (2.2) can be expressed in terms of the Hamiltonian by the formulas

$$\frac{dx_i}{dt} = \frac{\partial \mathcal{H}}{\partial \psi_i}, \quad i = 0, 1, \cdots, n,$$
$$\frac{d\psi_i}{dt} = -\frac{\partial \mathcal{H}}{\partial x_i}, \quad i = 0, 1, \cdots, n.$$

With this notation, the statement of Pontryagin's minimum principle is as follows.

Theorem II.2. *(Pontryagin et al. (1962)) If the trajectory $\mathbf{x}(t)$ determined by $u(t) \in U$ is optimal, then there exists a non-zero continuous solution $\psi = (\psi_0, \psi_1, \psi_2, \cdots, \psi_n)$ such that*

(1) The control $u(t)$ minimizes the Hamiltonian at every time t; that is,

$$\mathcal{H}(\psi(t), \mathbf{x}(t), \mathbf{u}(t)) = \min_{z \in U} \mathcal{H}(\psi(t), \mathbf{x}(t), z).$$

(2) $\psi_0(t)$ *and* $\mathcal{H}(\psi, \mathbf{x}, \mathbf{u}(t))$ *are constant, and*

$$\psi_0(t) \geq 0 \text{ and } H(\psi(t), \mathbf{x}(t), \mathbf{u}(t)) = 0.$$

For the time-optimal problem, f_0 is a constant function, $f_0(\mathbf{x}(t), \mathbf{u}(t)) = 1$ for all t in $[0, T]$, and consequently $\psi_0(t)$ is constant. Let H be defined by the equation

$$H = \mathcal{H} - \psi_0 = \sum_{i=1}^{n} \psi_i f_i(\mathbf{x}, \mathbf{u}).$$

If the trajectory $\mathbf{x}(t)$ determined by $\mathbf{u}(t) \in \mathbf{U}$ is time-optimal, then it follows from Theorem II.2 that

$$\min_{z \in \mathbf{U}} \mathcal{H}(\psi(t), \mathbf{x}(t), z) = \min_{z \in \mathbf{U}} H(\psi(t), \mathbf{x}(t), z)$$

and $H(\psi(t), \mathbf{x}(t), \mathbf{u}(t))$ is a constant function such that $H(\psi(t), \mathbf{x}(t), \mathbf{u}(t)) \leq 0$. This fact leads to the following theorem:

Theorem II.3. *(Pontryagin et al. (1962)) If the trajectory* $\mathbf{x}(t)$ *determined by* $\mathbf{u}(t) \in \mathbf{U}$, $0 \leq t \leq T$, *is time-optimal, then there exists a non-zero continuous solution* $\psi(t) = (\psi_1(t), \psi_2(t), \cdots, \psi_n(t))$ *such that*

(1) The control $\mathbf{u}(t)$ *minimizes the Hamiltonian at every time* t*; that is,*

$$H(\psi(t), \mathbf{x}(t), \mathbf{u}(t)) = \min_{z \in \mathbf{U}} H(\psi(t), \mathbf{x}(t), z).$$

(2) $H(\psi(t), \mathbf{x}(t), \mathbf{u}(t))$ *is constant, and*

$$H(\psi(t), \mathbf{x}(t), \mathbf{u}(t)) \leq 0.$$

Therefore, condition (2) can be checked at any time t, $0 \leq t \leq T$.

2.4 Dubins Car Problem

The Dubins car problem (Dubins (1957)) defines length-optimal paths for a vehicle that moves forward in a plane with constant speed and constraint on turn rate. Variations of this problem have been studied over a wide range of motion planning applications. Reeds and Shepp (1990) conducted a study for a vehicle capable of both forward and backward motions, identifying shortest-length paths with cusps. Balkcom and Mason (2002) extended the Dubins problem to consider differential drive (i.e., two independently driven coaxial wheels), which yielded time-optimal paths with at most three straight segments and two turns. Balkcom et al. (2006) characterized time-optimal paths for a robot capable of instantaneously moving in any direction. Salaris et al. (2010) and (2012) presented a complete characterization for length-optimal paths of the unicycle with field-of-view constraints and visibility constraints. Bakolas and Tsiotras (2011) modified the Dubins problem to allow different minimum radii for clockwise versus counterclockwise turns. Dolinskaya and Maggiar (2012) characterized time-optimal paths for the Dubins vehicle with the speed function depending on the direction and the minimum-turning radius function.

The kinematic models of the above vehicles are based on the simplified kinematic model of the Dubins car. The optimal paths taken by the Dubins car and its variants were characterized by employing Pontryagin's minimum principle in numerous papers, e.g., Reister and Lenhart (1995), Balkcom and Mason (2002), Balkcom et al. (2006), Chitsaz and LaValle (2007), Bakolas and Tsiotras (2011). In particular, necessary conditions for the Dubins path were derived again by Boissonnat et al. (1994) and Sussmann and Tang (1991) using this principle because this method is much simpler and easier. In this section, the formulation of Boissonnat et al. (1994) for the Dubins car problem will be reviewed.

A path $(x,\, y)$ of the Dubins car is a solution of the system of differential equations

$$\begin{aligned} \dot{x}(t) &= \cos\phi(t), \\ \dot{y}(t) &= \sin\phi(t), \\ \dot{\phi}(t) &= u(t), \end{aligned} \tag{2.3}$$

where $\phi(t)$ represents the angle between unit tangent vector $(\dot{x},\, \dot{y})$ and the x-axis, and $u(t)$ represents the turn rate, called the control. The turning radius is assumed to be bounded by a given minimum turning radius $r > 0$. Therefore, the control $u(t)$ is bounded on control region

$$U = \left[-r^{-1},\, r^{-1}\right].$$

Note that the constraint on r (i.e., $r > 0$) will be changed when a maximum turning radius is given. Also note that if a path taken by the Dubins car has a non-zero constant speed, the path can be reparametrized by its length and have unit speed. In this case, the Hamiltonian is given by

$$H(\psi,\, \mathbf{x},\, u) = \psi_1 \cos\phi + \psi_2 \sin\phi + \psi_3 u, \tag{2.4}$$

and the adjoint system is given by

$$\begin{aligned} \dot{\psi}_1(t) &= -\frac{\partial H}{\partial x} = 0, \\ \dot{\psi}_2(t) &= -\frac{\partial H}{\partial y} = 0, \\ \dot{\psi}_3(t) &= -\frac{\partial H}{\partial \phi} = \psi_1 \sin\phi(t) - \psi_2 \cos\phi(t). \end{aligned} \tag{2.5}$$

In system (2.5), ψ_1 and ψ_2 are constant on $[0,\, T]$. To state the results in a more intuitive form, we introduce notations λ and θ defined by $\lambda = \sqrt{\psi_1^2 + \psi_2^2} \geq 0$ and $\theta = \tan^{-1}(\psi_2/\psi_1) \in (-\pi/2,\, \pi/2]$, respectively. Note that $\theta = \pi/2$ when $\psi_1 = 0$.

Then the Hamiltonian and system (2.5) become

$$\begin{aligned} H &= \lambda \cos(\phi - \theta) + \psi_3 u, \\ \dot{\psi}_3 &= \lambda \sin(\phi - \theta). \end{aligned} \tag{2.6}$$

Since the Dubins car problem is time-optimal, it follows from Theorem II.3 that

$$\psi_3(t)\, u(t) \leq \psi_3(t)\, \zeta(t) \tag{2.7}$$

for all piecewise continuous $\zeta(t)$ and for all t in $[0, T]$, and the Hamiltonian (2.4) is constant. The optimal control found from (2.7) is then

$$u(t) = \begin{cases} -r^{-1} & \text{if } \psi_3 > 0, \\ \zeta \in U & \text{if } \psi_3 = 0, \\ r^{-1} & \text{if } \psi_3 < 0. \end{cases} \tag{2.8}$$

It may appear as though (2.8) does not provide information on open intervals for which $\psi_3(t) = 0$. However, it can be shown that $u(t) = 0$ on those intervals, and consequently (2.8) becomes

$$u(t) = \begin{cases} -r^{-1} & \text{if } \psi_3 > 0, \\ 0 & \text{if } \psi_3 = 0, \\ r^{-1} & \text{if } \psi_3 < 0. \end{cases} \tag{2.9}$$

Using (2.9) with further geometric analysis, Boissonnat et al. (1994) proved the following theorem:

Theorem II.4. *(Boissonnat et al. (1994)). Every shortest path in* $\mathbb{R}^2$ *is either (1) an arc of a circle of radius* r*, followed by a line segment, followed by an arc of a circle*

of radius r; or (2) an arc of a circle of radius r, followed by an arc of a circle of radius r and length greater than πr, followed by an arc of a circle of radius r; or (3) a subpath of a path of type (1) or (2). For every path of type (2), it is oriented either clockwise-counterclockwise-clockwise or counterclockwise-clockwise-counterclockwise.

2.5 Dubins Airplane Problem

The Dubins car problem and its variations in the preceding section only considered motion in two-dimensional Euclidean space, i.e., planar motions. $\sim$ To allow changes in altitude, the Dubins car problem has been extended into three-dimensional Euclidean space. Walsh et al. (1994) solved the problem of determining an optimal path for an airplane on the Lie group $SE(3)$ to minimize the sum of the squares of the inputs. Sussmann (1995) formulated the Dubins car problem in $\mathbb{R}^3$ based on Pontryagin's minimum principle on manifolds. He provided the structure of the shortest path for the Dubins car in three-dimensional Euclidean space. Chitsaz and LaValle (2007) characterized time-optimal paths for the Dubins airplane with independently-bounded vertical and turn rates.

The problem of aircraft path planning in this dissertation is a variant of the Dubins airplane problem, thus we briefly review this problem. Note that the Dubins airplane is an extension of the Dubins car that considers altitude. A path $(x,\, y,\, z)$ of the Dubins airplane is a solution of the system of differential equations

$$\begin{aligned} \dot{x}(t) &= \cos\phi(t), \\ \dot{y}(t) &= \sin\phi(t), \\ \dot{z}(t) &= v(t) \in V, \\ \dot{\phi}(t) &= u(t) \in U. \end{aligned} \tag{2.10}$$

In this case, the Hamiltonian is given by

$$H(\psi,\, \mathbf{x},\, u) = \psi_1 \cos\phi + \psi_2 \sin\phi + \psi_3 v + \psi_4 u, \tag{2.11}$$

and the adjoint system is given by

$$\begin{aligned}
\dot{\psi}_1(t) &= -\frac{\partial H}{\partial x} = 0, \\
\dot{\psi}_2(t) &= -\frac{\partial H}{\partial y} = 0, \\
\dot{\psi}_3(t) &= -\frac{\partial H}{\partial z} = 0, \\
\dot{\psi}_4(t) &= -\frac{\partial H}{\partial \phi} = \psi_1 \sin\phi(t) - \psi_2 \cos\phi(t).
\end{aligned} \tag{2.12}$$

Using the notations λ and θ defined in Section 2.4, the Hamiltonian and system (2.12) are given by

$$\begin{aligned}
H &= \lambda \cos(\phi - \theta) + \psi_3 v + \psi_4 u, \\
\dot{\psi}_4 &= \lambda \sin(\phi - \theta).
\end{aligned} \tag{2.13}$$

It follows from Theorem II.3 that

$$\psi_3(t)\, v(t) + \psi_4(t)\, u(t) \leq \psi_3(t)\, \zeta(t) + \psi_4(t)\, \eta(t) \tag{2.14}$$

for all piecewise continuous $\zeta(t)$ and $\eta(t)$ and for all t in $[0,\, T]$, and the Hamiltonian (2.11) is constant. Therefore, the optimal control found from (2.14) is

$$v(t) = \begin{cases} -\operatorname{sgn}(\psi_3) & \text{if } \psi_3 \neq 0, \\ \zeta \in V & \text{if } \psi_3 = 0, \end{cases} \tag{2.15}$$

and

$$u(t) = \begin{cases} -r^{-1} & \text{if } \psi_4 > 0, \\ \eta \in U & \text{if } \psi_4 = 0, \\ r^{-1} & \text{if } \psi_4 < 0. \end{cases} \tag{2.16}$$

Using (2.15) and (2.16) with further geometric analysis, Chitsaz and LaValle (2007) proved the following theorem:

Theorem II.5. *(Chitsaz and LaValle (2007)). Every time-optimal path in* $\mathbb{R}^3$ *has either (1) the shortest time for the Dubins car problem or (2) the time equal to the time required to climb (or descend) between initial and final altitudes at maximum rate.*

CHAPTER III

Admissible Paths

3.1 Introduction

This chapter includes a compilation of initial efforts to explore unidirectional Dubins path geometries. We define admissible but not necessarily optimal paths and investigate their use in aircraft emergency path planning with and without transitions connecting path segments of different turning radii. These admissible paths will be subsequently used to guarantee the existence of minimum-time paths for the unidirectional Dubins car (Chapter IV) and airplane (Chapter V) where Pontryagin's minimum principle is used to characterize time-optimal paths.

In this chapter, admissible paths for a unidirectional Dubins car are defined as concatenations of alternating circular arcs of two different radii that each follows an arc or line segment connecting centers of two circular arcs containing prescribed initial and final oriented points. For a unidirectional Dubins airplane, a concatenation of alternating circular helices of two different radii and constant pitch is defined whose projection onto the xy plane is a concatenation of alternating circular arcs. The geometric properties of these concatenations will be shown to guarantee the existence of admissible paths.

We extend the problem of finding admissible paths for a unidirectional Dubins car to consider continuous curvature. Admissible paths having continuous curvature

allow the robot or vehicle to more precisely follow these paths. A clothoid whose curvature is a linear function with constant slope is used to connect circular arcs of different radii. Finding such clothoids proves the existence of admissible paths having continuous curvature.

The chapter is organized as follows. Section 3.2 defines the concatenation of alternating circular arcs connecting given initial and final oriented points and shows the existence of admissible paths for all unidirectional Dubins car cases. Section 3.3 applies an algorithm to find the admissible path to the planar unidirectional Dubins problem. Section 3.4 defines the concatenation of alternating circular helices connecting given initial and final oriented points and shows the existence of admissible paths for a unidirectional Dubins airplane. Section 3.5 applies an algorithm to find the admissible path to an emergency landing problem. In Section 3.6, we find admissible paths having continuous curvature. In Section 3.7, we show the existence of optimal paths for unidirectional Dubins vehicles.

3.2 Admissible Paths for Unidirectional Dubins Cars

In this section, we define admissible paths for a unidirectional Dubins car joining an initial oriented point with a final oriented point. Given two points (x_0, y_0) and (x_T, y_T) in $\mathbb{R}^2$ with corresponding directions ϕ_0 and ϕ_T, we want to find a continuous and piecewise $\mathcal{C}^2$ path (x, y) subject to the following constraints:

(i) The radius of curvature lies between r and 1 where $0 < r < 1$. The reciprocal of the radius, called the control (or the curvature) and denoted u, is also bounded on control region U. Since a path is continuous and piecewise $\mathcal{C}^2$, the control is piecewise continuous.

(ii) The sign of the curvature remains unchanged. Therefore, the control region U is $[1, r^{-1}]$. The case $U = [-r^{-1}, -1]$ can be treated similarly to $U = [1, r^{-1}]$.

(iii) The path $(x,\, y)$ has unit speed. Even if the path has non-zero constant speed, the path has a unit-speed reparametrization (do Carmo (1976)), so the path with unit speed produces no loss of generality.

Throughout this section, it will be assumed that the control $u(t)$ is a switching function whose values are 1 and r^{-1}. Paths which correspond to the constant controls $u \equiv 1$ and $u \equiv r^{-1}$ are circular arcs of radius 1 and radius r, respectively. It follows that extremal controls produce a concatenation of alternating circular arcs of radius 1 and r. The initial and final segments are also circular arcs of radius 1 or r. Thus, given an initial state $\mathbf{x}_0$ and a final state $\mathbf{x}_T$, we can draw two possible circular arcs that lead away from the initial state and two possible circular arcs that lead into the final state. Since we have two possible initial circular arcs and two possible final circular arcs, we have four possible combinations of initial and final arcs. Each combination is determined by the values of the extremals at $t = 0$ and $t = T$. We will refer to each combination as an ordered pair $(u(0),\, u(T))$. For simplicity, only the combinations $(1,\, 1)$ and $(r^{-1},\, r^{-1})$ are considered in this chapter. All four cases will be considered in subsequent chapters.

Given any combination $(u(0),\, u(T))$ with $u(0) = u(T)$, we seek to find centers of a concatenation of alternating circular arcs. We assume all these centers lie on a circular arc from P and Q. Such a circular arc will be referred to as a *reference arc* and denoted $\mathcal{A}$. The center of a reference arc $\mathcal{A}$ is a point on the perpendicular bisector of the line segment $\overline{PQ}$, as shown in Figure 3.1. Let $r_{\mathcal{A}}$ be the radius of $\mathcal{A}$. Then $r_{\mathcal{A}} \geq \left|\overline{PQ}\right|/2$, and the central angle corresponding to $\overline{PQ}$, denoted α, is defined as follows: $\alpha = 2\sin^{-1}\left(\left|\overline{PQ}\right|/(2r_{\mathcal{A}})\right)$ for a semicircle or minor reference arc and $\alpha = 2\pi - 2\sin^{-1}\left(\left|\overline{PQ}\right|/(2r_{\mathcal{A}})\right)$ for a major reference arc. Note that a reference arc is a straight line when $r_{\mathcal{A}} = \infty$.

Given any combination $(u(0),\, u(T))$ with $u(0) = u(T)$ and any reference arc $\mathcal{A}$, we construct centers of the concatenation of alternating circular arcs. Let P and Q

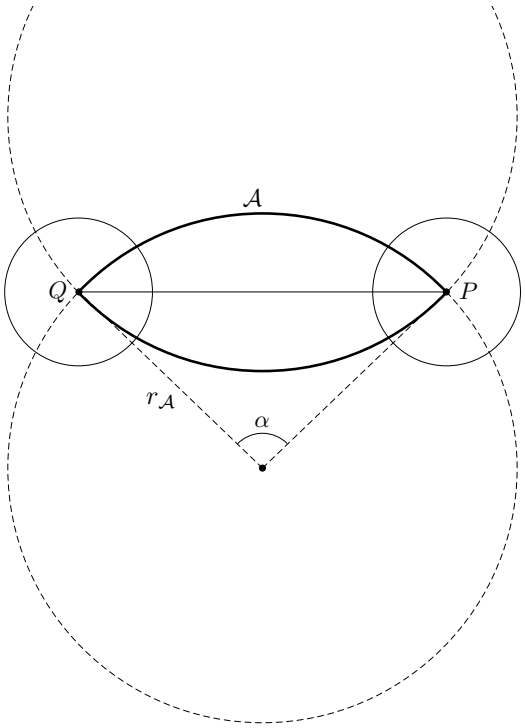

Figure 3.1: A reference arc $\mathcal{A}$.

be two centers of the initial circular arc and the final circular arc, respectively. By the definition of a reference arc, two centers P and Q are the end points of the reference arc $\mathcal{A}$. The center of the second circular arc (i.e., the arc immediately following and tangent to the initial arc) is defined as the intersection of $\mathcal{A}$ and its chord with length $1 - r$ through P, as shown in Figure 3.2. In general, given n centers of the concatenation of alternating circular arcs, the center of the $n + 1$th circular arc is defined as an end point of a chord of $\mathcal{A}$ with length $1 - r$ that has as the other end point the center of the nth circular arc.

By construction, the centers of each pair of alternating circular arcs with radius 1 and r are the end points of a chord of a reference arc $\mathcal{A}$ with length $1 - r$. Since the distance between these two centers is $1 - r$, each pair has a common tangent vector where $u(t)$ switches between 1 and r^{-1}. Each point where $u(t)$ switches is the intersection of each pair and the line through its centers. It follows that all circles of radius 1 and r have the same angular path change, denoted $\Delta\phi$, as shown in

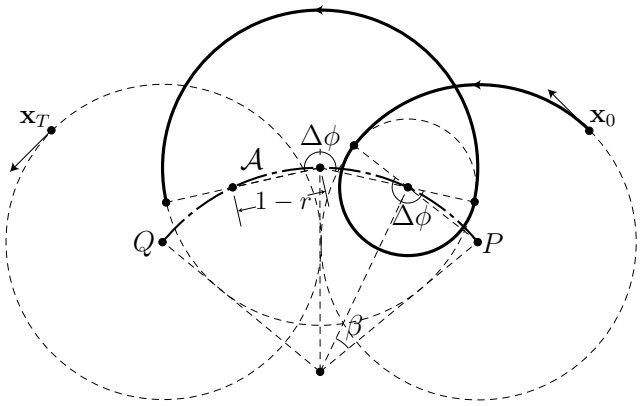

Figure 3.2: The construction of a concatenation of alternating circular arcs on $\mathcal{A}$.

Figure 3.2. Let β be the central angle corresponding to the chord of $\mathcal{A}$ with length $1-r$. Then $\beta = 2\sin^{-1}\left((1-r)/(2r_{\mathcal{A}})\right)$, thus $\Delta\phi$ is either $\pi-\beta$ or $\pi+\beta$, depending on $\mathcal{A}$. For n distinct pairs, the central angle corresponding to the chord of $\mathcal{A}$ joining two centers of the initial and $2n$th circular arcs equals $(2n-1)\,\beta$.

Even if reference arcs can be characterized for all radii $r_{\mathcal{A}} \geq \left|\overline{PQ}\right|/2$, not all reference arcs allow extremal paths to join the initial state $\mathbf{x}_0$ with the final state $\mathbf{x}_T$. Thus, we need to formulate the condition for extremal paths to satisfy boundary conditions $\mathbf{x}(0) = \mathbf{x}_0$ and $\mathbf{x}(T) = \mathbf{x}_T$. This condition will guarantees the existence and uniqueness of such extremal paths from $\mathbf{x}_0$ to $\mathbf{x}_T$.

Except for the initial and final circular arcs, circular arcs are specified as pairs of tangent circular arcs of radius 1 and r whose angular path changes are $\Delta\phi$. referred to as *basic pairs*. Although a pair of an initial arc and arc following it is not a basic pair, this pair will be considered as the first basic pair to include cases where the extremal path is a circular arc.

For some number n of basic pairs, their centers together with center Q are joined to form a polygon with $2n+1$ edges inscribed in the circle including a reference arc $\mathcal{A}$ such that:

(1) $2n-1$ edges have length $1-r$.

(2) One edge of the remaining edges has length $\left|\overline{PQ}\right|$.

(3) The other edge has length equal to the distance between the centers of the $2n$th and final circular arcs.

Such a polygon will be called a *cyclic polygon*, as indicated in Figure 3.3 (a). If the chord of $\mathcal{A}$ joining the centers of the $2n$th and final circular arcs has length $1-r$, then these circular arcs have a common tangent vector where $u(t)$ switches, as shown in Figure 3.3 (b). Thus, the extremal path constructed on a reference arc $\mathcal{A}$ satisfies boundary conditions $\mathbf{x}(0)=\mathbf{x}_0$ and $\mathbf{x}(T)=\mathbf{x}_T$ if

$$\alpha = 2n\beta \tag{3.1}$$

for some number n of basic pairs.

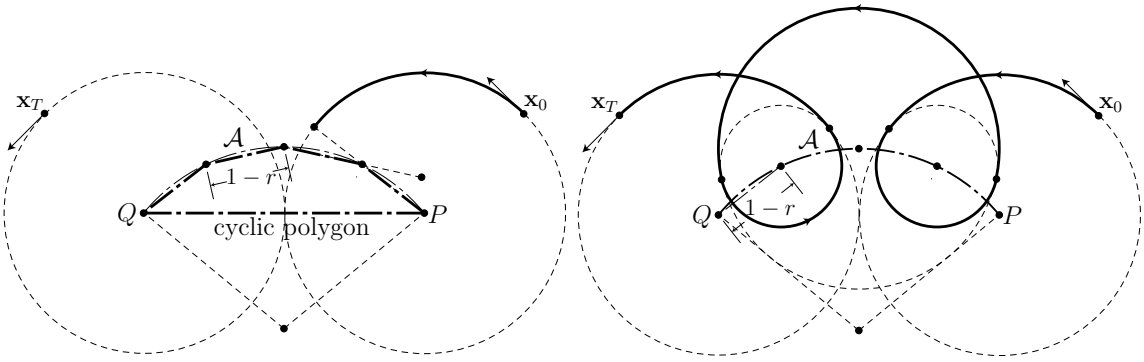

(a) A cyclic polygon. (b) An admissible path constructed on $\mathcal{A}$.

Figure 3.3: A concatenation of alternating circular arcs satisfying boundary conditions $\mathbf{x}(0)=\mathbf{x}_0$ and $\mathbf{x}(T)=\mathbf{x}_T$.

The number n of basic pairs for which condition (3.1) holds is in

$$\left\{n\in\mathbb{N}\,:\,n>\left|\overline{PQ}\right|/\left(2\left(1-r\right)\right)\right\}. \tag{3.2}$$

Let $n>\left|\overline{PQ}\right|/\left(2\left(1-r\right)\right)$. Then there exists a unique cyclic polygon for a reference arc $\mathcal{A}$ having $2n$ edges of length $1-r$ and an edge of length $\left|\overline{PQ}\right|$. This follows from

the existence and uniqueness theorem for convex cyclic polygons (Pinelis (2005)) and the fact that each of the edge lengths of a cyclic polygon for $\mathcal{A}$ is less than the sum of all other edge lengths. Note that such a polygon is convex. Thus, condition (3.1) holds for n, and consequently the extremal path constructed on $\mathcal{A}$ joins $\mathbf{x}_0$ with $\mathbf{x}_T$.

The set in (3.2) is a nonempty set of positive integers that is bounded below, and thus has a minimum which is denoted n_m. The minimum number n_m of basic pairs is then defined by

$$n_m = \begin{cases} \lceil \dfrac{\left|\overline{PQ}\right|}{2\left(1-r\right)} \rceil & \text{if } \dfrac{\left|\overline{PQ}\right|}{2\left(1-r\right)} \notin \mathbb{N} \\ \lceil \dfrac{\left|\overline{PQ}\right|}{2\left(1-r\right)} \rceil + 1 & \text{if } \dfrac{\left|\overline{PQ}\right|}{2\left(1-r\right)} \in \mathbb{N} \end{cases} \tag{3.3}$$

where $\lceil \ \rceil$ denotes the ceiling function.

The condition that $\left|\overline{PQ}\right| / \left(2\left(1-r\right)\right)$ is an integer implies that the extremal path constructed on the line segment $\overline{PQ}$ joins an initial oriented point $\mathbf{x}_0$ with a final oriented point $\mathbf{x}_T$. If the centers of a concatenation of alternating circular arcs lie on $\overline{PQ}$ and their distance is $1-r$, then each pair of alternating circular arcs has a common tangent vector at its intersection with the line $\overleftrightarrow{PQ}$ (Figure 3.4). At its intersection, the control $u\left(t\right)$ switches between 1 and r^{-1}. It follows that all circles of radius 1 and r have the same angular path change $\Delta\phi$ as π. Since the center of the initial circular arc is the end point of $\overline{PQ}$, the sequence of centers of a concatenation is then defined recursively.

For n distinct pairs of alternating circular arcs, the line segment between the centers of the initial and $2n$th circular arcs has length $\left(2n-1\right)\left(1-r\right)$. If the distance between the centers of the $2n$th and final circular arcs equals $1-r$, then these circular arcs have a common tangent vector where $u\left(t\right)$ switches. Thus, the extremal path

constructed on $\overline{PQ}$ joins an initial oriented point $\mathbf{x}_0$ with a final oriented point $\mathbf{x}_T$ if

$$\left|\overline{PQ}\right| = 2n\,(1-r) \tag{3.4}$$

for some number n of basic pairs.

The construction of extremal paths on $\overline{PQ}$ requires slight modification to the set in (3.2) and the minimum number n_m of basic pairs. The number n of basic pairs for which condition (3.1) or condition (3.4) holds is contained in

$$\left\{n \in \mathbb{N} \,:\, n \geq \left|\overline{PQ}\right| / \left(2\,(1-r)\right)\right\}. \tag{3.5}$$

The minimum number n_m becomes

$$n_m = \lceil \frac{\left|\overline{PQ}\right|}{2\,(1-r)} \rceil. \tag{3.6}$$

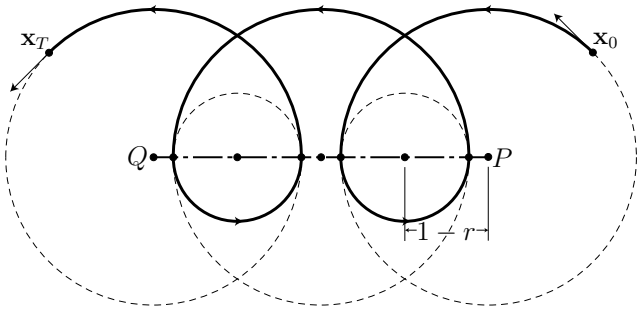

Figure 3.4: The construction of a concatenation of alternating circular arcs on $\overline{PQ}$.

Previously, we constructed a concatenation of alternating circular arcs on a reference arc $\mathcal{A}$ or the line segment $\overline{PQ}$, and enumerated its geometric properties to derive the conditions under which it joins $\mathbf{x}_0$ with $\mathbf{x}_T$. In summary, the concatenation of alternating circular arcs of radius 1 and r constructed on a reference arc $\mathcal{A}$ or the line segment $\overline{PQ}$ has the following properties:

(1) It is smooth in the sense that at juncture points of the concatenation the two

circles have a common tangent vector.

(2) The angular path changes for all circles of radius 1 and r are $\Delta\phi$ which is either $\pi - \beta$ or $\pi + \beta$ where $\beta = 2\sin^{-1}\left((1-r)/(2r_{\mathcal{A}})\right)$ for $\mathcal{A}$ and $\beta = 0$ for $\overline{PQ}$.

Since the set in (3.5) is nonempty for $\left|\overline{PQ}\right| \neq 0$, we conclude with the following theorem:

Theorem III.1. *There exists an admissible path* $(x,\, y)$ *from an initial oriented point* $(x_0,\, y_0,\, \phi_0)$ *to a final oriented point* $(x_T,\, y_T,\, \phi_T)$ *subject to constraints (i)-(iii) (on page 26).*

Algorithm 3.1 presents a method to determine and generate a concatenation of alternating circular arcs from an initial state $\mathbf{x}_0$ to a final state $\mathbf{x}_T$. For each combination $(u(0),\, u(T))$ with $u(0) = u(T)$, we choose one between a reference arc $\mathcal{A}$ and the line segment $\overline{PQ}$ to construct such a concatenation. If $\overline{PQ}/(2(1-r))$ is an integer, the concatenation is constructed on $\overline{PQ}$. Otherwise, the minimum number n_m of basic pairs for $\mathcal{A}$ is evaluated using (3.6). To identify $\mathcal{A}$ which is either a minor arc or a major arc, it suffices to compute the number of basic pairs when $\mathcal{A}$ is a semicircle, denoted by n_s. Note that $\alpha = \pi$ and $r_{\mathcal{A}} = \left|\overline{PQ}\right|/2$ for a semicircle $\mathcal{A}$. If $n_m \leq n_s$, then the concatenation of alternating circular arcs with n_m basic pairs is constructed on a semicircle or minor reference arc $\mathcal{A}$. Otherwise, $\mathcal{A}$ is a major arc. This procedure is summarized in Step I of Algorithm 3.1. Since $\mathcal{A}$ is determined by its radius $r_{\mathcal{A}}$, $r_{\mathcal{A}}$ allows the concatenation to be constructed on $\mathcal{A}$.

For each radius $r_{\mathcal{A}}$ in $\left[\left|\overline{PQ}\right|, \infty\right)$, there are two reference arcs from P and Q, one for which $\Delta\phi = \pi + \beta$ and the other for which $\Delta\phi = \pi - \beta$, denoted by $\mathcal{A}_+$ and $\mathcal{A}_-$, respectively. If a reference arc $\mathcal{A}$ is chosen to construct the extremal path, each combination $(u(0),\, u(T))$ has two concatenations of alternating circular arcs with n_m basic pairs from $\mathbf{x}_0$ to $\mathbf{x}_T$. Note that every combination $(u(0),\, u(T))$ has one concatenation for the line segment $\overline{PQ}$. For each $(u(0),\, u(T))$, every reference

arc $\mathcal{A}$ in $\{\mathcal{A}_+, \mathcal{A}_-\}$ or the line segment $\overline{PQ}$ yields a family of extremal controls that concatenate circular arcs. Therefore, the sequence of points of the concatenation at which $u(t)$ switches can be found as stated in Step II of Algorithm 3.1.

Algorithm 3.1. Generating admissible paths with n_m basic pairs constructed on a reference arc $\mathcal{A}$ or line segment $\overline{PQ}$.

Given initial state $\mathbf{x}_0 = (x_0, y_0, \phi_0)$, final state $\mathbf{x}_T = (x_T, y_T, \phi_T)$, minimum radius of curvature r and maximum radius of curvature 1, generate admissible paths with n_m basic pairs constructed on a reference arc $\mathcal{A}$ or line segment $\overline{PQ}$ for each combination $(u(0), u(T)) \in \{(1, 1), (r^{-1}, r^{-1})\}$.

I. **For** each combination $(u(0), u(T)) \in \{(1, 1), (r^{-1}, r^{-1})\}$,
   1. Determine the two centers P and Q of the initial and final circular arcs and compute the length of $\overline{PQ}$.
   2. Compute the minimum number n_m of basic pairs using
   $$n_m = \lceil \left|\overline{PQ}\right| / (2(1-r)) \rceil$$
   and the number n_s of basic pairs when reference arc $\mathcal{A}$ is a semicircle using (3.1) with the floor function:
   $$n_s = \lfloor \pi / \left(4 \sin^{-1}\left((1-r) / \left|\overline{PQ}\right|\right)\right) \rfloor.$$
   3. **If** $\left|\overline{PQ}\right| / (2(1-r))$ is an integer, **then** the admissible path constructed on the line segment $\overline{PQ}$ has n_m basic pairs. Go to Step 1 for the next combination. **Otherwise,** continue.
   4. Compute the radius $r_{\mathcal{A}}$ of a reference arc $\mathcal{A}$ which is a solution to $\alpha = 2n_m\beta$ in the interval $\left[\left|\overline{PQ}\right|/2, \infty\right)$ using conventional numerical methods, e.g., Newton-Raphson.
   5. Determine the type of the reference arc $\mathcal{A}$ on which the admissible path with n_m basic paris for the current combination is constructed.
      5a. **If** $n_m \leq n_s$, **then** the admissible path with n_m basic pairs is constructed on the semicircle or minor reference arc $\mathcal{A}$ of radius $r_{\mathcal{A}}$.
      5b. **Otherwise,** the admissible path with n_m basic pairs is constructed on the major reference arc $\mathcal{A}$ of radius $r_{\mathcal{A}}$.

   Go to Step 1 for the next combination.

II. **For** each combination $(u(0), u(T)) \in \{(1, 1), (r^{-1}, r^{-1})\}$, compute the sequence of points at which $u(t)$ switches. If a reference arc $\mathcal{A}$ is chosen in Step I, two admissible paths are constructed on each $\mathcal{A}$ in $\{\mathcal{A}_+, \mathcal{A}_-\}$. If the line segment $\overline{PQ}$ is chosen in Step I, one admissible path is constructed on $\overline{PQ}$.
   1. Determine the first time (or length) t_1 at which $u(t)$ switches between 1 and r^{-1}.
      1a. **If** $u(0) = 1$, **then** $t_1 = \theta + \beta/2 - \phi_0 + \pi$ for $\mathcal{A}_+$, $t_1 = \theta - \beta/2 - \phi_0$ for $\mathcal{A}_-$ and $t_1 = \theta - \phi_0 + \pi/2$ for $\overline{PQ}$.
      1b. **If** $u(0) = r^{-1}$, **then** $t_1 = r(\theta + \beta/2 - \phi_0)$ for $\mathcal{A}_+$, $t_1 = r(\theta - \beta/2 - \phi_0 + \pi)$ for $\mathcal{A}_-$ and $t_1 = r(\theta - \phi_0 - \pi/2)$ for $\overline{PQ}$.

Note that, for $\mathcal{A}_+$ and $\mathcal{A}_-$, θ represents the angle between $\overrightarrow{RP}$ and the x-axis. For $\overline{PQ}$, θ represents the angle between $\overrightarrow{PQ}$ and the x-axis.

2. Compute the point $(x(t_1), y(t_1))$ by integrating $\dot{x}(t) = \cos\phi(t)$, $\dot{y}(t) = \sin\phi(t)$ and $\dot{\phi}(t) = u(t)$ over $[0, t_1]$.
3. **For** $i = 2, 3, \cdots, 2n_m$,
   3a. Determine the ith time (or length) t_i at which $u(t)$ switches between 1 and r^{-1}.
   $$t_i = u^{-1}\left(\left(t_{i-1} + t_i\right)/2\right)\Delta\phi + t_{i-1}$$
   where $\Delta\phi = \pi + \beta$ for $\mathcal{A}_+$, $\Delta\phi = \pi - \beta$ for $\mathcal{A}_-$ and $\Delta\phi = \pi$ for $\overline{PQ}$.
   3b. Compute the point $(x(t_i), y(t_i))$ by integrating $\dot{x}(t) = \cos\phi(t)$, $\dot{y}(t) = \sin\phi(t)$ and $\dot{\phi}(t) = u(t)$ over $[t_{i-1}, t_i]$.

3.3 Case Study: The Unidirectional Dubins Car

In this section, we apply Algorithm 3.1 to a series of test cases and evaluate its completeness and solution computation times. We consider an Unmanned Ground Vehicle (UGV) in the unobstructed plane and assume the UGV is constrained to clockwise turning motions after its steering wheel is locked. Specifically, control u (i.e., the curvature) is bounded on the interval $[\pi/24$ rad/sec, $\pi/18$ rad/sec$]$. The initial state $\mathbf{x_0} = (x_0, y_0, \phi_0)$ is uniformly distributed on

$$[73.7104^\circ\,\mathrm{W}, 73.8475^\circ\,\mathrm{W}] \times [40.5712^\circ\,\mathrm{N}, 40.7083^\circ\,\mathrm{N}] \times \times [0, 2\pi).$$

Ten sample points on each axis (i.e., the x-axis, y-axis and ϕ-axis) are considered as each component of $\mathbf{x}_0$. For every initial state $\mathbf{x}_0$, the UGV is asked to return to base at latitude 40.6398°N and longitude 73.7789°W with a final orientation of 130 degrees.

For every initial state $\mathbf{x}_0$, we evaluate the computation times of Algorithm 3.1 for finding admissible paths constructed on $\mathcal{A}$ or $\overline{PQ}$, implemented in Matlab. Over 1,000 initial states, the average computation time of Algorithm 3.1 is 3.9×10^{-3} seconds

on a 2.93GHz Intel® Xeon® X5570 processor, running Linux. Figure 3.5 shows a histogram of computation times for Algorithm 3.1 over 1,000 initial states. Each bar represents an execution time interval of width 1.8×10^{-3}. In about 50% of the test cases, the computation time of Algorithm 3.1 is near the mean value. Since the minimum number n_m of basic pairs is proportional to $\left|\overline{PQ}\right|$, the computation time of Algorithm 3.1 increases approximately linearly with $\left|\overline{PQ}\right|$.

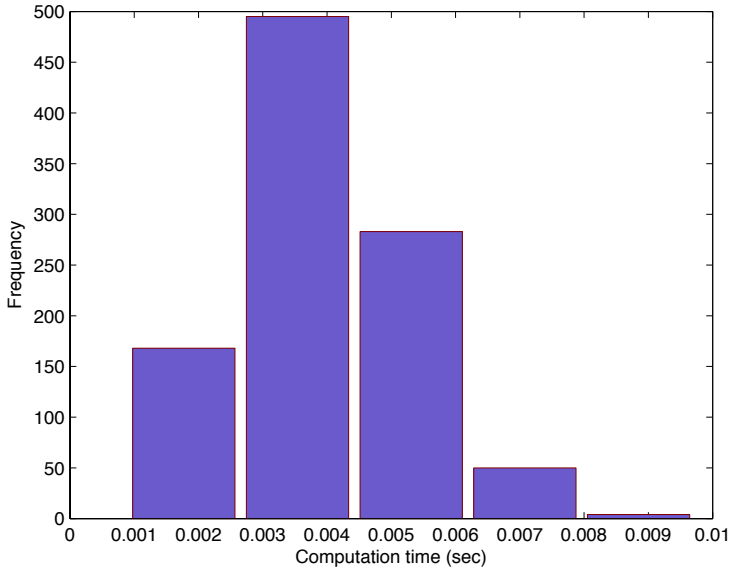

Figure 3.5: Histogram of computation times of Algorithm 3.1 over 1,000 initial states.

Figure 3.6 illustrates concatenations of alternating circular arcs joining $\mathbf{x}_0$ with $\mathbf{x}_T$ for combination (1, 1). In Figure 3.6 (a) and (b), concatenations of alternating circular arcs joining $\mathbf{x}_0$ with $\mathbf{x}_T$ have the minimum and the maximum n_m of 1 and 47, respectively, over the 1,000 initial states $\mathbf{x}_0$. These minimum and maximum n_m occur when $\overline{PQ}$ is minimum and maximum, respectively. The concatenation in Figure 3.6 (a) is constructed on a major reference arc $\mathcal{A}$. In contrast, the concatenation in Figure 3.6 (b) is constructed on a minor reference arc $\mathcal{A}$. In Figure 3.6 (c), a concatenation of alternating circular arcs is constructed on the line segment $\overline{PQ}$ because $\left|\overline{PQ}\right| = 2n_m\,(1-r)$ for $n_m = 3$. Note that one admissible path is constructed

on $\overline{PQ}$.

3.4 Admissible Paths for Unidirectional Dubins Airplanes

In Section 3.2, we constructed an admissible path $(x,\, y)$ from an initial oriented point $(x_0,\, y_0,\, \phi_0)$ to a final oriented point $(x_T,\, y_T,\, \phi_T)$. Such an admissible path was defined as a concatenation of alternating circular arcs constructed on a reference arc $\mathcal{A}$ or the line segment $\overline{PQ}$. This concatenation always exists because there exists a number of basic pairs in $\left\{n \in \mathbb{N} : n \geq \left|\overline{PQ}\right| / \left(2\left(1 - r\right)\right)\right\}$. We now extend this result to define admissible solutions for the unidirectional Dubins airplane as follows: Given two oriented points $(x_0,\, y_0,\, z_0,\, \phi_0)$ and $(x_T,\, y_T,\, z_T,\, \phi_T)$ in $\mathbb{R}^3 \times S^1$, define a continuous and piecewise $\mathcal{C}^2$ path $(x,\, y,\, z)$ subject to constraints (i), (ii) and (iii), and the following additional constraints:

(iv) The rate of change in altitude, called the control (or the vertical rate) and denoted v, is bounded on control region $V = [-v_{\max},\, v_{\max}]$ where $0 < v_{\max} < 1$. [1] The control is piecewise continuous.

(v) The controls u and v are independent of each other.

An algorithm to find a sequence of admissible controls is also developed.

Under constraints (iv) and (v), altitude z is a solution of the differential equation

$$\dot{z}\left(t\right) = v\left(t\right) \in V. \tag{3.7}$$

Without loss of generality, we assume that $z_0 = 0$.

[1] A value $v_{\max} = 1$ would imply a 45° flight path angle. Fixed-wing aircraft will climb and descend at a more shallow angle. Additionally, an aircraft may have asymmetric bounds on vertical rate, e.g., it may be capable of descending faster than climbing. Each Dubins airplane problem posed will require either a climb or descent, indicating the appropriate value of $v_{\max}$ for that particular path planning activity.

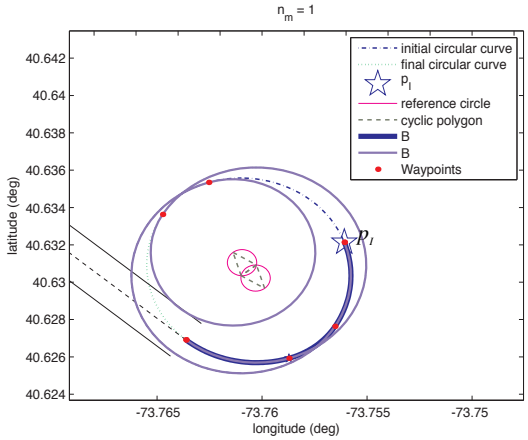

(a) An admissible path with the minimum n_m over 1,000 initial states.

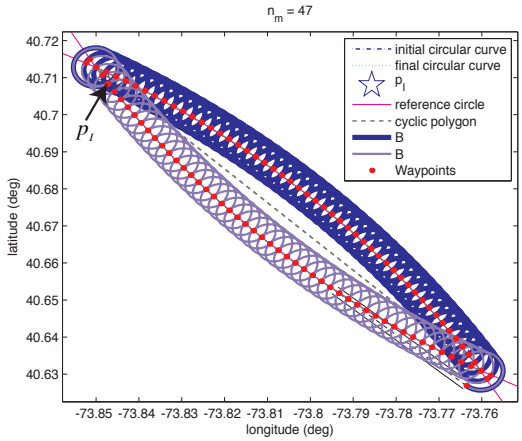

(b) An admissible path with the maximum n_m over 1,000 initial states.

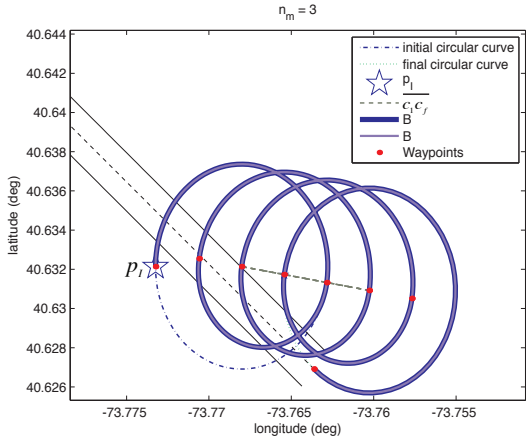

(c) An admissible path constructed on $\overline{PQ}$.

Figure 3.6: Some Concatenations of alternating circular arcs joining 1,000 initial states with $\mathbf{x}_T = (73.7789^\circ\,\mathrm{W},\ 40.6398^\circ\,\mathrm{N},\ 130^\circ)$.

The projection of a path $(x,\, y,\, z)$ onto the xy plane is a continuous and piecewise $\mathcal{C}^2$ path $(x,\, y)$ subject to constraints (i), (ii) and (iii). It follows from Theorem III.1 that an admissible path $(x,\, y)$ exists. The length of such an admissible path approaches ∞ as the number n of basic pairs approaches ∞. This follows from the fact that such a concatenation joins an initial oriented point with a final oriented point for the number of basic pairs in $\left\{n \in \mathbb{N} \,:\, n \geq \left|\overline{PQ}\right| / \left(2\left(1-r\right)\right)\right\}$. Thus, we can construct a sequence of alternating circular arcs joining an initial oriented point with a final oriented point (Section 3.2), denoted by (T_n).

To find an admissible path $(x,\, y,\, z)$, it suffices to find control v that transfers z_0 to z_T for a given (T_n). The result follows from constraint (v). Let $T_{\Delta z} = \left|z_T\right| / v_{\max}$ and T_1 be the first term of the sequence (T_n). There are two cases to consider: $T_1 \geq T_{\Delta z}$ and $T_1 < T_{\Delta z}$. For $T_1 \geq T_{\Delta z}$, $\left|z_T\right| / T_1 \leq v_{\max}$, and thus $v \equiv z_T / T_1$ transfers z_0 to z_T. For $T_1 \leq T_{\Delta z}$, an extremal path $(x,\, y)$ of length (or time) T_1 constructed on a reference arc $\mathcal{A}$ or line segment $\overline{PQ}$ satisfies boundary conditions $(x_0,\, y_0,\, \phi_0)$ and $(x_T,\, y_T,\, \phi_T)$ before the final altitude z_T can be reached. Since the sequence (T_n) diverges to $+\infty$, there exists a time $T_n > T_1$ such that $T_n \geq T_{\Delta z}$. Thus, an initial oriented point $(x_0,\, y_0,\, z_0,\, \phi_0)$ is joined to a final oriented point $(x_T,\, y_T,\, z_T,\, \phi_T)$ by a path $(x,\, y,\, z)$ of length T_n whose projection onto the xy plane is a concatenation of alternating circular arcs constructed on $\mathcal{A}$ or $\overline{PQ}$. Using these results, we can state the following theorem:

Theorem III.2. *There exists an admissible path* $(x,\, y,\, z)$ *from an initial oriented point* $(x_0,\, y_0,\, z_0,\, \phi_0)$ *to a final oriented point* $(x_T,\, y_T,\, z_T,\, \phi_T)$ *subject to constraints (i)-(v).*

For such an admissible path, the control u is a switching function whose values are 1 and r^{-1}, and the control v is a constant function whose value is a final altitude divided by the length T_n of a concatenation of alternating circular arcs. Note that the value of the control v is in $V = [-v_{\max},\, v_{\max}]$. Paths which correspond to the

constant controls $u \equiv 1$ and $u \equiv r^{-1}$ with the constant control v are circular helices of radius 1 and radius r, respectively, and of pitch $2\pi |v|$. These circular helices have a common tangent vector where $u(t)$ switches between 1 and r^{-1}. This follows from the fact that $\phi(t)$ and $v(t)$ are continuous functions that define the direction of the tangent vector. Therefore, controls produce a concatenation of alternating circular helices of radius 1 and r and of pitch $2\pi |z_T/T_n|$ where T_n is a length of its projection onto the xy plane such that $T_n \geq T_{\Delta z}$. Algorithm 3.2 finds the minimum value of n such that $T_n \geq T_{\Delta z}$. It then generates the sequence of points at which $u(t)$ switches. Note that control $v(t)$ is constant in this algorithm.

Algorithm 3.2. Generating admissible concatenations of alternating circular helices.

Given initial state $\mathbf{x}_0 = (x_0, y_0, z_0, \phi_0)$, final state $\mathbf{x}_T = (x_T, y_T, z_T, \phi_T)$, and minimum radius of curvature r, generate admissible concatenations of alternating circular helices for each combination $(u(0), u(T)) \in \{(1, 1), (r^{-1}, r^{-1})\}$. Note that the maximum radius of curvature is assumed to be 1, the vertical rate (i.e., the rate of change in altitude) is bounded on $[-1, 1]$ and $z_0 = 0$.

I. **For** each combination $(u(0), u(T)) \in \{(1, 1), (r^{-1}, r^{-1})\}$,

1. Determine the two centers P and Q of the initial and final circular arcs and compute the length of $\overline{PQ}$.
2. Compute the minimum number n_m of basic pairs using
$$n_m = \lceil \left|\overline{PQ}\right| / (2(1-r)) \rceil$$
and the number n_s of basic pairs when a reference arc $\mathcal{A}$ is a semicircle using (3.1) with the floor function:
$$n_s = \lfloor \pi / \left(4 \sin^{-1}(1-r) / \left|\overline{PQ}\right|\right) \rfloor.$$
3. Set $n = n_m$.
4. **If** $n = \left|\overline{PQ}\right| / (2(1-r))$, **then** the admissible path with n basic pairs is constructed on the line segment $\overline{PQ}$. **Otherwise,** continue.
5. Compute the radius $r_{\mathcal{A}}$ of a reference arc $\mathcal{A}$ which is a solution to $\alpha = 2n\beta$ in the interval $\left[\left|\overline{PQ}\right|/2, \infty\right)$ using conventional numerical methods, e.g., Newton-Raphson.
6. Determine the type of the reference arc $\mathcal{A}$ on which the admissible path with n basic paris for the current combination is constructed.
   - 6a. **If** $n \leq n_s$, **then** the admissible path with n basic pairs is constructed on the semicircle or minor reference arc $\mathcal{A}$ of radius $r_{\mathcal{A}}$.
   - 6b. **Otherwise,** the admissible path with n basic pairs is constructed on the major reference arc $\mathcal{A}$ of radius $r_{\mathcal{A}}$.

7. Compute the length T_n of the admissible path with n basic pairs constructed on $\mathcal{A}$ or $\overline{PQ}$. If a reference arc $\mathcal{A}$ is chosen, compute the lengths of two admissible paths constructed on each $\mathcal{A}$ in $\{\mathcal{A}_+, \mathcal{A}_-\}$. If the line segment $\overline{PQ}$ is chosen, compute the length of the one admissible path constructed on $\overline{PQ}$.

   7a. Compute the first time (or length) t_1 at which $u(t)$ switches between 1 and r^{-1}.

   If $u(0) = 1$, **then** $t_1 = \theta + \beta/2 - \phi_0 + \pi$ for $\mathcal{A}_+$, $t_1 = \theta - \beta/2 - \phi_0$ for $\mathcal{A}_-$ and $t_1 = \theta - \phi_0 + \pi/2$ for $\overline{PQ}$.

   If $u(0) = r^{-1}$, **then** $t_1 = r(\theta + \beta/2 - \phi_0)$ for $\mathcal{A}_+$, $t_1 = r(\theta - \beta/2 - \phi_0 + \pi)$ for $\mathcal{A}_-$ and $t_1 = r(\theta - \phi_0 - \pi/2)$ for $\overline{PQ}$.

   Note that, for $\mathcal{A}_+$ and $\mathcal{A}_-$, θ represents the angle between $\overrightarrow{RP}$ and the x-axis. For $\overline{PQ}$, θ represents the angle between $\overrightarrow{PQ}$ and the x-axis.

   7b. Compute the angular path change $\Delta\phi$ as follows: $\Delta\phi = \pi + \beta$ for $\mathcal{A}_+$, $\Delta\phi = \pi - \beta$ for $\mathcal{A}_-$ and $\Delta\phi = \pi$ for $\overline{PQ}$.

   7c. Compute the length T_n.

$$T_n = t_1 + (n-1)(1+r)\Delta\phi + ru(0)\Delta\phi + u^{-1}(0)(\phi_T - \phi(t_{2n})).$$

8. Determine the control v (i.e. the vertical rate) transferring z_0 to z_T.

   8a. **If** $T_n \geq T_{\Delta z}$ for some T_n, **then** the control $v = z_T/T_n$ transfers z_0 to z_T. Go to Step 1 for the next combination.

   8b. **Otherwise,** set $n = n + 1$, and go to Step 4.

II. **For** each combination $(u(0), u(T)) \in \{(1, 1), (r^{-1}, r^{-1})\}$, compute the sequence of points at which $u(t)$ switches. If a reference arc $\mathcal{A}$ is chosen in Step I, two admissible concatenations are constructed. If the line segment $\overline{PQ}$ is chosen in Step I, one admissible concatenation is constructed.

1. Compute the point $(x(t_1), y(t_1), z(t_1))$ by integrating $\dot{x}(t) = \cos\phi(t)$, $\dot{y}(t) = \sin\phi(t)$, $\dot{z}(t) = w$ and $\dot{\phi}(t) = u(t)$ over $[0, t_1]$.
2. **For** $i = 2, 3, \cdots, 2n$,

   2a. Determine the ith time (or length) t_i at which $u(t)$ switches between 1 and r^{-1}.

$$t_i = u^{-1}((t_{i-1} + t_i)/2)\Delta\phi + t_{i-1}.$$

   2b. Compute the point $(x(t_i), y(t_i), z(t_i))$ by integrating $\dot{x}(t) = \cos\phi(t)$, $\dot{y}(t) = \sin\phi(t)$, $\dot{z}(t) = v$ and $\dot{\phi}(t) = u(t)$ over $[t_{i-1}, t_i]$.

3.5 Application: An Emergency Landing Problem for Unidirectional Dubins Airplanes

In this section, we present an application of Algorithm 3.2 to the emergency landing planning problem that motivated our work. Figure 3.7 illustrates the discretized flight envelope of an F-16 for aileron jam over a range of altitude from 0 ft to $10,000$ ft. Axes in Figure 3.7 are airspeed V, turn rate $\dot{\phi}$ and climb rate $\dot{z}$. Each trim point shown in Figure 3.7 is feasible over the full range of specified jam angles and altitudes.

We assume that a -10° aileron jam occurs at an altitude of $10,000$ ft, and that the true airspeed is 250 ft/sec. At the given altitude of $10,000$ ft and true airspeed of 250 ft/sec, the F-16 has a range of turn rates varying from -10 deg/sec to -7.5 deg/sec and from 7.5 deg/sec to 10 deg/sec; non-turning (straight flight) states are not feasible except at slower airspeeds. We assume the F-16 is in an initial left-turning state; as shown it cannot transition through straight flight to a right turning state so it is commmanded to land with a unidirectional left turning path. Thus, the control u (i.e., the curvature) is bounded on the interval $[\pi/24$ rad/sec, $\pi/18$ rad/sec$]$ assuming z is positive up. Moreover, the F-16 has a range of vertical rates varying from -25 ft/sec to 0 ft/sec, thus the control v (i.e., the vertical rate) is bounded on the interval $[-25, 0]$.

The initial state $\mathbf{x}_0$ of the F-16 is given by

$$\mathbf{x}_0 = (x_0, y_0, z_0, \phi_0) = (73.76^\circ\,\mathbf{W}, 40.64^\circ\,\mathbf{N}, 10,000\,\mathbf{ft}, 210^\circ)\,.$$

The final oriented point state $\mathbf{x}_T$ is the end of JFK runway 31L at latitude 40.6398°N and longitude 73.7789°W and at an altitude of 11.8 ft. Figure 3.8 illustrates example concatenations of alternating circular helices joining $\mathbf{x}_0$ with $\mathbf{x}_T$. Consequently, the F-16 can land on JFK runway 31L by following each admissible path corresponding to the given $\mathbf{x}_0$. Although the minimum number n_m of basic pairs are 4 and 3 for

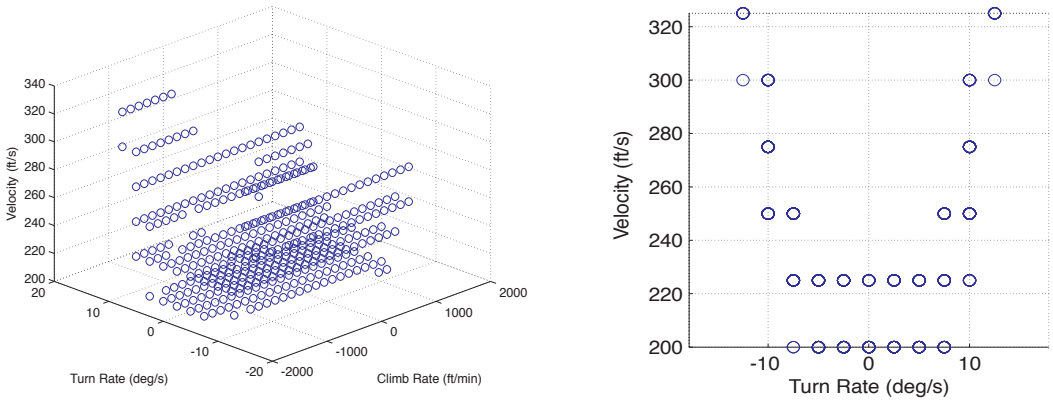

(a) $\left(V,\, \dot{\phi},\, \dot{z}\right)$-space (b) $\left(V,\, \dot{\phi}\right)$-space

Figure 3.7: Flight Envelope for an F-16 aircraft over an Aileron Jam Interval $[-10,\, 10]$ degrees and Altitude Interval $[0,\, 10000]$ ft (Strube (2005) and Choi et al. (2010)).

combinations $(1,\, 1)$ and $(r^{-1},\, r^{-1})$, respectively, the determined emergency landing trajectories have an increased number 6 and 7 of basic pairs to yield the necessary altitude change from the initial state to the final (landing) state. In Figures 3.8 (a) and (b), the concatenations of alternating circular helices have vertical rates of -23.86 ft/sec and -22.53 ft/sec, respectively. These vertical rates lie in the control region $[-25,\, 0]$.

3.6 Admissible Paths with Smooth Transitions for Unidirectional Dubins Cars

In Sections 3.2 and 3.4, we presumed switching the curvature (i.e., the control $u\,(t)$) was instantaneous. However, it is likely the robot or vehicle would require a finite switching interval over which curvature is smoothly transitioned. It then follows that the robot or vehicle can more precisely follow the path with continuous curvature. We investigate such a solution for the Dubins car problem given unidirectional turning constraints. Given two oriented points $(x_0,\, y_0,\, \phi_0)$ and $(x_T,\, y_T,\, \phi_T)$ in $\mathbb{R}^2 \times S^1$, we

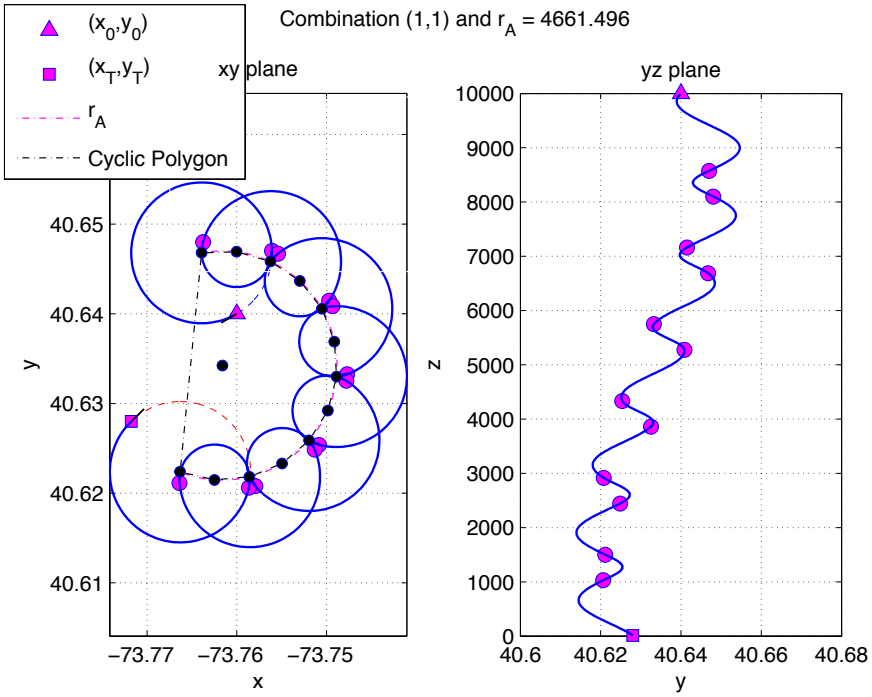

(a) A combination $(u(0), u(T)) = (1, 1)$.

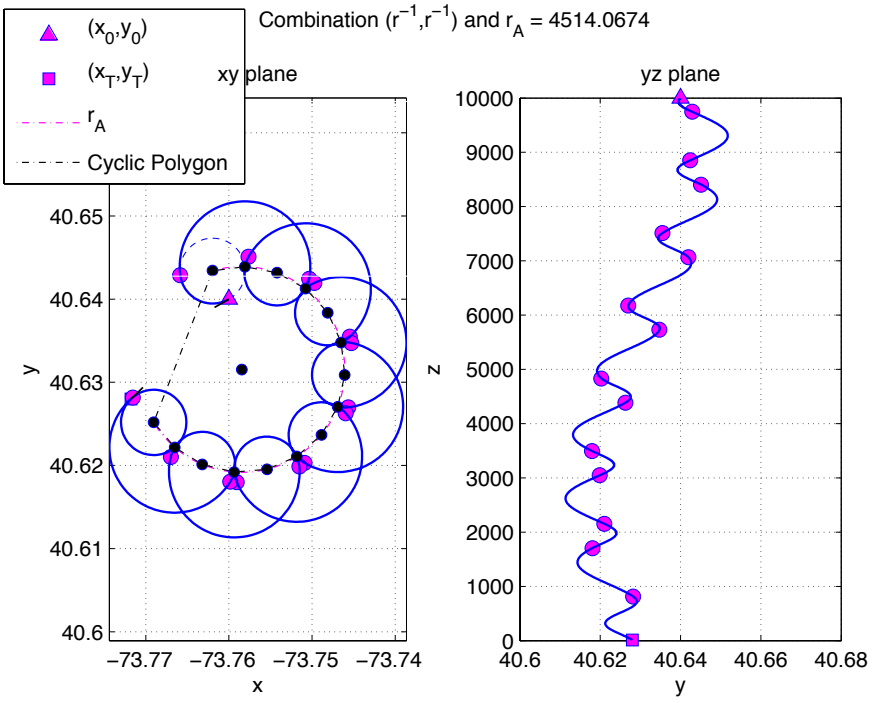

(b) A combination $(u(0), u(T)) = (r^{-1}, r^{-1})$.

Figure 3.8: Example admissible paths comprised of alternating circular helices from $\mathbf{x}_0 = (73.76^\circ\,\mathbf{W}, 40.64^\circ\,\mathbf{N}, 10,000\,\mathbf{ft}, 210^\circ)$ to the JFK 31L runway threshold.

now want to find a $\mathcal{C}^2$ and piecewise $\mathcal{C}^3$ path $(x,\, y)$ subject to constraints (i), (ii) and (iii), and the following additional constraints:

(iv) The derivative of the curvature with respect to the path's length, called the control and denoted w, is bounded on the control region $W = [-m,\, m]$.

For unidirectional Dubins cars, we defined a concatenation of alternating circular arcs constructed on the reference arc $\mathcal{A}$ or the line segment $\overline{PQ}$. All centers of alternating circular arcs lie on $\mathcal{A}$ or $\overline{PQ}$ at a distance $1-r$ from each other, depending on whether $\left|\overline{PQ}\right| / (2\,(1-r))$ is an integer. In the same manner, we assume all centers of alternating circular arcs of radius 1 and radius $\bar{r}$ in $[r,\, 1)$ lie on $\mathcal{A}$ or $\overline{PQ}$ at a distance $\Delta d \in (0,\, 1-r)$ from each other. All statements in Section 3.2 hold if $|1-r|$ is replaced by Δd, except for the properties of the concatenation of alternating circular arcs. Thus, if the number n of pairs of alternating arcs of radius 1 and $\bar{r}$ is in $\left\{n \in \mathbb{N} : n > \left|\overline{PQ}\right| / (2\Delta d)\right\}$, then some cyclic polygon of $\mathcal{A}$ has $2n$ edges of length Δd and an edge of length $\overline{PQ}$. If $n = \left|\overline{PQ}\right| / (2\Delta d)$, the line segment $\overline{PQ}$ consists of $2n$ line segments of length Δd. Thus, alternating circular arcs with the minimum number n_m of basic pairs can be constructed on a reference arc $\mathcal{A}$ or the line segment $\overline{PQ}$, as shown in Figure 3.9.

Since Δd is arbitrary, alternating circular arcs of radius 1 and radius $\bar{r}$ may have no juncture point at which the arcs have a common tangent vector. Now we want to find a smooth curve joining each pair of alternating arcs so that at each juncture point the curve has the same tangent vector and control $u\,(t)$ (i.e., curvature) as the corresponding circular arc. Throughout this section, it is assumed that the curvature of such a smooth curve is a linear function with slope m or $-m$. Paths which correspond to the constant controls $v \equiv -m$ and $v \equiv m$ are arcs of clothoids. Such a clothoid joining two arcs of radius 1 and $\bar{r}$ can be uniquely characterized by radius $\bar{r}$ if $\bar{r}$ is in some restricted interval (to be established below). This follows from the results of Meek and Walton (1989).

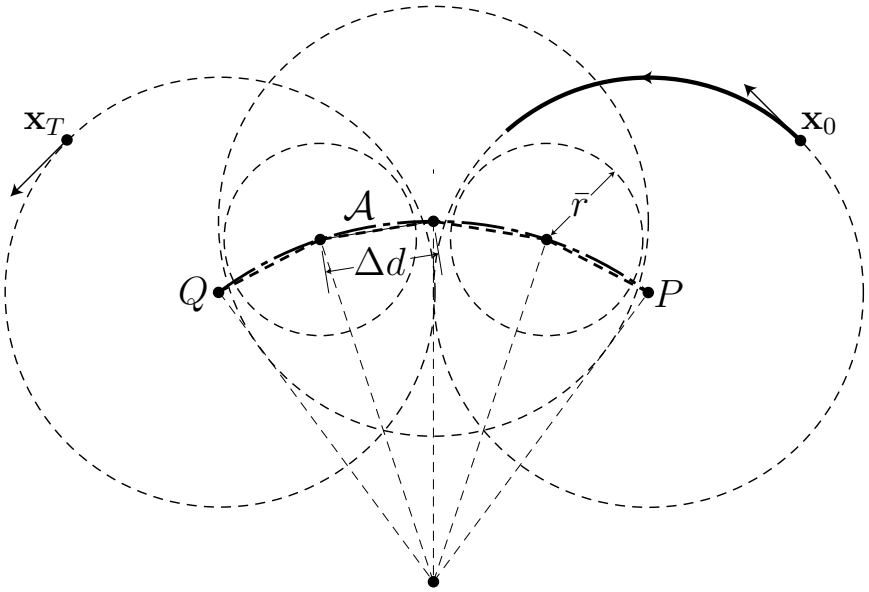

Figure 3.9: The construction of alternating circular arcs of radius 1 and radius $\bar{r}$ on $\mathcal{A}$.

By the construction of alternating circular arcs on a reference arc $\mathcal{A}$ or the line segment $\overline{PQ}$, it suffices to find a clothoid connecting the one pair of such alternating arcs, as shown in Figure 3.10. For simplicity, we choose a coordinate system in such a way that the centers of this one pair are in the first quadrant and the clothoid is defined by

$$x(t) = C(t) \quad \text{and} \quad y(t) = S(t), \tag{3.8}$$

where $C(t)$ and $S(t)$ are the Fresnel integrals defined by

$$C(t) = \int_0^t \cos\left(\frac{m}{2}\tau^2\right) d\tau \quad \text{and} \quad S(t) = \int_0^t \sin\left(\frac{m}{2}\tau^2\right) d\tau. \tag{3.9}$$

Then the center of curvature of the clothoid at t is given by

$$\left(\frac{C_I(t)}{t}, \frac{S_I(t) + m^{-1}}{t}\right), \tag{3.10}$$

where $C_I(t)$ and $S_I(t)$ represent the integrals of the Fresnel integrals $C(t)$ and $S(t)$, respectively, defined by

$$\begin{aligned} C_I(t) &= \int_0^t C(\tau)\, d\tau = tC(t) - \frac{1}{m}\sin\left(\frac{m}{2}t^2\right) \\ S_I(t) &= \int_0^t S(\tau)\, d\tau = tS(t) + \frac{1}{m}\cos\left(\frac{m}{2}t^2\right) - \frac{1}{m}. \end{aligned} \tag{3.11}$$

The circle of radius $\bar{r}$ must be inside that of radius 1, that is $\Delta d < 1 - \bar{r}$. The proof of this result will be found in Stoer (1982).

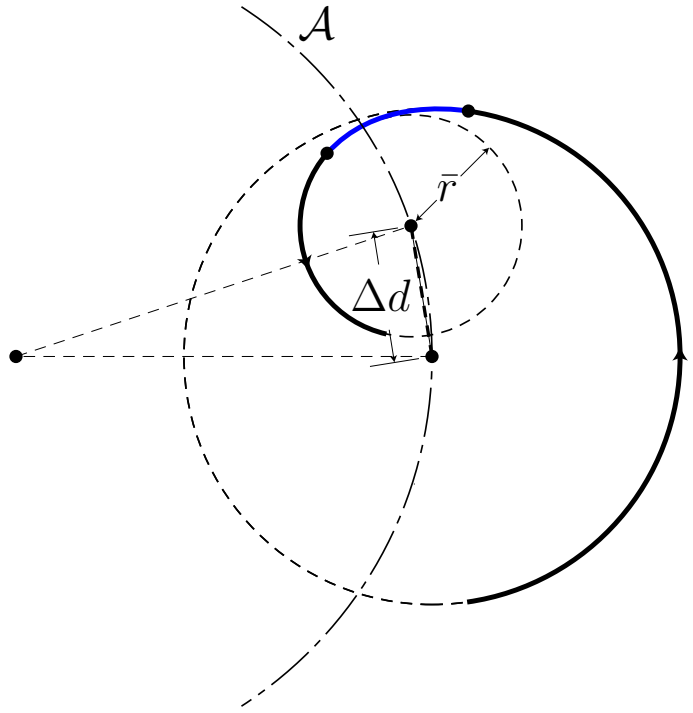

Figure 3.10: A clothoid connecting a pair of alternating circular arcs of radius 1 and $\bar{r}$.

Let t_1 and t_2 be the times at which the clothoid meets the circular arcs of radius 1 and radius $\bar{r}$, respectively. Since $u(t) = mt$ for the clothoid and since the control $u(t)$ equals 1 at $t = t_1$ and $\bar{r}^{-1}$ at $t = t_2$,

$$t_1 = m^{-1} \quad \text{and} \quad t_2 = m^{-1}\bar{r}^{-1}. \tag{3.12}$$

Since the centers of curvature $u(t)$ of the clothoid at $t = t_1$ and $t = t_2$ are the centers of alternating arcs, it follows from (3.10) that

$$\begin{aligned}&\Delta d\\&= \sqrt{m^2\left(\bar{r}\cdot C_I\left(m^{-1}\bar{r}^{-1}\right) - C_I\left(m^{-1}\right)\right)^2 + \left(m\left(\bar{r}\cdot S_I\left(m^{-1}\bar{r}^{-1}\right) - S_I\left(m^{-1}\right)\right) + \bar{r} - 1\right)^2}.\end{aligned} \tag{3.13}$$

Therefore, the behavior of Δd depends only on the radius $\bar{r}$.

By the results in Meek and Walton (1989), there is a one-to-one correspondence between $\bar{r}$ and Δd for all $\bar{r}$ in $\left[\max\left\{r,\, 1/\sqrt{m^2+1}\right\},\, 1\right)$. Note that $r \leq \bar{r} < 1$. Thus, the clothoid connecting two circular arcs of radius 1 and radius $\bar{r}$ whose centers are at a distance Δd can be uniquely characterized by each value of $\bar{r}$ in $\left[\max\left\{r,\, 1/\sqrt{m^2+1}\right\},\, 1\right)$. This follows from the fact that the geometry of this clothoid depends only on $\bar{r}$ for given m. Furthermore, the geometry of this clothoid can be employed for any alternating circular arcs of radius 1 and radius $\bar{r}$ in $\left[\max\left\{r,\, 1/\sqrt{m^2+1}\right\},\, 1\right)$ because its geometry does not depend on the choice of coordinate system. Therefore, if all centers of alternating circular arcs of radius 1 and radius $\bar{r}$ in $\left[\max\left\{r,\, 1/\sqrt{m^2+1}\right\},\, 1\right)$ lie on a reference arc $\mathcal{A}$ or the line segment $\overline{PQ}$ at a distance Δd given by (3.13), then there exists a unique clothoid joining each pair of these alternating circular arcs so that at each juncture point the curve has the same tangent vector and control $u(t)$ (i.e., curvature) as the corresponding circular arc (Figure 3.11). Using the preceding results, we obtain the following theorem:

Theorem III.3. *There exists an admissible path $(x,\, y)$ from an initial oriented point $(x_0,\, y_0,\, \phi_0)$ to a final oriented point $(x_T,\, y_T,\, \phi_T)$ subject to constraints (i)-(iii) and (vi).*

A concatenation of a circular arc with radius 1, a clothoid arc with m, a circular arc with radius $\bar{r}$ and a clothoid arc with $-m$ is such an admissible path that correspond

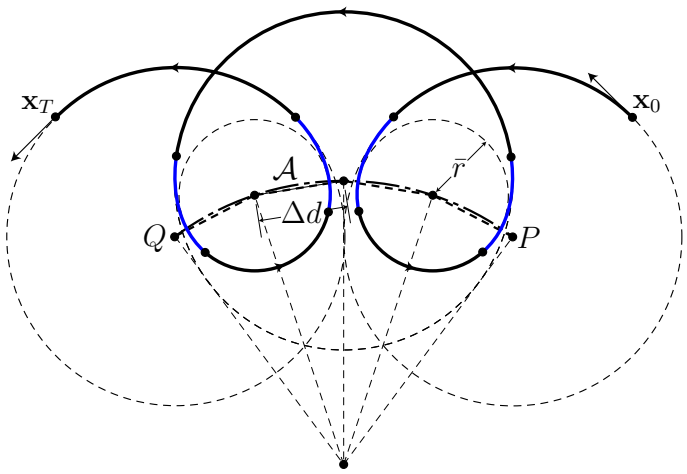

Figure 3.11: A concatenation of a circular arc with radius 1, a clothoid arc with m, a circular arc with radius $\bar{r}$ and a clothoid arc with $-m$

to the constant controls $v \equiv 0$, $v \equiv m$, $v \equiv 0$ and $v \equiv -m$, respectively, as shown in Figure 3.12. At each juncture point, $v(t)$ switches between 0 and m or between $-m$ and 0. The control $u(t)$ (i.e., the curvature) is a constant function for $v \equiv 0$ and a linear function of the path's length for $v \equiv \pm m$. It follows that the curvature $u(t)$ and angle $\phi(t)$ are continuous.

Figure 3.13 illustrates example concatenations of a circular arc with radius 1 and alternating clothoid arcs with curvature slope of $\pm m$ joined by a circular arc with radius $\bar{r}$ for different m. In both these figures, initial state $\mathbf{x}_0$ is given by $\mathbf{x}_0 = (x_0, y_0, \phi_0) = (4, 4, 2\pi/3)$, the final state $\mathbf{x}_T$ is given by $\mathbf{x}_T = (x_T, y_T, \phi_T) = (0, 0, 3\pi/2)$, and $r = 1/4$. Note that the maximum radius of curvature is assumed to be 1. In Figure 3.13 (a) and (b), m equals 10, and thus we can find a unique clothoid joining the each pair of alternating circular arcs of radius 1 and radius $\bar{r}$ in the interval $\left[\max\left\{r, 1/\sqrt{m^2+1}\right\}, 1\right) = [r, 1)$. For $\bar{r} = r$, all centers of these arcs lie on a reference arc $\mathcal{A}$ at a distance $\Delta d = 7.39 \times 10^{-1}$ and the number n of basic pairs is 3. Note that $\Delta d < 1 - r$. As m is decreased to 2, as shown in Figure 3.13 (c) and (d), the interval $\left[\max\left\{r, 1/\sqrt{m^2+1}\right\}, 1\right)$ becomes $\left[1/\sqrt{m^2+1}, 1\right)$. Thus, the end point $1/\sqrt{m^2+1}$ approaches 1 as m approaches 0. Note that the clothoid may

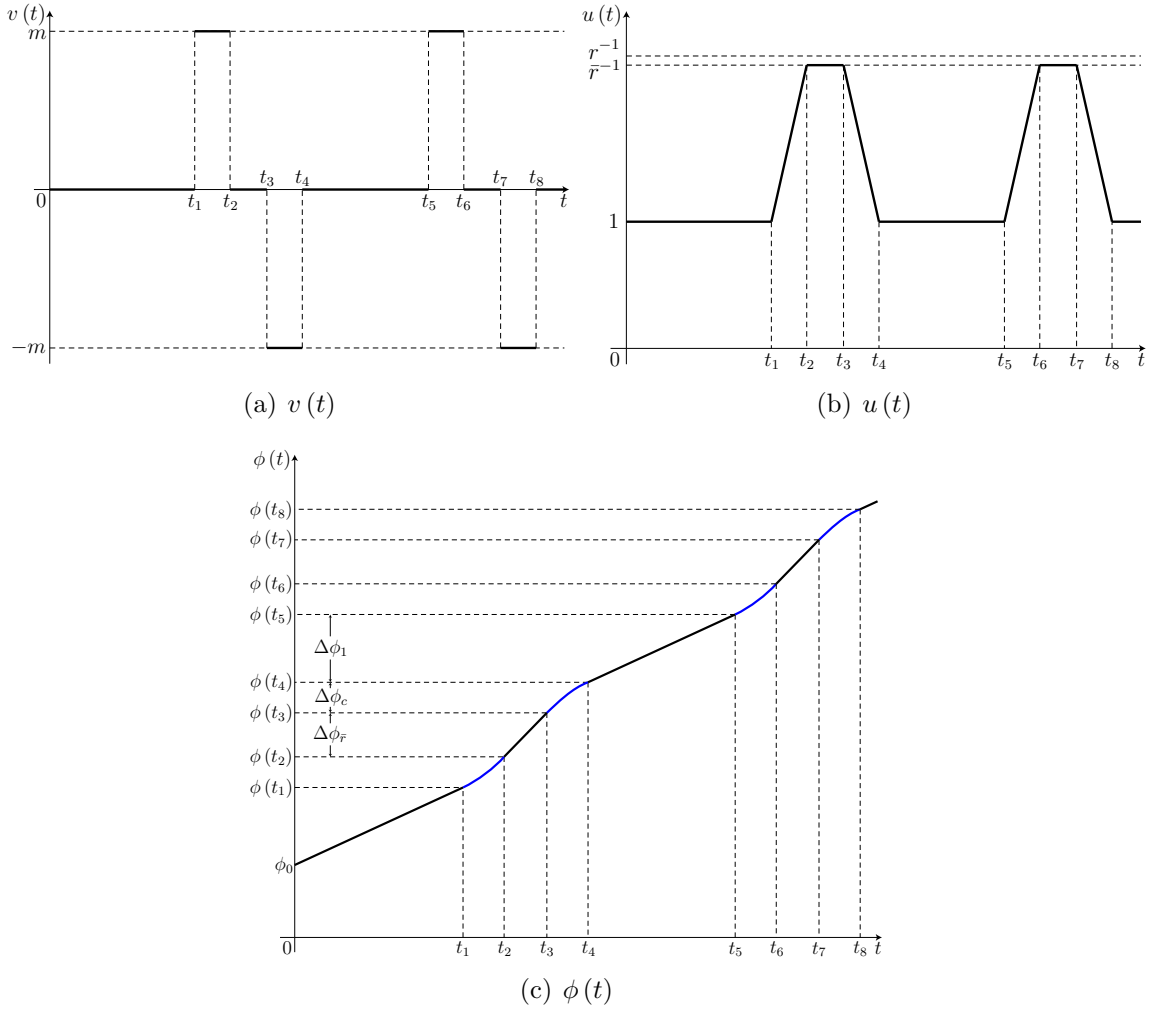

(a) $v(t)$ (b) $u(t)$

(c) $\phi(t)$

Figure 3.12: $v(t)$, $u(t)$ and $\phi(t)$.

be not uniquely determined for alternating circular arcs of radius 1 and radius r. For $\bar{r} = 1/\sqrt{m^2+1} = 1/\sqrt{5}$, the distance Δd is decreased to 5.33×10^{-1} and the number n is increased to 4.

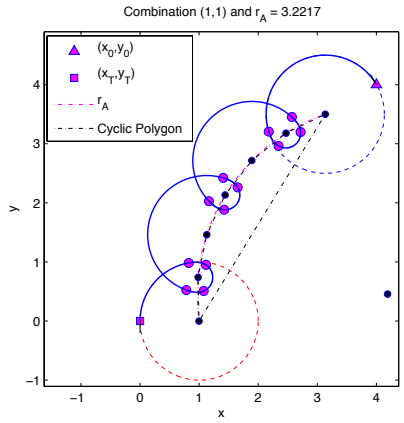

(a) An admissible path for $m = 10$.

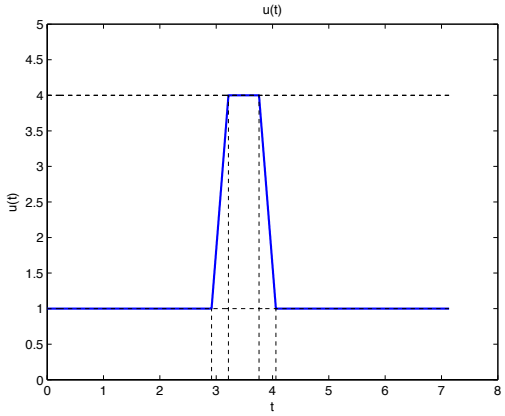

(b) $u(t)$ for $m = 10$.

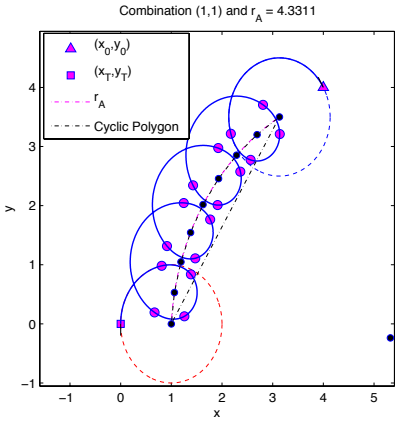

(c) An admissible path for $m = 2$

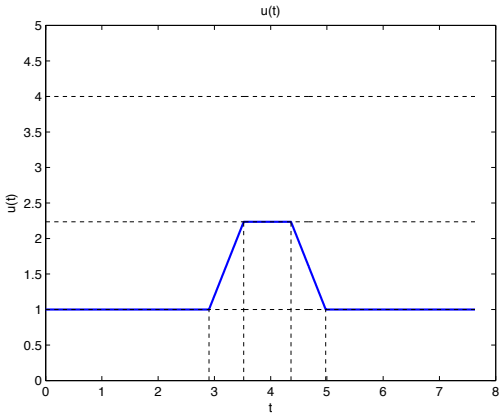

(d) $u(t)$ for $m = 2$

Figure 3.13: Concatenations of a circular arc with radius 1 and alternating clothoid arcs with $\pm m$ joined by a circular arc with radius $\bar{r}$ from $\mathbf{x}_0 = (x_0, y_0, \phi_0) = (4, 4, 2\pi/3)$ to $\mathbf{x}_T = (x_T, y_T, \phi_T) = (0, 0, 3\pi/2)$ for different m.

3.7 Existence of Optimal Paths for Unidirectional Dubins Vehicles.

In this section, we demonstrate the existence of optimal paths for unidirectional Dubins vehicles using Filippov's theorem II.1. In the preceding sections, we showed the existence of admissible paths for the unidirectional Dubins car and airplane given two oriented points $\mathbf{x}_0$ and $\mathbf{x}_T$. Moreover, the systems (2.3) and (2.10) are continuous functions of t, $\mathbf{u}$, $\mathbf{x}$ and a continuously differentiable function of $\mathbf{x}$. Thus, it suffices to show that conditions (2) and (3) in Filippov's theorem II.1 hold for the unidirectional Dubins car and airplane.

We first consider the unidirectional Dubins car. We verify condition (2) as follows. Let $C = \sqrt{1 + 1/r^2}/2$. Then $C > 0$ and

$$\begin{aligned}\langle \mathbf{x}, f(t, \mathbf{x}, \mathbf{u})\rangle &\leq \|\mathbf{x}\| \cdot \|f(t, \mathbf{x}, \mathbf{u})\| \leq 1/2 \|f(t, \mathbf{x}, \mathbf{u})\| \left(1 + \|\mathbf{x}\|^2\right) \\ &\leq \sqrt{1 + 1/r^2}/2 \left(1 + \|\mathbf{x}\|^2\right) = C\left(1 + \|\mathbf{x}\|^2\right)\end{aligned}$$

where f is system (2.3). For condition (3), since the control region $U = [1, r^{-1}]$ is bounded and closed, U is compact. Furthermore, it follows from the continueity of f in the u variable, the image set described by f is convex for all t and $\mathbf{x}$. By Filippov's theorem II.1, we conclude with the following theorem:

Theorem III.4. *There exists an optimal path (x, y) from an initial oriented point (x_0, y_0, ϕ_0) to a final oriented point (x_T, y_T, ϕ_T) subject to constraints (i)-(iii) (on page 26).*

We next consider the unidirectional Dubins airplane. For condition (2), let $C = \sqrt{1 + v_{\max}^2 + 1/r^2}/2$. Then $C > 0$ and

$$\begin{aligned}\langle \mathbf{x}, f(t, \mathbf{x}, \mathbf{u})\rangle &\leq \|\mathbf{x}\| \cdot \|f(t, \mathbf{x}, \mathbf{u})\| \leq 1/2 \|f(t, \mathbf{x}, \mathbf{u})\| \left(1 + \|\mathbf{x}\|^2\right) \\ &\leq \sqrt{1 + v_{\max}^2 + 1/r^2}/2 \left(1 + \|\mathbf{x}\|^2\right) = C\left(1 + \|\mathbf{x}\|^2\right)\end{aligned}$$

where f is system (2.10). Thus, condition (2) holds for the unidirectional Dubins airplane. Since f is continuous in the u and v variables, the image set described by f is convex for all t and $\mathbf{x}$. By Filippov's theorem II.1, we also conclude with the following theorem:

Theorem III.5. *There exists an optimal path* $(x,\ y,\ z)$ *from an initial oriented point* $(x_0,\ y_0,\ z_0,\ \phi_0)$ *to a final oriented point* $(x_T,\ y_T,\ z_T,\ \phi_T)$ *subject to constraints (i)-(v).*

3.8 Conclusion

This chapter has presented admissible paths for an object moving at a constant horizontal speed. The object's path are subject to the turn rate bounded on an interval whose end points are either both positive or both negative and the vertical rate bounded by its maximum rate. For simplicity, the turn and vertical rates are independent of each other. These admissible paths can be used as emergency landing trajectories for cases where steady straight flight is not possible.

For the unidirectional Dubins car, admissible paths generated by extremal controls are concatenations of alternating circular arcs of two different radii at every switching point. For the unidirectional Dubins airplane, admissible paths are concatenations of alternating circular helices of two different radii with constant vertical (climb/descent) rate. The concatenations for unidirectional Dubins vehicles exist. Using Filippov's theorem, we showed the existence of optimal paths for the unidirectional Dubins car and airplane.

In this chapter, we developed efficient algorithms for generating admissible paths joining an initial state with a final state. Both algorithms are applied to find emergency landing trajectories. These algorithms have real-time performance and completeness.

CHAPTER IV

Time-Optimal Paths for Unidirectional Dubins Cars

4.1 Introduction

This chapter characterizes minimum-length paths for a unidirectional Dubins vehicle that can only follow paths comprised of unidirectional (clockwise or counterclockwise) turns. Recall that Dubins paths specify shortest paths comprised of at most three segments, each of which is either a line segment or a circular arc with minimum radius. This chapter extends the Dubins formulation to consider cases in which bounds on curvature are either both positive or both negative. Thus, the turns are either always clockwise or always counterclockwise.

Variations of the Dubins problem have been studied over a wide range of motion planning applications. Reeds and Shepp (1990) conducted a similar study for a vehicle with forward and backward motions, identifying shortest-length paths with cusps. Balkcom and Mason (2002) extended the Dubins problem to consider the differential drive (i.e., two independently driven coaxial wheels), which yielded time-optimal paths with at most three straight segments and two turns. Balkcom et al. (2006) characterized time-optimal paths for a robot capable of instantaneously moving in any direction. Chitsaz and LaValle (2007) derived necessary conditions for time-optimal

paths of the Dubins airplane with independently bounded climb (or descent) and turn rates. Salaris et al. (2010) and (2012) presented a complete characterization for length-optimal paths of the unicycle with field-of-view constraints and visibility constraints. Bakolas and Tsiotras (2011) modified the Dubins problem to allow different minimum radii for clockwise versus counterclockwise turns. Dolinskaya and Maggiar (2012) characterized time-optimal paths for the Dubins vehicle with the speed function depending on the direction and the minimum-turning radius function.

All these existing solutions presume a vehicle has the ability to follow a straight path and turn in both directions. Under the unidirectional turning constraint motivated above, a new solution is required. We employ Pontryagin's minimum principle to characterize the length-optimal path for a unidirectional Dubins vehicle. This principle has previously been applied to solve a number of path planning problems, as discussed previously in Chapter II.

The chapter is organized as follows. Section 4.2 applies the minimum principle of Pontryagin to characterize length-optimal paths subject to prescribed initial and final conditions. Section 4.3 enumerates the geometric properties of the identified extremal paths given arbitrary boundary conditions. Section 4.4 presents algorithms to find the optimal path using these properties and provides example solution paths. Section 4.5 analyzes algorithm efficiency and optimal solution properties.

4.2 Necessary Conditions for Optimality

Given two points (x_0, y_0) and (x_T, y_T) in $\mathbb{R}^2$ with corresponding directions ϕ_0 and ϕ_T, we want to find a continuous and piecewise $\mathcal{C}^2$

path (x, y) of minimal length subject to the following constraints:

(i) The radius of curvature lies between r and 1 where $0 < r < 1$. The reciprocal of the radius, called the control (or the curvature) and denoted u, is also bounded

on control region U. Since a path is continuous and piecewise $\mathcal{C}^2$, the control is piecewise continuous.

(ii) The sign of the curvature remains unchanged. Therefore, the control region U is $[1,\, r^{-1}]$. The case $U = [-r^{-1},\, -1]$ can be treated similarly to $U = [1,\, r^{-1}]$.

(iii) The path $(x,\, y)$ has unit speed. Even if the path has non-zero constant speed, the path has a unit-speed reparametrization (do Carmo (1976)), and thus the path with unit speed produces no loss of generality.

Under these constraints, a path $(x,\, y)$ is a solution of the system of differential equations

$$\begin{aligned} \dot{x}\,(t) &= \cos\phi\,(t)\,, \\ \dot{y}\,(t) &= \sin\phi\,(t)\,, \\ \dot{\phi}\,(t) &= u\,(t) \in U. \end{aligned} \tag{4.1}$$

Let $\mathbf{x} = (x\,(t)\,,\, y\,(t)\,,\, \phi\,(t))$. Then the boundary conditions are

$$\mathbf{x}\,(0) = (x_0,\, y_0,\, \phi_0) \triangleq \mathbf{x}_0 \text{ and } \mathbf{x}\,(T) = (x_T,\, y_T,\, \phi_T) \triangleq \mathbf{x}_T, \tag{4.2}$$

where $\phi\,(t)$ is the angle between unit tangent vector $(\dot{x},\, \dot{y})$ and the x-axis and is a real number modulo 2π. The cost to be minimized is the length of the path $(x\,(t)\,,\, y\,(t))$ from 0 to T given by

$$J\,(u) = \int_0^T dt = T.$$

Therefore, our problem becomes a time-optimal problem.

We now characterize the necessary conditions for the path $(x,\, y)$ of minimal length using Pontryagin's minimum principle in Section 2.3. Let ψ_1, ψ_2 and ψ_3 be the adjoint variables corresponding to x, y and ϕ, respectively. The Hamiltonian is then defined

by

$$H(\psi, \mathbf{x}, u) = \psi_1 \cos\phi + \psi_2 \sin\phi + \psi_3 u,$$

where $\psi = (\psi_1, \psi_2, \psi_3)$, and the adjoint system is defined by

$$\begin{aligned} \dot{\psi}_1(t) &= -\frac{\partial H}{\partial x} = 0, \\ \dot{\psi}_2(t) &= -\frac{\partial H}{\partial y} = 0, \\ \dot{\psi}_3(t) &= -\frac{\partial H}{\partial \phi} = \psi_1 \sin\phi(t) - \psi_2 \cos\phi(t). \end{aligned} \tag{4.3}$$

Therefore, ψ_1 and ψ_2 are constant on $[0, T]$. To state our results in a more intuitive form, we introduce the notations λ and θ defined by $\lambda = \sqrt{\psi_1^2 + \psi_2^2} \geq 0$ and $\theta = \tan^{-1}(\psi_2/\psi_1) \in (-\pi/2, \pi/2]$, respectively. Note that $\theta = \pi/2$ when $\psi_1 = 0$. Then the Hamiltonian and system (4.3) become

$$\begin{aligned} H &= \lambda \cos(\phi - \theta) + \psi_3 u, \\ \dot{\psi}_3 &= \lambda \sin(\phi - \theta). \end{aligned} \tag{4.4}$$

By Pontryagin's minimum principle, if the trajectory $\mathbf{x}(t)$ determined by $u(t) \in U$ is time-optimal, then there exists a non-zero continuous solution $\psi = (\psi_1, \psi_2, \psi_3)$ such that

(1) The control $u(t)$ minimizes the Hamiltonian at every time t; that is,

$$H(\psi(t), \mathbf{x}(t), u(t)) = \min_{z \in U} H(\psi(t), \mathbf{x}(t), z).$$

(2) $H(\psi, \mathbf{x}(t), u(t))$ is constant, and

$$H(\psi(t), \mathbf{x}(t), u(t)) \leq 0.$$

It follows from condition (1) that $\psi_3(t)\,u(t) \leq \psi_3(t)\,\xi(t)$ for all piecewise continuous $\xi(t)$ and for all t in $[0,\, T]$. Since there is no open interval on which $\psi_3(t) = 0$, the optimal control is

$$u(t) \triangleq u_{\min}(\psi_3(t)) = \begin{cases} 1 & \text{if } \psi_3(t) > 0, \\ r^{-1} & \text{if } \psi_3(t) \leq 0. \end{cases} \tag{4.5}$$

Accordingly,

$$\psi_3(t) \cdot u_{\min}(\psi_3(t)) = H - \lambda \cos(\phi(t) - \theta).$$

For $\lambda = 0$, it follows that $\psi_3(t)$ is constant and non-positive. Since $\psi(t) \neq 0$, $\psi_3(t)$ is negative. Thus, $u \equiv r^{-1}$. For $\lambda > 0$, the minimum principle remains invariant when the adjoint vector is multiplied by λ. Therefore, we can hereafter assume without loss of generality that $\lambda = 1$. Then system (4.4) can be simplified to

$$\begin{aligned} \dot{\psi}_3(t) &= \sin(\phi(t) - \theta), \\ \psi_3(t) \cdot u_{\min}(\psi_3(t)) &= H - \cos(\phi(t) - \theta). \end{aligned} \tag{4.6}$$

For $H \leq -1$, it follows that $\psi_3(t) \leq 0$ and $u \equiv r^{-1}$, that is, the same possible result as when $\lambda = 0$. Thus, hereafter we only consider $-1 \leq H \leq 0$. Since $u(t) \geq 1$, it follows that $\phi(t)$ is strictly increasing and there is a one-to-one correspondence between t and $\phi(t)$ for all t. For $-1 < H \leq 0$, the variation in $\psi_3(t) \cdot u_{\min}(\psi_3(t))$ versus $\phi(t)$ is illustrated in Figure 4.1. In Figure 4.1, $\psi_3(t_1) = \psi_3(t_2) = 0$. Thus, $\psi_3(t)$ changes sign from negative to positive at t_1 and from positive to negative at t_2. This follows from the fact that $\dot{\psi}_3(t_1) > 0$ and $\dot{\psi}_3(t_2) < 0$. Therefore, extremal $u(t)$ changes magnitude from r^{-1} to 1 at t_1 and from 1 to r^{-1} at t_2. It is clear that $u(t) = 1$ for $t_1 < t < t_2$ and $u(t) = r^{-1}$ for $t_2 < t < t_3$. Since $\psi_3(t_1) = \psi_3(t_2) = \psi_3(t_3) = 0$

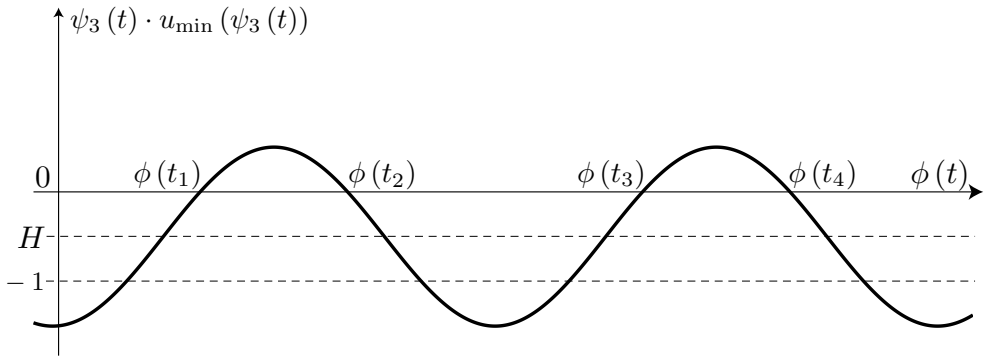

Figure 4.1: $\psi_3(t) \cdot u_{\min}(\psi_3(t))$ for $H = -0.5$.

and $\phi(t)$ is strictly increasing,

$$\phi(t_2) - \phi(t_1) = \Delta\phi \quad \text{and} \quad \phi(t_3) - \phi(t_2) = 2\pi - \Delta\phi. \tag{4.7}$$

where $\Delta\phi \triangleq 2\cos^{-1}(-H)$. Consequently, $t_2 - t_1 = \Delta\phi$ and $t_3 - t_2 = r(2\pi - \Delta\phi)$. For $-1 \leq H \leq 0$, $0 \leq \Delta\phi \leq \pi$. Note that $u \equiv r^{-1}$ when $H = -1$ or $\Delta\phi = 0$. It is also clear that $\phi(t_3) - \phi(t_1) = 2\pi$.

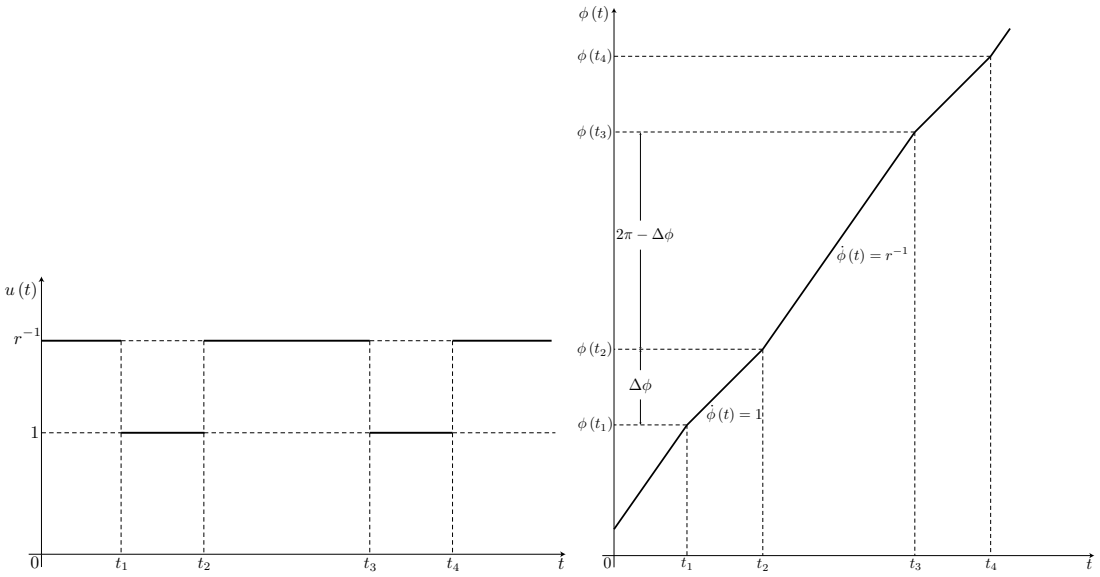

(a) $u(t)$ (b) $\phi(t)$

Figure 4.2: $\phi(t)$ and $u(t)$.

Since the variation in $\psi_3(t) \cdot u_{\min}(\psi_3(t))$ versus $\phi(t)$ has period 2π, the above

argument can also be applied for $t > t_3$. As shown in Figure 4.2, $u(t)$ is a periodic function with values 1 and r^{-1} and $\phi(t)$ is a periodic function with modulo 2π. Since $\Delta\phi \triangleq 2\cos^{-1}(-H)$, there is a one-to-one correspondence between H and $\Delta\phi$ for $-1 \leq H \leq 0$. Therefore, either of these variables together with θ can be used to characterize the family of extremal controls. Note that θ, as seen from (4.6), corresponds to shifting the extremal $u(t)$ in time and $-\pi < \theta \leq \pi$.

Now we can geometrically characterize the path generated by extremal controls. Control $u(t)$ is a periodic switching function whose values are 1 and r^{-1}. Paths which correspond to the constant controls $u \equiv 1$ and $u \equiv r^{-1}$ are circular arcs of radius 1 and radius r, respectively. These circular arcs of radius 1 and radius r have lengths $\Delta\phi$ and $r(2\pi - \Delta\phi)$, respectively, as shown in Figure 4.3. In addition, these circular arcs have a common tangent vector where $u(t)$ switches between 1 and r^{-1}. This follows from the fact that $\phi(t)$ is a continuous function that defines the direction of the tangent vector. Since $u(t)$ is periodic, extremal controls produce a concatenation of alternating circular arcs of radius 1 and r. The preceding results are summarized in the following theorem:

Theorem IV.1. *The planar paths generated by extremal controls are concatenations of alternating circular arcs of radius* 1 *and* r. *The concatenation has the following properties:*

(1) It is smooth in the sense that at juncture points of the concatenation the two circles have a common tangent vector.

(2) The angular path change for all circles of radius 1 *is* $\Delta\phi$ *where* $0 \leq \Delta\phi \leq \pi$.

(3) The angular path change for all circles of radius r *is* $2\pi - \Delta\phi$.

Note that $u \equiv r^{-1}$ for $\Delta\phi = 0$. A pair of circular arcs of radius 1 and r having the above properties of the concatenation will be referred to as a *basic pair* of circular

arcs of radius 1 and r. This basic pair has length $\Delta T \triangleq (1-r)\,\Delta\phi + 2r\pi$. The distance between the beginning and ending points of this pair equals

$$\Delta d \triangleq 2\,(1-r)\sin\left(\Delta\phi/2\right), \tag{4.8}$$

as shown in Figure 4.3.

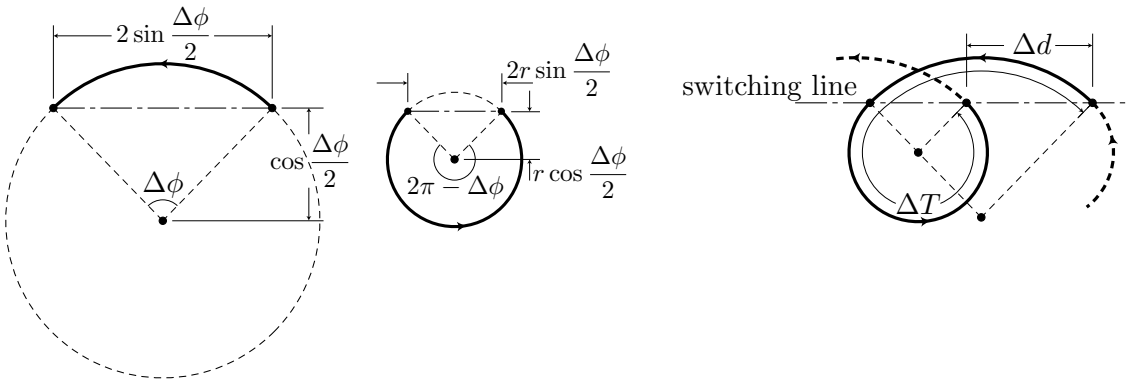

(a) A circular arc of radius 1

(b) A circular arc of radius r

(c) The concatenation of alternating circular arcs of radius 1 and r (A basic pair appears in solid line and its adjoining arcs of radius 1 and r appear in dotted line.)

Figure 4.3: Circular arcs of radius 1 and radius r.

As illustrated in Figure 4.3, all circular arcs have juncture points that lie on a common "secant line". At these juncture points, $\psi_3(t)$ changes sign, so extremal $u(t)$ switches between 1 and r^{-1}. This secant line will be called the *switching line* and denoted by L. This follows from the fact that $\phi(t)$ defines the direction of the tangent vector and the adjoint system is defined by (4.3). From this fact, θ is the angle between the switching line L and the x-axis. Since the distances between L and circle centers of radius 1 and between L and circle centers of radius r are constant, the locus of circle centers for radius 1 and the locus of circle centers for radius r are parallel to the switching line, and denoted by L_1 and L_r, as shown in Figure 4.4.

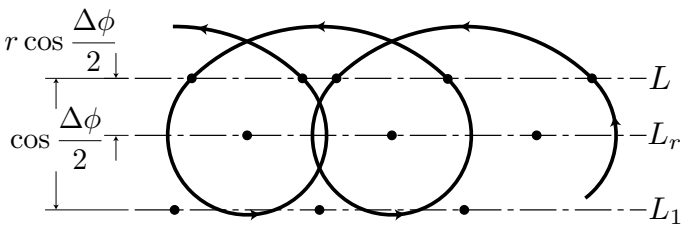

Figure 4.4: L, L_r and L_1.

4.3 Geometric Interpretation of Switching Lines

In this section, we describe the geometric properties of extremal paths. For simplicity, only the case $u(t) > 0$ is considered. By Pontryagin's minimum principle, extremal paths are concatenations of alternating circular arcs of radius 1 and r. Their initial and final segments are circular arcs of radius 1 or r. Thus, given an initial state $\mathbf{x}_0$ and a final state $\mathbf{x}_T$, we can draw two possible circular arcs that lead away from the initial state and two possible circular arcs that lead into the final state. Since we have two possible initial circular arcs and two possible final circular arcs, we have four possible combinations of initial arc and final arc. Each combination is determined by the values of the externals at $t = 0$ and $t = T$. Thus we will refer to a combination as an ordered pair $(u(0), u(T))$.

Given any combination $(u(0), u(T))$, we seek to find points at which the extremal $u(t)$ switches between 1 and r^{-1}. All these points lie on the switching line L. Therefore, the first point is the intersection of L and the initial arc with radius $u^{-1}(0)$. At this intersection, the initial arc and arc following it have a common tangent vector. According to Theorem IV.1, the next arc also intersects L if $0 < \Delta\phi \leq \pi$. By repeatedly finding these intersection points, the concatenation of alternating circular arcs can be constructed. Note that if $\Delta\phi = 0$, then $u \equiv r^{-1}$; it follows that all intersection points are the same.

We now construct the switching line L for each combination $(u(0), u(T))$. It will be seen that each switching line L is uniquely characterized by $\Delta\phi \in [0, \pi]$. For

each combination $(u(0), u(T))$ of initial and final arcs, the center of each respective arc lies on either of the loci L_1 or L_r depending on which of the four combinations is considered. Since the distances between the switching line L and the loci L_1 and L_r are $\cos(\Delta\phi/2)$ and $r\cos(\Delta\phi/2)$, respectively, the switching line L is a common external tangent line to two circles of radii $u^{-1}(0)\cos(\Delta\phi/2)$ and $u^{-1}(T)\cos(\Delta\phi/2)$, as indicated in Figure 4.5. One of these two circles has the same center as the initial circular arc, and the other has the same center as the final circular arc. Note that $u^{-1}(t)$ represents the reciprocal of the control (or the curvature) and is either r or 1.

Let P and Q be two centers of the initial circular arc and the final circular arc, respectively. For $u(0) = u(T)$, P and Q both lie either on L_1 or L_r, and thus the line through P and Q is parallel to the loci L_1 and L_r. For two circles with centers P and Q with radii $u^{-1}(0)\cos(\Delta\phi/2)$, their common external tangent line (i.e., L) is parallel to the line passing through P and Q. Therefore, for $u(0) = u(T)$, the switching line L is a line obtained by translating the line passing through P and Q by a vector which has magnitude $u^{-1}(0)\cos(\Delta\phi/2)$ and is formed by rotating $\overrightarrow{PQ}$ by $-\pi/2$ (Figure 4.5 (a)).

For $u(0) \neq u(T)$, two centers P and Q lie on different loci L_1 and L_r (i.e., one is on L_1, the other on L_r). For two circles with centers P and Q and with radii $u^{-1}(0)\cos(\Delta\phi/2)$ and $u^{-1}(T)\cos(\Delta\phi/2)$, their common external tangent line (i.e., L) passes through their external center of similitude, denoted by S. As illustrated in Figure 4.5, the external center S of similitude is a fixed point on the line passing through P and Q which makes an angle α with L given by

$$\alpha = \sin^{-1}\left(\frac{u^{-1}(0) - u^{-1}(T)}{\left|\overline{PQ}\right|}\cos\frac{\Delta\phi}{2}\right), \tag{4.9}$$

where $\left|\overline{PQ}\right|$ is the length of the line segment $\overline{PQ}$. Therefore, for $u(0) \neq u(T)$, the switching line L is a line obtained by rotating the line passing through P and Q

through an angle α in the xy-plane (Figure 4.5 (b)).

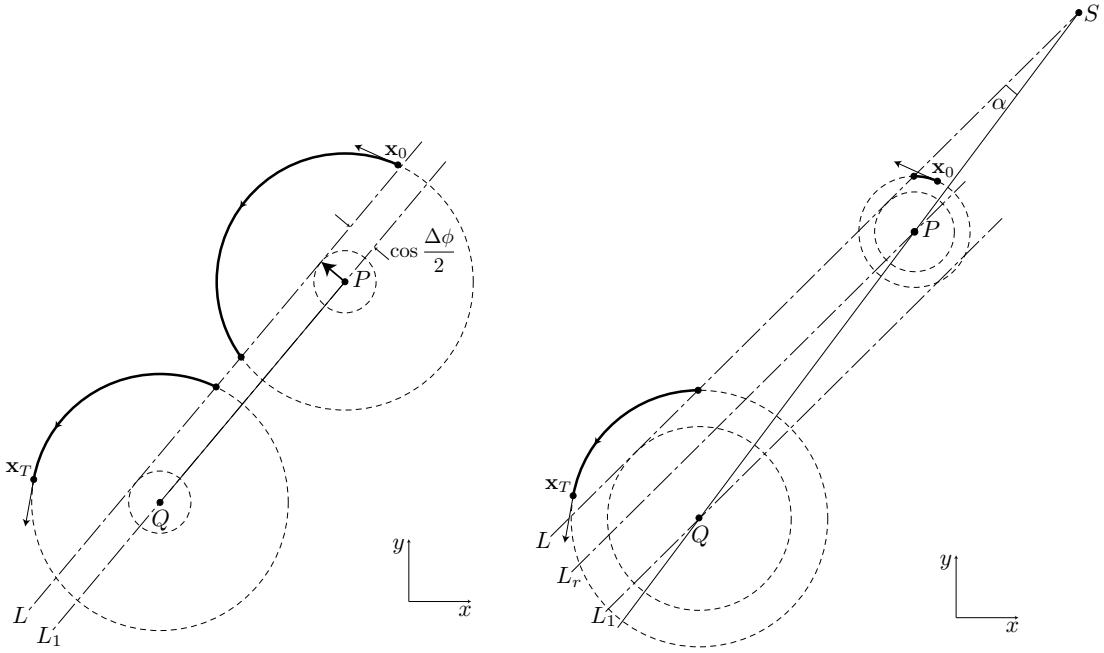

(a) A combination $(u(0), u(T)) = (1, 1)$. (b) A combination $(u(0), u(T)) = (r^{-1}, 1)$.

Figure 4.5: The construction of switching line L.

Although the switching lines are uniquely determined for all values of $\Delta\phi$, not every switching line generates an extremal path having the properties of Theorem IV.1. Let I denote the set of values for $\Delta\phi$ where the conditions of Theorem IV.1 are met. We obtain the determination of I by considering each of the four combinations for $(u(0), u(T))$.

Since $\dot{x} = \cos\phi$ and $\dot{y} = \sin\phi$ in (4.1), it follows from (4.3) that $\dot{\psi}_3 = \psi_1\dot{y} - \psi_2\dot{x}$ where ψ_1 and ψ_2 are constant on $[0, T]$. Then there is a constant $c \in \mathbb{R}$ such that

$$\psi_3(t) = \psi_1 y(t) - \psi_2 x(t) + c \tag{4.10}$$

for $0 \leq t \leq T$. In the above equation, the right-hand side represents the signed distance from a point $(x(t), y(t))$ to the switching line L. This follows from the facts that $\psi_3 = 0$ on the switching line L. If $\psi_3(t) > 0$, that is, if $u(t) = 1$, then the

distance between $(x(t), y(t))$ and L must be nonnegative. Otherwise, the distance between $(x(t), y(t))$ and L must be nonpositive.

To illustrate the sign of the distance between $(x(t), y(t))$ and L, we define two regions divided by L. One of these two regions includes both L_r and L_1, and the other does not. For $u(t) = 1$, the positive distance between $(x(t), y(t))$ and L is equivalent to $(x(t)\ y(t))$ in the region without both L_r and L_1. For $u(t) = 0$, the negative distance between $(x(t), y(t))$ and L is equivalent to $(x(t)\ y(t))$ in the region with both L_r and L_1.

Let $\Delta\phi_t$ be $\Delta\phi$ in $[0, \pi]$ such that L characterized by $\Delta\phi$ contains $(x(t)\ y(t))$. If we can find $\Delta\phi_t$, L characterized by $\Delta\phi$ in $[\Delta\phi_t, \pi]$ is a nonnegative distance away from $(x(t), y(t))$ when $u(t) = 1$, and L characterized by $\Delta\phi$ in $[0, \Delta\phi_t]$ is a nonpositive distance away from $(x(t), y(t))$ when $u(t) = r^{-1}$. Otherwise, $u(t)$ must equal r^{-1}, that is, $u(t)$ cannot be 1. Depending on whether $\Delta\phi_0$ and $\Delta\phi_T$ exist, the possible values of $\Delta\phi$ can thus be evaluated for each combination $(u(0), u(T))$. See Table 1.

Table 4.1: The set I for each combination.

$(u(0), u(T))$	I
$(1, 1)$	If both $\Delta\phi_0$ and $\Delta\phi_T$ exist, set $I = [\Delta\phi_0, \pi] \bigcap [\Delta\phi_T, \pi]$. Otherwise, set $I = \emptyset$.
(r^{-1}, r^{-1})	If both $\Delta\phi_0$ and $\Delta\phi_T$ exist, set $I = [0, \Delta\phi_0] \bigcap [0, \Delta\phi_T]$. If only $\Delta\phi_0$ exists, set $I = [0, \Delta\phi_0]$. If only $\Delta\phi_T$ exists, set $I = [0, \Delta\phi_T]$. Otherwise, $I = [0, \pi]$.
$(1, r^{-1})$	If both $\Delta\phi_0$ and $\Delta\phi_T$ exist and $\Delta\phi_0 \leq \Delta\phi_T$, set $I = [\Delta\phi_0, \Delta\phi_T]$. If only $\Delta\phi_0$ exists, set $I = [\Delta\phi_0, \pi]$. Otherwise, $I = \emptyset$.
$(r^{-1}, 1)$	If both $\Delta\phi_0$ and $\Delta\phi_T$ exist and $\Delta\phi_0 \geq \Delta\phi_T$, set $I = [\Delta\phi_T, \Delta\phi_0]$. If only $\Delta\phi_T$ exists, set $I = [\Delta\phi_T, \pi]$. Otherwise, $I = \emptyset$.

Not all switching lines defined by each $\Delta\phi$ in I allow extremal paths to join the

initial state $\mathbf{x}_0$ with the final state $\mathbf{x}_T$. Thus, we next need to formulate the condition for extremal paths to satisfy boundary conditions $\mathbf{x}(0) = \mathbf{x}_0$ and $\mathbf{x}(T) = \mathbf{x}_T$. This condition will provide values of $\Delta\phi$ in I for defining such extremal paths.

Except for the initial and final circular arcs, the circular arcs are specified as basic pairs of length ΔT. Given an initial angle ϕ_0 and a final angle ϕ_T, it is obvious that each basic pair has a point of an extremal path with ϕ_T. This follows from the fact that the angular path change for each basic pair is 2π. The time at which the ith basic pair has a point with ϕ_T will be denoted by T_i. Although a pair of an initial arc and arc following it is not a basic pair, this pair will be considered as the first basic pair to include cases where the optimal path is a circular arc or a pair of initial and final arcs. This argument is also applied for a final arc. Then $T_{i+1} - T_i = \Delta T$ and the distance between two points at T_i and T_{i+1} equals Δd, as shown in Figure 4.6. Note that Δd is also the distance between the centers of two circular arcs with the same radius.

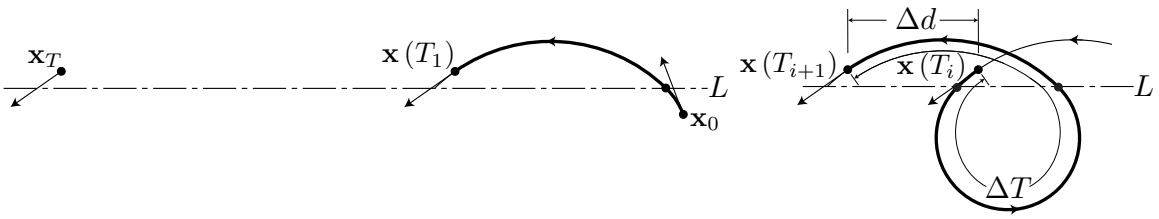

(a) T_1. (b) T_i and T_{i+1}.

Figure 4.6: T_1, T_i and T_{i+1}.

Given an initial state $\mathbf{x}_0$ and a final state $\mathbf{x}_T$, the line segment connecting $(x(T_1),$ $y(T_1))$ and (x_T, y_T) is parallel to the switching line L, as indicated in Figure 4.7. The distance of this line segment is denoted by $\mathcal{D}$. This follows from the fact that $\phi(T_1) = \phi_T$ and the loci L_1 and L_r are parallel to L. Moreover, the line segment connecting two points at T_i and T_{i+1} is also parallel to L and its length is Δd. Thus, the extremal path characterized by $\Delta\phi$ satisfies boundary conditions $\mathbf{x}(0) = \mathbf{x}_0$ and

$\mathbf{x}(T) = \mathbf{x}_T$ if

$$\mathcal{D} = (n-1)\,\Delta d \tag{4.11}$$

for some number n of basic pairs. (4.11) implies that $T = T_n = T_1 + (n-1)\,\Delta T$.

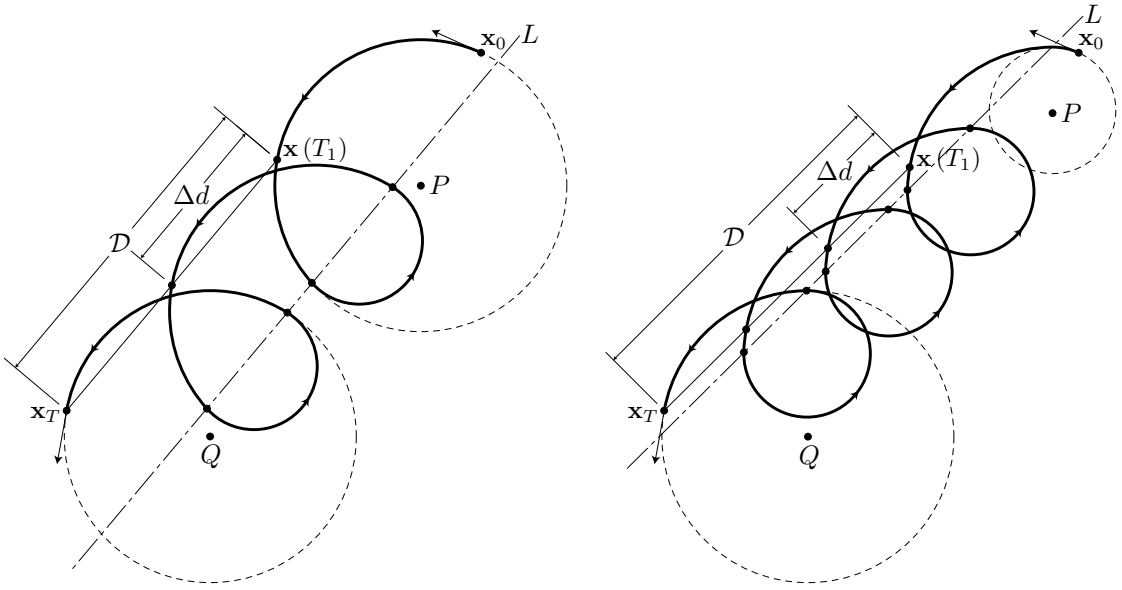

(a) A case where $u(0) = u(T) = 1$.

(b) A case where $u(0) = r^{-1}$ and $u(T) = 1$.

Figure 4.7: Paths satisfying the boundary conditions $\mathbf{x}(0) = \mathbf{x}_0$ and $\mathbf{x}(T) = \mathbf{x}_T$.

To evaluate the value of $\Delta\phi$ for which (4.11) holds, we derive a formula for $\mathcal{D}$ that involves $\left|\overline{PQ}\right|$. This formula together with (4.11) provides an exact value of $\Delta\phi$ for the given number n of basic pairs. For $u(0) = u(T)$, the initial and final circular arcs contain points of the extremal path at T_1 and T, respectively, as shown in Figure 4.8 (a). For $u(0) \neq u(T)$, the second circular arc (i.e., the arc following the initial arc) and the final arc contain the points of the extremal path at T_1 and T, respectively, as shown in Figure 4.8 (b). Since the tangent direction of the extremal path at T_1 is identical to that at T, $\mathcal{D} = \left|\overline{PQ}\right|$ for $u(0) = u(T)$ and $\mathcal{D} = \left|\overline{RQ}\right|$ for $u(0) \neq u(T)$ where R is the center of circular arc following the initial arc. When $u(0) \neq u(T)$, two centers P and Q and the intersection point of the line through Q and R with a perpendicular transversal of the loci L_1 and L_r, passing through P, form a right

triangle, as shown in Figure 4.8 (b). Thus,

$$\mathcal{D} = \begin{cases} \left|\overline{PQ}\right| & \text{if } u(0) = u(T) \\ \sqrt{\left|\overline{PQ}\right| - (1-r)^2 \cos^2(\Delta\phi/2)} & \\ \quad - \Delta d/2 & \text{if } u(0) \neq u(T) \end{cases} \tag{4.12}$$

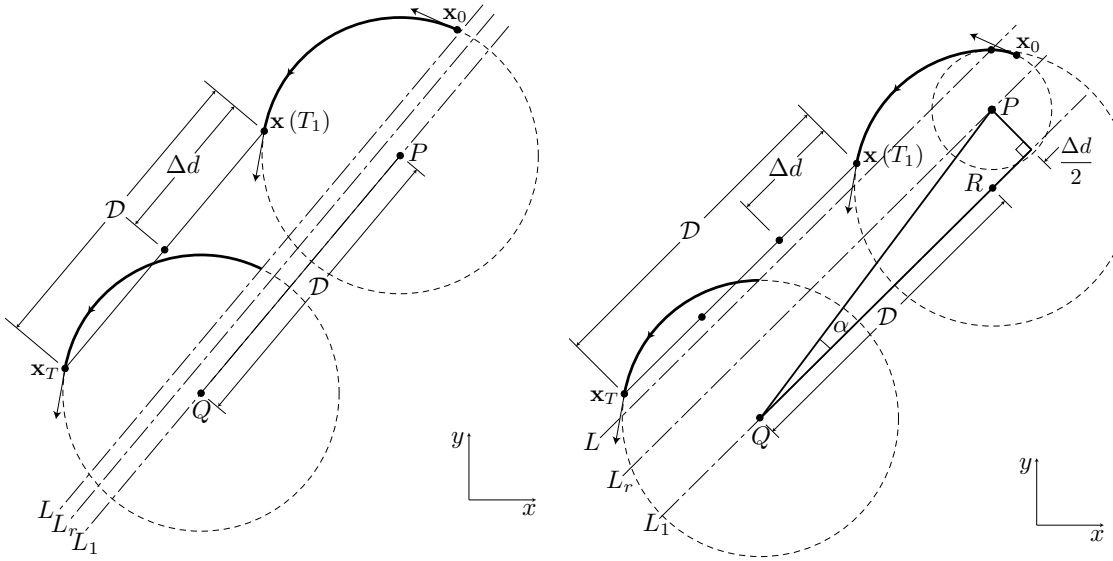

(a) A combination $(u(0), u(T)) = (1, 1)$. (b) A combination $(u(0), u(T)) = (r^{-1}, 1)$.

Figure 4.8: The distance between two points at T_1 and T.

4.4 Algorithm for Finding the Optimal Path

We now present an algorithm to determine the optimal path from an initial state $\mathbf{x}_0$ to a final state $\mathbf{x}_T$. This algorithm first determines extremal paths according to their geometric interpretations (Section 4.3) and then finds the one with the least time of transit which corresponds to minimal length. For each combination $(u(0), u(T))$, we define switching lines for extremal paths joining $\mathbf{x}_0$ with $\mathbf{x}_T$. The switching line can be characterized by a value of $\Delta\phi$ which is a function of the number n of basic pairs. Since each combination $(u(0), u(T))$ has its own domain I of possible values of $\Delta\phi$ and since n decreases as $\Delta\phi$ increases, the minimum number of basic pairs,

denoted n_m, can be evaluated by the supremum of I. The value of $\Delta\phi$ corresponding to n_m generates a switching line and thus an extremal path from $\mathbf{x}_0$ to $\mathbf{x}_T$.

The sequence of feasible extremal paths is then defined recursively by increasing n. This procedure is continued until the length of the current extremal path is greater than that of the previous extremal path or until $\Delta\phi$ determined by n is not in the domain I. This iterative process results in an extremal path with minimal length among all paths of the same combination. Consequently, we can have at most four candidate paths, one for each $(u(0), u(T))$, joining $\mathbf{x}_0$ with $\mathbf{x}_T$. By comparing the lengths of these paths, we can choose the shortest path from the initial state to the final state.

Algorithm 4.1 describes this procedure to find the optimal path connecting two oriented points $\mathbf{x}_0$ and $\mathbf{x}_T$. The algorithm first determines the two centers P and Q of the initial and final circular arcs for each of the four possible combinations (1, 1), (1, r^{-1}), (r^{-1}, r^{-1}) and (r^{-1}, 1). We consider as an example the combination (r^{-1}, 1), as shown in Figure 4.9 (b). Since we can only find a value $\Delta\phi_T$ such that the switching line characterized by this value contains the final point, $I = [\Delta\phi_T, \pi]$ as shown in Table 1. From the supremum of I (i.e., π), n_m can be evaluated, as stated in Step 3 of Algorithm 4.1. This follows from the fact that the number of basic pairs decreases as $\Delta\phi$ increases.

If $n_m = 1$, then the length T of the extremal path can be calculated directly from the geometry of each combination. When $u(0) = u(T)$, the initial and final circular arcs are the same. When $u(0) \neq u(T)$, the initial and final circular arcs must be tangent at the one point. As $n_m > 1$, (4.11) together with (4.12) provides a value of $\Delta\phi$ for n_m. The switching line L characterized by this value defines the extremal path from $\mathbf{x}_0$ to $\mathbf{x}_T$. This follows from the fact that every intersection point of L with a concatenation of alternating arcs is a point at which the extremal $u(t)$ switches. For combination (r^{-1}, 1), the values of $\Delta\phi$ are determined recursively by incrementing n,

and by using (4.11) and (4.12). Since the length of the extremal path with n_m basic pairs is less than that with $n_m + 1$ basic pairs in this case, the extremal path with n_m basic pairs has minimal length among all paths of combination $(r^{-1}, 1)$. A similar argument applies to the remaining combinations $(1, 1)$, $(1, r^{-1})$ and (r^{-1}, r^{-1}).

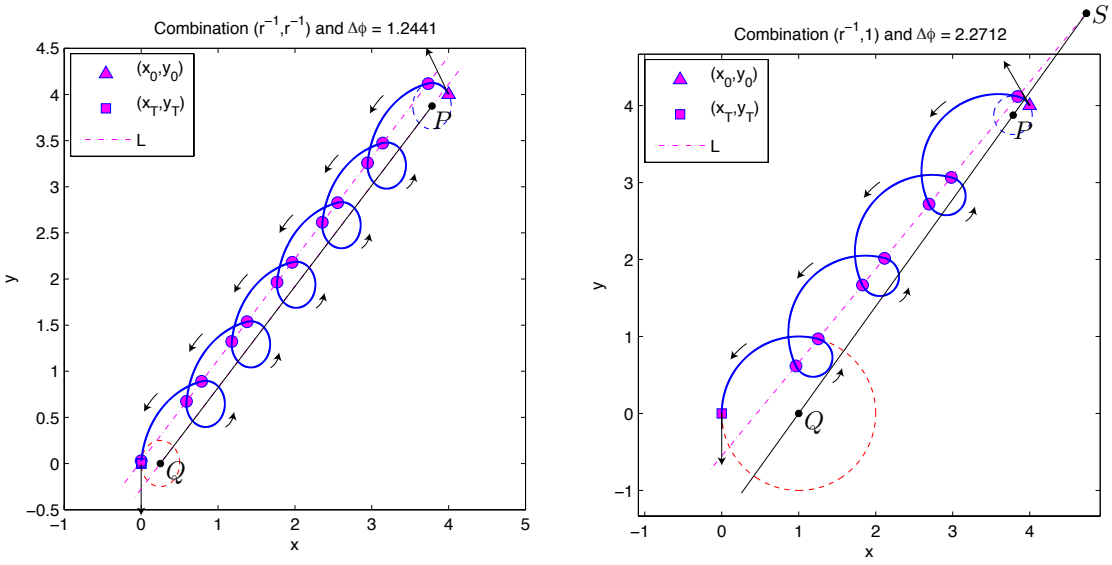

(a) Extremal path with minimal length for a combination $(u(0), u(T)) = (r^{-1}, r^{-1})$. (The number of basic pairs is $n_m = 7$.)

(b) Extremal path with minimal length for a combination $(u(0), u(T)) = (r^{-1}, 1)$. (The number of basic paris is $n_m = 4$.)

Figure 4.9: Extremal paths from $\mathbf{x}_0 = (x_0, y_0, \phi_0) = (4, 4, 2\pi/3)$ to $\mathbf{x}_T = (x_T, y_T, \phi_T) = (0, 0, 3\pi/2)$.

Figure 4.9 illustrates extremal paths for combinations (r^{-1}, r^{-1}) and $(r^{-1}, 1)$ generated by Step I of Algorithm 4.1 when $\mathbf{x}_0 = (x_0, y_0, \phi_0) = (4, 4, 2\pi/3)$, $\mathbf{x}_T = (x_T, y_T, \phi_T) = (0, 0, 3\pi/2)$ and $r = 1/4$. Since the maximum radius of curvature is 1, it suffices to deal only with combinations (r^{-1}, r^{-1}) and $(r^{-1}, 1)$. The other two combinations have no values of $\Delta\phi$ such that the switching line contains $\mathbf{x}_0$. By computing and comparing the lengths of the extremal paths in Figure 4.9, the optimal path is the extremal path for combination $(r^{-1}, 1)$.

To represent the run time of Algorithm 4.1, we use O-notation providing an asymptotic upper bound and Ω-notation providing an asymptotic lower bound (Cor-

Algorithm 4.1. Finding the optimal path using n_m.

Given initial state $\mathbf{x}_0 = (x_0, y_0, \phi_0)$, final state $\mathbf{x}_T = (x_T, y_T, \phi_T)$, and minimum radius of curvature r, find an optimal path which is characterized by a combination $(u(0), u(T))$ and $\Delta\phi$. Note that the maximum radius of curvature is assumed to be 1.

I. **For** each combination $(u(0), u(T)) \in \{(1, 1), (1, r^{-1}), (r^{-1}, r^{-1}), (r^{-1}, 1)\}$,

1. Determine the two centers P and Q of the initial and final circular arcs and compute the length of $\overline{PQ}$.
2. Determine $\Delta\phi_0$ and $\Delta\phi_T$ in $[0, \pi]$ and determine I using Table 1. **If** $I = \emptyset$, **then** go to Step 1 for the next combination because the current combination is impossible. **Otherwise,** continue.
3. Compute the minimum number n_m of basic pairs using (4.11) and (4.12) with the ceiling function.
$$n_m = \lceil \mathcal{D}/\Delta d + 1 \rceil.$$
where $\mathcal{D} = \left|\overline{PQ}\right|$ for $u(0) = u(T)$ and $\mathcal{D} = \sqrt{|\overline{PQ}| - (1-r)^2 \cos^2(\Delta\phi/2)} - \Delta d/2$ for $u(0) \neq u(T)$, and $\Delta d = 2(1-r)\sin(\Delta\phi/2)$ with $\Delta\phi = \sup I$.
4. Set $n = n_m$ and $T_m = \infty$.
5. **If** $n = 1$, **then** compute the length T_n of the extremal path and go to Step 9. **Otherwise,** continue.
6. Compute the value of $\Delta\phi$ corresponding to n using (4.11) and (4.12).
$$\Delta\phi(n) = 2\sin^{-1}(\mathcal{D}/(2n(1-r))).$$
If $\Delta\phi(n_m) \notin I$, **then** go to Step 1 for the next combination. **Otherwise,** continue.
7. Determine the switching line L characterized by the value of $\Delta\phi$ found in Step 6.
   7a. **If** $u(0) = u(T)$, **then** find L by translating the line passing through P and Q by a vector which has magnitude $u^{-1}(0)\cos(\Delta\phi/2)$ and is formed by rotating $\overrightarrow{PQ}$ by $-\pi/2$.
   7b. **If** $u(0) \neq u(T)$, **then** find L by rotating the line passing through P and Q through an angle α defined by (4.9).
8. Compute the length T_n of the extremal path using the switching line L determined in Step 7.
9. Find the extremal path with minimal length for the current combination.
   9a. **If** $T_n > T_m$ or $\Delta\phi(n) \notin I$, **then** the extremal path characterized by the value of $\Delta\phi(n-1)$ has minimal length T_m for the current combination. Go to Step 1 for the next combination.
   9b. **Otherwise,** set $T_m = T_n$ and $n = n + 1$, and go to Step 6.

II. Choose the one among the (at most four) combinations of $\Delta\phi$ with the shortest path length. The extremal path defined by the chosen combination $(u(0), u(T))$ and the corresponding value of $\Delta\phi$ is optimal. Return this optimal path.

men et al. (2001)). The worst-case and best-case run times for Algorithm 4.1 are $O(n^* - n_m)$ and $\Omega(1)$, respectively, where n^* is the number of basic pairs of the optimal path. Since n^* approaches ∞ as r approaches 0, finding an optimal path could theoretically require a very long time for some input. In practical applications, however, robots or vehicles under damage and/or failure conditions have their own constraints, e.g., maximum fuel available, or environmental constraints. If these constraints are considered in Algorithm 4.1, its run time can be within acceptable bounds. Therefore, a hard upper bound can be given for the run time for real-time applications.

Although Algorithm 4.1 is acceptable for real-time implementation, it is possible to modify Algorithm 4.1 so as to find an optimal path even more efficiently. The modified algorithm uses a reference value of $\Delta\phi$ to enable direct identification of the extremal path with the shortest length for each combination $(u(0), u(T))$. To find this reference value, we now turn to the study of the path length (or time) T as a function of $\Delta\phi$. Since $T = T_1 + (n-1)\Delta d$, we derive formulas for the time T_1 and the number n of basic pairs. By the definition of T_1, it is easy to see that for every combination

$$T_1 = u^{-1}(T)\,\phi_T - u^{-1}(0)\,\phi_0 - \left(u^{-1}(T) - u^{-1}(0)\right)\phi(t_1) \tag{4.13}$$

where t_1 represents the first time when $u(t)$ switches. If $u(0) = 1$, then $\phi(t_1) = \pi + \Delta\phi/2 + \theta$. If $u(0) = r^{-1}$, then $\phi(t_1) = \pi - \Delta\phi/2 + \theta$. Note that T_1 is negative when $u(0) = u(T)$ and $\phi_0 > \phi_T$. Since θ is the angle between the switching line L and the x-axis, it is the sum of two angles; one is the angle α in (4.9), and the other is the angle between the vector $\overrightarrow{PQ}$ and the x-axis. For each combination, the number n of basic pairs is defined by the expression inside the ceiling function in Step 3 of Algorithm 4.1.

For each combination $(u(0), u(T))$, both T_1 and n are functions of $\Delta\phi$, and thus T is a function of $\Delta\phi$. If $\Delta\phi$ is a continuous variable, then it follows from the second derivative test that the path length T has a minimum at the same $\Delta\phi$ on $[0, \pi]$ for all combinations. The value of $\Delta\phi$ at which T is minimum for each combination is a solution of the equation

$$\Delta T \cos(\Delta\phi/2) = \Delta d, \tag{4.14}$$

or equivalently,

$$\tan(\Delta\phi/2) = \Delta\phi/2 + r\pi/(1-r). \tag{4.15}$$

This value of $\Delta\phi$ is denoted $\Delta\phi_R$. Note that (4.15) has only one solution between 0 and π and can be solved by conventional numerical methods, e.g., Newton-Raphson.

For each combination $(u(0), u(T))$, as $\Delta\phi$ decreases from π, T first decreases, reaches a minimum at the solution of (4.14), and then increases. Note that this behavior of T, as a function of $\Delta\phi$, guarantees that the sequence of extremal paths generated by Step I of Algorithm 4.1 converges in a finite number of iterations to the extremal path with the shortest length for each combination. Since each combination has its own domain I of possible values of $\Delta\phi$, using $\Delta\phi_R$ allows direct identification of $\Delta\phi$ that minimizes length among all paths for the same combination.

If the interior of the domain I (i.e., the set excluding its endpoints) does not contain $\Delta\phi_R$, the path length $T(\Delta\phi)$ is strictly decreasing or increasing on I. In the former case, the supremum of I can be used to evaluate the number n of basic pairs which corresponds to a value $\Delta\phi$ in I closest to $\Delta\phi_R$. In the latter case, the infimum of I can be used to evaluate n. By contrast, if the interior of the domain I contains $\Delta\phi_R$, $T(\Delta\phi)$ is strictly decreasing and increasing on the interval $[\inf I, \Delta\phi_R]$ and the interval $[\Delta\phi_R, \sup I]$, respectively. To find the extremal path with minimal length for each combination, the two candidates for n corresponding to a value of $\Delta\phi$ in each interval closest to $\Delta\phi_R$ are considered. One candidate is computed by using $\Delta\phi_R$ and

the ceiling function, and the other is calculated by using $\Delta\phi_R$ and the floor function to choose values of $\Delta\phi$ in I. Table 2 summarizes candidates of such n.

Table 4.2: Candidates of n for the shortest path among all paths of the same combination. (Here $\Delta d = 2(1-r)\sin(\Delta\phi/2)$, and $\lceil\ \rceil$ and $\lfloor\ \rfloor$ denote the ceiling function and the floor function, respectively.)

Case	n
$\Delta\phi_R \notin \text{Interior}\, I$ and $\sup I \leq \Delta\phi_R$	$n = \lceil \mathcal{D}/\Delta d + 1 \rceil$ and $\Delta\phi = \sup I$
$\Delta\phi_R \notin \text{Interior}\, I$ and $\Delta\phi_R \leq \inf I$	$n = \lfloor \mathcal{D}/\Delta d + 1 \rfloor$ and $\Delta\phi = \inf I$
$\Delta\phi_R \in \text{Interior}\, I$ and $[\inf I,\, \Delta\phi_R]$	$n = \lceil \mathcal{D}/\Delta d + 1 \rceil$ and $\Delta\phi = \Delta\phi_R$
$\Delta\phi_R \in \text{Interior}\, I$ and $[\Delta\phi_R,\, \sup I]$	$n = \lfloor \mathcal{D}/\Delta d + 1 \rfloor$ and $\Delta\phi = \Delta\phi_R$

Algorithm 4.2 finds the optimal path using the reference value $\Delta\phi_R$. In the first step, (4.15) is solved to obtain $\Delta\phi_R$. Let us again consider the combination $(r^{-1},\, 1)$, as shown in Figure 4.9 (b), in the same manner as for Algorithm 4.1. As previously discussed, $I = [\Delta\phi_T,\, \pi]$. Since $\Delta\phi_R$ lies in the interior of I, the switching line characterized by $\Delta\phi_R$ lies between the line $\overleftrightarrow{PQ}$ and the switching line characterized by $\Delta\phi_T$. Thus, for combination $(r^{-1},\, 1)$, the extremal path with minimal length is defined by one of two switching lines, one lying between the switching lines defined by $\Delta\phi_T$ and $\Delta\phi_R$ and the other lying between $\overleftrightarrow{PQ}$ and the switching line defined by $\Delta\phi_R$. This follows from the fact that T is decreasing and increasing on $[\Delta\phi_T,\, \Delta\phi_R]$ and $[\Delta\phi_R,\, \pi]$, respectively. These two candidates for the switching line are characterized by n, as shown in Table 2.

The candidate path with shorter length is then selected for combination $(r^{-1},\, 1)$. In Figure 4.9 (b), the extremal path with minimal length comes from a switching line defined by $\Delta\phi$ between $\Delta\phi_T$ and $\Delta\phi_R$. Note that if $\Delta\phi_R$ does not lie in the interior of I, the value of $\Delta\phi$ corresponding to n determined by Table 2 defines the extremal path with minimal length among all paths of the same combination. A similar argument applies to the remaining combinations $(1,\, 1)$, $(1,\, r^{-1})$ and $(r^{-1},\, r^{-1})$. Of the (at most

four) paths, the shortest can then be chosen, as stated in Step III of Algorithm 4.2.

Algorithm 4.2. Finding the optimal path using $\Delta\phi_R$.

Given initial state $\mathbf{x}_0 = (x_0,\, y_0,\, \phi_0)$, final state $\mathbf{x}_T = (x_T,\, y_T,\, \phi_T)$, and minimum radius of curvature r, find an optimal path characterized by combination $(u(0),\, u(T))$ and $\Delta\phi$. Note that the maximum radius of curvature is assumed to be 1.

I. Find a solution to $\tan(\Delta\phi/2) = \Delta\phi/2 + r\pi/(1-r)$ in the interval $[0,\, \pi]$ using conventional numerical methods, e.g., the Newton-Raphson method; let $\Delta\phi_R$ represent this solution.

II. **For** each combination $(u(0),\, u(T)) \in \{(1,\, 1),\, (1,\, r^{-1}),\, (r^{-1},\, r^{-1}),\, (r^{-1},\, 1)\}$,

1. Determine the two centers P and Q of the initial and final circular arcs and compute the length of $\overline{PQ}$.
2. Determine $\Delta\phi_0$ and $\Delta\phi_T$ in $[0,\, \pi]$ and determine I using Table 1. **If** $I = \emptyset$, **then** go to Step 1 for the next combination because the current combination is impossible. **Otherwise,** go to Step 3.
3. Compute the number n of basic pairs using Table 2. **If** $\Delta\phi_R \in \text{Interior}\, I$, **then** compute n for the interval $[\Delta\phi_R,\, \sup I]$.
4. Set $m = n$.
5. **If** $m = 1$, **then** compute the length T_m of the extremal path and go to Step 9. **Otherwise,** continue.
6. Compute the value of $\Delta\phi$ corresponding to m using (4.11) and (4.12).
$$\Delta\phi(m) = 2\sin^{-1}(\mathcal{D}/(2m(1-r))).$$
If $\Delta\phi(n) \notin I$, **then** go to Step 9. **Otherwise,** continue.
7. Determine the switching line L characterized by the value of $\Delta\phi$ found in Step 6.
   - 7a. **If** $u(0) = u(T)$, **then** find L by translating the line passing through P and Q by a vector which has magnitude $u^{-1}(0)\cos(\Delta\phi/2)$ and is formed by rotating $\overrightarrow{PQ}$ by $-\pi/2$.
   - 7b. **If** $u(0) \neq u(T)$, **then** find L by rotating the line passing through P and Q through an angle α defined by (4.9).
8. Compute the length T_m of the extremal path using the switching line L determined in Step 7 and go to Step 10.
9. **If** $\Delta\phi(m) \notin I$, **then** check whether or not $\Delta\phi_R \in \text{Interior}\, I$.
   - 9a. **If** $\Delta\phi_R \notin \text{Interior}\, I$, **then** go to Step 1 for the next combination because the current combination is impossible.
   - 9b. **If** $\Delta\phi_R \in \text{Interior}\, I$ and $m = n$, **then** set m equal to the number of basic pairs for the interval $[\inf I,\, \Delta\phi_R]$ in Table 2 and return to Step 6.
   - 9c. **If** $\Delta\phi_R \in \text{Interior}\, I$ and $m \neq n$, **then** check whether or not $\Delta\phi(n) \in I$. **If** $\Delta\phi(n) \notin I$, **then** go to Step 1 for the next combination because the current combination is impossible. **Otherwise,** the extremal path characterized by the value of $\Delta\phi(n)$ has minimal length T_n for the current combination. Go to Step 1 for the next combination.

10. **If** $\Delta\phi(m) \in I$, **then** check whether or not $\Delta\phi_R \in \text{Interior}\, I$.
    - 10a. **If** $\Delta\phi_R \notin \text{Interior}\, I$; **then** the extremal path characterized by the value of $\Delta\phi(m)$ has minimal length T_m for the current combination. Go to Step 1 for the next combination.
    - 10b. **If** $\Delta\phi_R \in \text{Interior}\, I$ and $m = n$, **then** set m equal to the number of basic pairs for the interval $[\inf I,\ \Delta\phi_R]$ in Table 2 and return to Step 6.
    - 10c. **If** $\Delta\phi_R \in \text{Interior}\, I$ and $m \neq n$, **then** check whether or not $\Delta\phi(n) \in I$. **If** $\Delta\phi(n) \notin I$, **then** the extremal path characterized by the value of $\Delta\phi(m)$ has minimal length T_n for the current combination. Go to Step 1 for the next combination. **Otherwise,** choose the one between $\Delta\phi(m)$ and $\Delta\phi(n)$ with the shorter path length. The extremal path characterized by the chosen value of $\Delta\phi$ has minimal length for the current combination. Go to Step 1 for the next combination.

III. Choose the one among the (at most four) combinations of $\Delta\phi$ with the shortest path length. The extremal path defined by the chosen combination $(u(0),\ u(T))$ and the corresponding value of $\Delta\phi$ is optimal. Return this optimal path.

It follows from the behavior of the path length (or time) T that both Algorithms 1 and 2 generate the same time-optimal solution. Except for Step I of Algorithm 4.2 to find the reference value $\Delta\phi_R$, there is no recursive procedure, so Algorithm 4.2 runs in $\Theta(1)$ for any input (where Θ-notation refers to an asymptotically tight bound (Cormen et al. (2001))). This enables Algorithm 4.2 to find an optimal path more efficiently than Algorithm 4.1 as $n^* - n_m$ grows large.

By Algorithm 4.1 or 4.2, we can select combination $(u(0),\ u(T))$ and the corresponding $\Delta\phi$ that define the optimal path from the initial state $\mathbf{x}_0$ to the final state $\mathbf{x}_T$. The combination $(u(0),\ u(T))$ and the corresponding value of $\Delta\phi$ uniquely characterize the switching line yielding the family of extremal controls of the optimal path. Therefore, the sequence of points of the optimal path that lie on its switching line L can be found as stated in Algorithm 4.3.

Algorithm 4.3. Compute points of an optimal path lying on its switching line L.

Given the combination $(u(0), u(T))$ and the corresponding value of $\Delta\phi$ that define the optimal path determined in Algorithm 4.1 or 4.2, compute the sequence of points of the optimal path lying on its switching line L.

I. Determine the first time (or length) t_1 at which $u(t)$ switches between 1 and r^{-1}.
   1. **If** $u(0) = 1$, **then** $t_1 = \pi + \Delta\phi/2 + \theta - \phi_0$.
   2. **If** $u(0) = r^{-1}$, **then** $t_1 = r(\pi - \Delta\phi/2 + \theta - \phi_0)$.

   Note that θ represents the angle between L and the x-axis and is determined in Step 7 of Algorithm 4.1 or 4.2.

II. Compute the point $(x(t_1), y(t_1))$ by integrating $\dot{x}(t) = \cos\phi(t)$, $\dot{y}(t) = \sin\phi(t)$ and $\dot{\phi}(t) = u(t)$ over $[0, t_1]$.

III. Set $N = 2n - 2$ for combinations $(1, 1)$ and (r^{-1}, r^{-1}) and $N = 2n - 1$ for combinations $(1, r^{-1})$ and $(r^{-1}, 1)$ where n is the number of basic pairs corresponding to $\Delta\phi$.

IV. **For** $i = 2, 3, \cdots, N$,
   1. Determine the ith time (or length) t_i at which $u(t)$ switches between 1 and r^{-1}.
      1a. **If** $u(t) = 1$ for $t_{i-1} < t < t_i$, **then** $t_i = \Delta\phi + t_{i-1}$.
      1b. **If** $u(t) = 1/r$ for $t_{i-1} < t < t_i$, **then** $t_i = r(2\pi - \Delta\phi) + t_{i-1}$.
   2. Compute the point $(x(t_i), y(t_i))$ by integrating $\dot{x}(t) = \cos\phi(t)$, $\dot{y}(t) = \sin\phi(t)$ and $\dot{\phi}(t) = u(t)$ over $[t_{i-1}, t_i]$.

4.5 Algorithm Performance

We investigated the performance of Algorithms 1 and 2 over 1,000 different cases. Two performance metrics were considered: computation time and extremal path's existence for each combination. The initial state $\mathbf{x_0} = (x_0, y_0, \phi_0)$ was uniformly distributed on $[-100, 100] \times [-100, 100] \times [0, 2\pi)$. Ten sample points on each axis (i.e., the x-axis, y-axis and ϕ-axis) were considered as each component of $\mathbf{x}_0$. For every initial state $\mathbf{x}_0$, the final state $\mathbf{x}_T$ was given by $\mathbf{x}_T = (x_T, y_T, \phi_T) = (0, 0, \pi/2)$ and $r = 1/4$.

For every initial state $\mathbf{x}_0$, we evaluated the computation times of Algorithms 1 and 2, for finding the optimal path, implemented in Matlab. Over 1,000 initial states, the average computation times of Algorithms 1 and 2 were 3.07×10^{-3} seconds and 1.99×10^{-3} seconds, respectively, on a 2.66 GHz Intel Core i7, running Mac OS X.

Figure 4.10 shows a histogram of computation times for Algorithms 1 and 2 over 1,000 initial states. The bars are for intervals of width 0.5. The computation times for Algorithm 2 are nearly constant as expected. In about 50% of the test cases, the computation time of Algorithm 1 is near the mean value which is slightly higher than the average execution time for Algorithm 2. Since $n^* - n_m$ is proportional to $\left|\overline{PQ}\right|$, the computation time of Algorithm 1 increases approximately linearly with $\left|\overline{PQ}\right|$. Therefore, while both algorithms have good real-time performance, Algorithm 2 is slightly better in terms of average run time and run time variance with $\left|\overline{PQ}\right|$. Note that the average computation time of Algorithm 3 is 9.0×10^{-4} seconds and the same order of magnitude as the running times for Algorithms 1 and 2 with little variation.

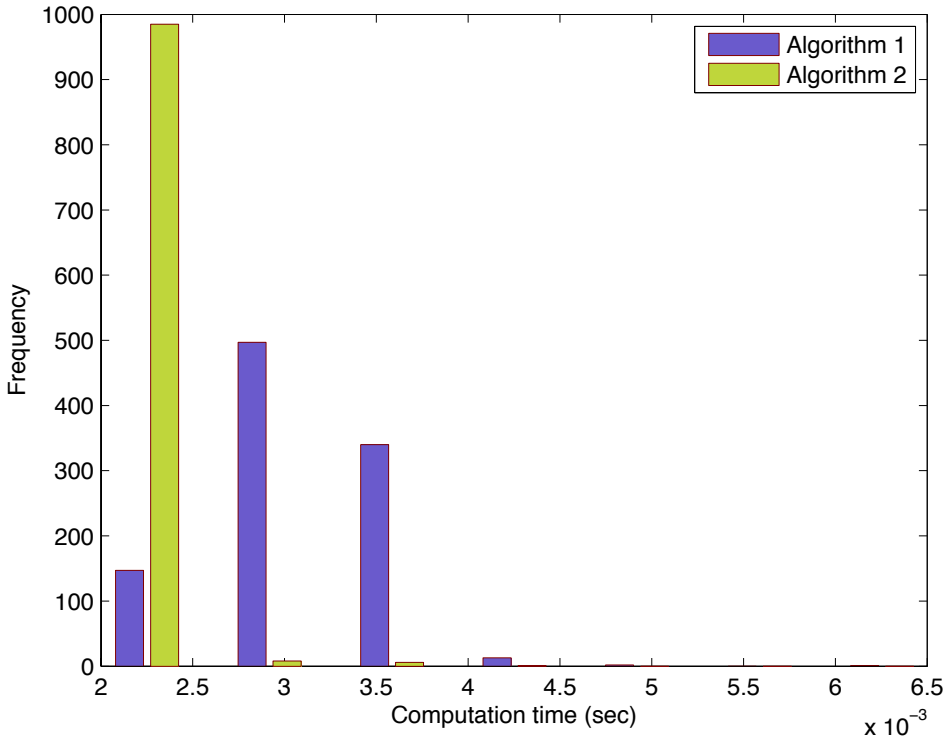

Figure 4.10: Histogram of computation times of Algorithms 1 and 2 over 1,000 initial states.

Figures 4.11 (a) and (b) respectively illustrate histograms of feasible combinations

for which there is an extremal path satisfying the boundary conditions and of the optimal path's combination for each case. Figure 4.11 (a) indicates the existence of extremal paths as the following percentages of the 1,000 test cases: 21.8 % for combination (1, 1), 35 % for combination (1, r^{-1}), 100 % for combination (r^{-1}, r^{-1}) and 35.4 % for combination (r^{-1}, 1). Every initial state $\mathbf{x}_0$ is joined to the final state $\mathbf{x}_T$ by an extremal path of combination (r^{-1}, r^{-1}). This follows from the fact that the domain I for this combination is of the form $[0, \Delta\phi]$ for some $\Delta\phi \in [0, \pi]$ and the fact that the number n of basic pairs increases toward infinity as $\Delta\phi$ decreases.

As a final analysis, we examined the likelihoods of selecting each of the four possible combinations as optimal over our 1,000 initial states. Figure 4.11 (b) shows the results: 13.7% selection of combination (1, 1), 23.1% selection of combination (1, r^{-1}), 38.9% selection of combination (r^{-1}, r^{-1}) and 24.3% selection of combination (r^{-1}, 1). Thus, in the simulation, the most common and least common combinations of optimal paths are (r^{-1}, r^{-1}) and (1, 1), respectively. Normalizing the frequency of each optimal path's combination in Figure 4.11 (b) by its extremal path's feasibility frequency in Figure 4.11 (a) shows that more than 60% of the extremal paths for combination (1, 1), (1, r^{-1}) or (r^{-1}, 1) were selected as an optimal path. For combination (r^{-1}, r^{-1}), less than 40% of the extremal paths were optimal even though extremal paths always exist. These results are related to the value of r and domain I for each combination. Since $\Delta\phi_R$ increases with r and $\Delta\phi$ of the optimal path is close to $\Delta\phi_R$, the percentages of combinations (1, 1) and (r^{-1}, r^{-1}) for an optimal path, respectively, increase and decrease as r approaches 1.

4.6 Conclusions

This chapter has presented the a characterization of shortest paths for a unidirectional Dubins car, subject to the turn rate bounded on an interval whose end points are either both positive or negative. While previous studies have extensively dealt

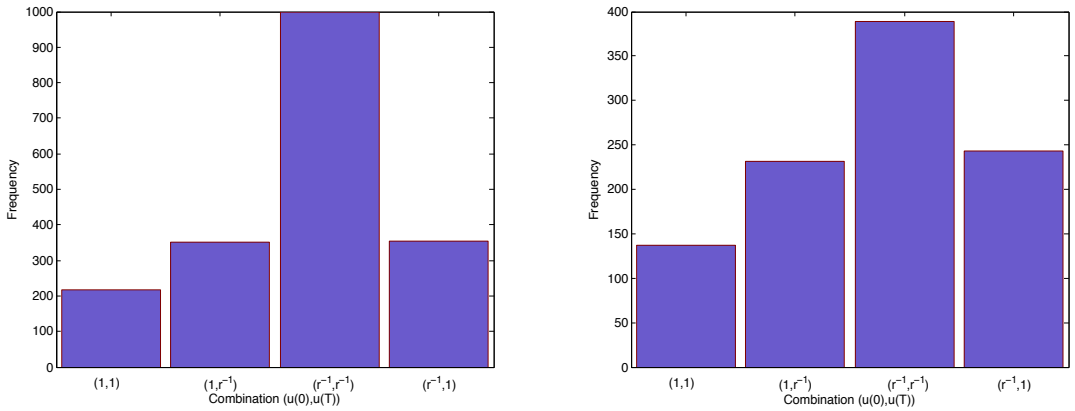

(a) Feasible combinations of extremal paths.

(b) Combinations of optimal paths.

Figure 4.11: Histograms of combinations over 1,000 initial states.

with finding the shortest path for objects able to travel along straight paths, this study for the first time finds optimal paths for objects unable to travel straight due to extreme kinematic constraints. We applied Pontryagin's minimum principle to characterize the optimal path. As a result, we were able to determine the following three possible candidates for the optimal path: a circular arc with normalized maximum radius 1, a circular arc with normalized minimum radius r, or the concatenation of alternating arcs of two tangent circles with radii r and 1 at every switching point.

Not all extremal paths are optimal. In Section 4.3, we derived geometric interpretations for each of the four possible combinations of initial arc and final arc. Each combination and each value of the Hamiltonian (or $\Delta\phi$) uniquely characterize the switching line yielding the family of extremal controls. The geometric interpretations for extremal paths were employed to develop an efficient algorithm for determining the optimal path (i.e. the combination and the value of the Hamiltonian).

CHAPTER V

Time-Optimal Paths for Unidirectional Dubins Airplanes

5.1 Introduction

Aircraft experiencing an emergency situation induced by damage or failure must rapidly identify a path to safe landing site to minimize risks associated with continued flight. A fixed-wing aircraft cannot travel in reverse, nor can it change heading instantly. Therefore, the traditional aircraft motion planning problem is to find an optimal path for a rigid-body aircraft, treated as a particle, moving only forward with a given maximum turn rate and maximum climb/descent rate. As shown in Chapter I, an aircraft can have unidirectional turning capabilities imposed by structural damage or jammed control surfaces.

This chapter extends the unidirectional Dubins car problem studied in Chapter IV to a Dubins airplane with unidirectional turning constraints. To simplify our problem, we suppose that vertical and turn rates are independent of each other. Additionally, we assume in this work that the aircraft travels at constant horizontal velocity. This assumption requires that we select a speed that is possible to maintain over all path segments.

For the unidirectional Dubins airplane, we again apply the minimum principle

of Pontryagin to characterize the time-optimal path to reach a given final oriented point. The optimal path will be divided into two paths, one with the same transition time as the shortest path for the unidirectional Dubins car (see Chapter IV), and the other with transition time determined by the difference between the initial and final altitudes. An algorithm is presented to find optimal paths for Dubins airplanes with unidirectional turning constraints. This algorithm selects the appropriate formulation based on initial and final 4-D states as well as turning and climbing constraints. To ensure completeness, the optimal algorithm is augmented by a feasible but suboptimal path planning option to handle rare but possible cases for which no optimal solution is defined.

The chapter is organized as follows. Section II of the chapter provides a characterization of the optimal 3D path using the minimum principle of Pontryagin. In Section III, the shortest unidirectional Dubins path is extended to pass through the final oriented point at the time determined by altitude difference and maximum climb (or descent) rate. Section IV presents an algorithm to find the optimal or suboptimal (but feasible) path given any initial and final oriented points. Section V validates the algorithm on a series of test cases, and Section VI applies the proposed algorithm to an aircraft emergency landing planning problem.

5.2 Necessary Conditions for Optimality

Given two points (x_0, y_0, z_0) and (x_T, y_T, z_T) in $\mathbb{R}^3$ with corresponding directions ϕ_0 and ϕ_T in $\mathbb{S}^1$, we want to find a continuous and piecewise $\mathcal{C}^2$ path (x, y, z) of minimal length subject to the following constraints:

(i) The radius of curvature lies between r and 1 where $0 < r < 1$. The reciprocal of the radius, called the control (or the curvature) and denoted u, is also bounded on control region U. Since every path is continuous and piecewise $\mathcal{C}^2$, the control

is piecewise continuous.

(ii) The sign of curvature remains unchanged. Therefore, the control region U is $[1,\, r^{-1}]$. The case $U = [-r^{-1},\, -1]$ can be treated similarly to $U = [1,\, r^{-1}]$.

(iii) The path $(x,\, y)$ has unit speed. Even if the path has non-zero constant speed, the path has a unit-speed reparametrization (do Carmo (1976)), and thus the path with unit speed produces no loss of generality.

(iv) The rate of change in altitude (or the vertical rate), called the control and denoted v, is bounded on the control region $V = [-v_{\max},\, v_{\max}]$ where $0 < v_{\max} < 1$. [1]

(v) Bounded controls u and v are independent of each other.

Under these constraints, a path $(x,\, y,\, z)$ is a solution of the system of differential equations

$$\begin{aligned} \dot{x}\,(t) &= \cos\phi\,(t)\,, \\ \dot{y}\,(t) &= \sin\phi\,(t)\,, \\ \dot{z}\,(t) &= v\,(t) \in V, \\ \dot{\phi}\,(t) &= u\,(t) \in U, \end{aligned} \tag{5.1}$$

where $\phi\,(t)$ is the angle between unit tangent vector $(\dot{x},\, \dot{y})$ in the xy plane and the x-axis, and $\phi\,(t)$ is a real number modulo 2π. Let $\mathbf{x} = (x\,(t)\,,\, y\,(t)\,,\, z\,(t)\,,\, \phi\,(t))$. Then the boundary conditions are

$$\mathbf{x}\,(0) = (x_0,\, y_0,\, z_0,\, \phi_0) \triangleq \mathbf{x}_0 \text{ and } \mathbf{x}\,(T) = (x_T,\, y_T,\, z_T,\, \phi_T) \triangleq \mathbf{x}_T. \tag{5.2}$$

[1] A value $v_{\max} = 1$ would imply a 45° flight path angle. Fixed-wing aircraft will climb and descend at a more shallow angle. Additionally, an aircraft may have asymmetric bounds on vertical rate, e.g., it may be capable of descending faster than climbing. Each Dubins airplane problem posed will require either a climb or descent, indicating the appropriate value of $v_{\max}$ for that particular path planning activity.

The cost to be minimized is the transition time from an initial oriented point $\mathbf{x}_0$ to a final oriented point $\mathbf{x}_T$ given by

$$J(u,\, v) = \int_0^T dt = T.$$

Therefore, our problem becomes a time-optimal problem.

We now characterize the necessary conditions for the time-optimal path $(x,\, y,\, z)$ using Pontryagin's minimum principle. Let ψ_1, ψ_2, ψ_3 and ψ_4 be the adjoint variables corresponding to x, y, z and ϕ, respectively. The Hamiltonian is then defined by

$$H(\psi,\, \mathbf{x},\, u,\, v) = \psi_1 \cos\phi + \psi_2 \sin\phi + \psi_3 v + \psi_4 u,$$

where $\psi = (\psi_1,\, \psi_2,\, \psi_3,\, \psi_4)$, and the adjoint system is defined by

$$\begin{aligned}
\dot{\psi}_1(t) &= -\frac{\partial H}{\partial x} = 0, \\
\dot{\psi}_2(t) &= -\frac{\partial H}{\partial y} = 0, \\
\dot{\psi}_3(t) &= -\frac{\partial H}{\partial z} = 0, \\
\dot{\psi}_4(t) &= -\frac{\partial H}{\partial \phi} = \psi_1 \sin\phi(t) - \psi_2 \cos\phi(t).
\end{aligned} \tag{5.3}$$

It follows from this adjoint system that ψ_1, ψ_2 and ψ_3 are constant on $[0,\, T]$. Using notations λ and θ defined in Section 4.2, the Hamiltonian and system (5.3) become

$$\begin{aligned}
H &= \lambda \cos(\phi - \theta) + \psi_3 v + \psi_4 u, \\
\dot{\psi}_4 &= \lambda \sin(\phi - \theta).
\end{aligned} \tag{5.4}$$

By Pontryagin's minimum principle, if the trajectory $\mathbf{x}(t)$ determined by $(u(t),\, v(t)) \in U \times V$ is time-optimal, then there exists a non-zero continuous solution $\psi = (\psi_1,\, \psi_2,\, \psi_3,\, \psi_4)$ such that

(1) The control $(u(t),\, v(t))$ minimizes the Hamiltonian at every time t; that is,

$$H(\psi(t),\, \mathbf{x}(t),\, u(t),\, v(t)) = \min_{(\zeta,\, \eta) \in U \times V} H(\psi(t),\, \mathbf{x}(t),\, \zeta,\, \eta).$$

(2) $H(\psi,\, \mathbf{x},\, u(t),\, v(t))$ is constant, and

$$H(\psi(t),\, \mathbf{x}(t),\, u(t),\, v(t)) \leq 0.$$

It follows from condition (1) that $\psi_3(t)\, v(t) + \psi_4(t)\, u(t) \leq \psi_3(t)\, \zeta(t) + \psi_4(t)\, \eta(t)$ for all $\zeta(t) \in U$ and $\eta(t) \in V$, and for all t in $[0,\, T]$. Thus, the optimal control is

$$v(t) = \begin{cases} -\operatorname{sgn}(\psi_3(t)) \cdot v_{\max} & \text{if } \psi_3(t) \neq 0, \\ \zeta \in V & \text{if } \psi_3(t) = 0, \end{cases} \tag{5.5}$$

and

$$u(t) = \begin{cases} 1 & \text{if } \psi_4(t) > 0, \\ \eta \in U & \text{if } \psi_4(t) = 0, \\ r^{-1} & \text{if } \psi_4(t) < 0. \end{cases} \tag{5.6}$$

For $\psi_3 = 0$, if $\psi_4(t) = 0$ on some open interval, then $\phi(t)$ is constant on that interval because $\psi(t)$ is non-zero. Thus, $u(t) = 0$, contradicting the assumption that $u(t) \geq 1$. Therefore, there is no open interval on which $\psi_4(t) = 0$, and consequently the optimal control $u(t)$ becomes

$$u(t) \triangleq u_{\min}(\psi_4(t)) = \begin{cases} 1 & \text{if } \psi_4(t) > 0, \\ r^{-1} & \text{if } \psi_4(t) \leq 0, \end{cases} \tag{5.7}$$

and system (5.4) becomes

$$\begin{aligned} \dot{\psi}_4(t) &= \sin(\phi(t) - \theta), \\ \psi_4(t) \cdot u_{\min}(\psi_4(t)) &= H - \lambda \cos(\phi(t) - \theta). \end{aligned} \tag{5.8}$$

Therefore, for $\psi_3 = 0$, the projection of a path (x, y, z) onto the xy plane is an extremal path for the Dubins car with unidirectional turning constraints. Note that in this case, the optimal control $v(t)$ can have any value in $V = [-v_{\max}, v_{\max}]$. For $\psi_3 \neq 0$, it follows from (5.1) and (5.5) that $T = |z(T) - z(0)| / v_{\max}$. Consequently, the transition time from an initial oriented point $\mathbf{x}_0$ to a final oriented point $\mathbf{x}_T$ is fixed. Therefore, for $\psi_3 \neq 0$, our problem is equivalent to the problem of finding a continuous and piecewise $\mathcal{C}^2$ path (x, y) of fixed time T with the prescribed $\mathbf{x}_0$ and $\mathbf{x}_T$ subject to constraints (i), (ii) and (iii). Thus, hereafter we only consider $\psi_3 \neq 0$.

For $\lambda = 0$, it follows that $\psi_4(t)$ is constant. Since $H + v_{\max} \cdot |\psi_3|$ is the constant function with value in $\mathbb{R}$, it follows that $u \equiv 1$ for $H + v_{\max} \cdot |\psi_3| > 0$ and $u \equiv r^{-1}$ for $H + v_{\max} \cdot |\psi_3| < 0$. When $H + v_{\max} \cdot |\psi_3| = 0$, the control $u(t)$ is singular. In this case, the minimum principle gives no information about control $u(t)$. For $\lambda > 0$, there is no open interval on which $\psi_4(t) = 0$. It follows that $u(t) \equiv u_{\min}(\psi_4(t))$, that is, the same result as when $\psi_3 = 0$. Since the minimum principle remains invariant when the adjoint vector is multiplied by λ, we can hereafter assume without loss of generality that $\lambda = 1$. Instead of working with H in (5.4), we work with $\mathbf{H} \triangleq H + v_{\max} \cdot |\psi_3|$ because $\mathbf{H}$ is a constant function with value in $\mathbb{R}$. Consequently, the system (5.4) can be simplified to

$$\begin{aligned} \dot{\psi}_4(t) &= \sin(\phi(t) - \theta), \\ \psi_4(t) \cdot u_{\min}(\psi_4(t)) &= \mathbf{H} - \cos(\phi(t) - \theta). \end{aligned} \tag{5.9}$$

For $\mathbf{H} \leq 0$, system (5.9) is equivalent to system (5.8) with $\lambda = 1$, so the extremal control $u(t)$ generates extremal paths for Dubins cars with unidirectional turning constraints. The only difference is that the optimal control $v(t)$ is defined as either $-v_{\max}$ or $v_{\max}$ instead of any value between $-v_{\max}$ and $v_{\max}$. For unidirectional Dubins cars, an extremal path is a concatenation of alternating circular arcs of radius 1 and r with the following properties:

(P1) It is smooth in the sense that at juncture points of the concatenation the two circles have a common tangent vector.

(P2) The angular path change for all circles of radius 1 is $\Delta\phi \triangleq 2\cos^{-1}(-\mathbf{H})$ where $0 \leq \Delta\phi \leq \pi$.

(P3) The angular path change for all circles of radius r is $2\pi - \Delta\phi$.

This follows from the results in Chapter IV.

For $\mathbf{H} > 0$, there are two cases to consider: $\mathbf{H} > 1$ and $0 < \mathbf{H} \leq 1$. For $\mathbf{H} > 1$, it follows that $\psi_4(t) > 0$ and $u \equiv 1$. For $0 < \mathbf{H} \leq 1$, the variation in $\psi_4(t) \cdot u_{\min}(\psi_4(t))$ versus $\phi(t)$ is illustrated in Figure 5.1. This variation is obtained from $-\mathbf{H} - \lambda\cos(\phi(t) - \theta)$ by translating vertically upward. Thus, in this case, the planar paths generated by extremal controls are concatenations of alternating circular arcs of radius 1 and r with smoothness property (P1) and the following reversed turning properties:

(P2′) The angular path change for all circles of radius 1 is $2\pi - \Delta\phi$.

(P3′) The angular path change for all circles of radius r is $\Delta\phi$.

The condition that $0 < \mathbf{H} \leq 1$ reverses the angular path changes for circles of radius 1 and radius r. A concatenation satisfying (P1), (P2′) and (P3′) is denoted as the *reverse* of a concatenation satisfying (P1), (P2) and (P3).

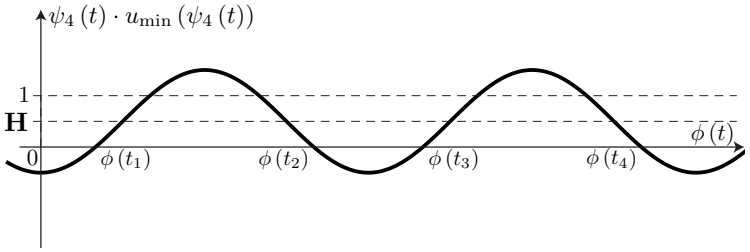

Figure 5.1: $\psi_4(t) \cdot u_{\min}(\psi_4(t))$ for $\mathbf{H} = 0.5$.

5.3 The Extension of Optimal Paths for Unidirectional Dubins Cars

We have shown that optimal paths have one of two transition times:

(1) The shortest time, denoted T^*, for the Dubins car with unidirectional turning constraints transferring from an initial oriented point (x_0, y_0, ϕ_0) to a final oriented point (x_T, y_T, ϕ_T).

(2) The time equal to the absolute altitude difference divided by the maximum vertical rate.

In case (1), optimal paths can be defined using the results from the unidirectional Dubins car problem. However, in case (2), the adjoint variable ψ_4 can be zero during the entire time interval so that the necessary condition provides no information about the relationship between $u(t)$ and $\psi_4(t)$. Moreover, it is rare for both the concatenations and their reversed concatenations to pass through a given final oriented point at the time corresponding to case (2). This follows from the fact that the lengths of extremal planar paths are not densely distributed throughout $\mathbb{R}$.

We show in this section that if a time-optimal path for the unidirectional Dubins car satisfies a certain condition, then it is extended to planar paths joining $\mathbf{x}_0$ and $\mathbf{x}_T$ whose length ranges over the closed interval with end points T^* and $T^* + 2\pi r$. The geometric properties of extremal paths for unidirectional Dubins cars in Chapter IV will be used to find the planar path. For simplicity, only the case $u(t) > 0$ is

considered. For the unidirectional Dubins car, it follows from Pontryagin's minimum principle that extremal paths are concatenations of alternating circular arcs of radius 1 and r with properties (P1), (P2) and (P3). These concatenations are categorized by four combinations of initial arc and final arc, depending on their radii which are either r or 1. Thus, we will refer to a combination as an ordered pair $(u(0), u(T))$ following the same notation as in Chapter IV.

Except for the initial and final circular arcs, the circular arcs are specified as basic pairs whose angular path change is 2π. We now extend the basic pair defined for extremal paths of unidirectional Dubins cars. The extended basic pair is used to construct feasible paths of length ranging from T^* to no less than $T^* + 2\pi r$. Let r_1 and r_2 be in $[r, 1]$ such that $r_1 \neq r_2$. Suppose that an arc of radius r_1 is followed by an arc of radius r_2, and both have property (P1) as well as the following properties:

(P2″) The angular path change for the circle of the larger of the radii r_1 and r_2 is $\Delta\phi$ where $0 \leq \Delta\phi \leq 2\pi$.

(P3″) The angular path change for the circle of the smaller of the radii r_1 and r_2 is $2\pi - \Delta\phi$.

Then the pair of arcs of radii r_1 and r_2 will be referred to as an *extended basic pair* of circular arcs of radii r_1 and r_2. Note that the order of radii r_1 and r_2 is crucial since extended basic pairs with radii r_1 and r_2 and with radii r_2 and r_1 are far from equal. Note also that $0 \leq \Delta\phi \leq \pi$ for every concatenation $\mathbf{C}$, and $\pi \leq \Delta\phi \leq 2\pi$ for every concatenation $\bar{\mathbf{C}}$. This extended basic pair has length

$$\Delta T_e \triangleq |r_1 - r_2| \Delta\phi + 2\pi\rho, \tag{5.10}$$

where $\rho \triangleq \min\{r_1, r_2\}$. The distance between the beginning and ending points of this pair equals

$$\Delta d_e \triangleq 2|r_1 - r_2| \sin(\Delta\phi/2), \tag{5.11}$$

as shown in Figure 5.2.

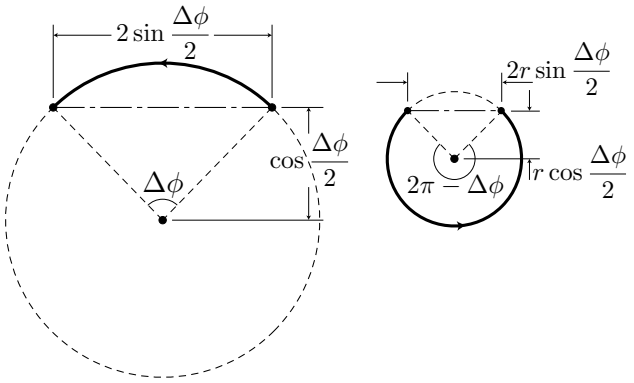

(a) A circular arc of radius r_1

(b) A circular arc of radius r_2

Figure 5.2: An extended basic pair of circular arcs of radius r_1 and radius r_2 for $r_1 > r_2$.

Using extended basic pairs, we can extend concatenations $\mathbf{C}$ and $\bar{\mathbf{C}}$ for unidirectional Dubins cars to allow for radius, denoted r_e, that varies over $r \leq r_e \leq 1$. Then it is possible for planar paths from $\mathbf{x}_0$ to $\mathbf{x}_T$ to have length ranging over $[T^*,\, T^* + 2\pi r]$. The extremal paths $\mathbf{C}$ and $\bar{\mathbf{C}}$ are extended to the following concatenations:

($\mathbf{C}$1) If $\mathbf{C}$ or $\bar{\mathbf{C}}$ belongs to the combination $(u\,(0)\,,\, u\,(T))$ with $u\,(0) = u\,(T)$, it is extended to a concatenation of extended basic pairs of two circular arcs of radius $u^{-1}\,(0)$ and r_e.

($\mathbf{C}$2) If $\mathbf{C}$ or $\bar{\mathbf{C}}$ belongs to the combination $(u\,(0)\,,\, u\,(T))$ with $u\,(0) \neq u\,(T)$, it is extended to a concatenation of extended basic pairs of two circular arcs of radius r_e and $u^{-1}\,(T)$ following the first basic pair with radii $u^{-1}\,(0)$ and $u^{-1}\,(T)$. The first time at which $u\,(t)$ switches between $u\,(0)$ and $u\,(T)$ remains unchanged.

These concatenations are referred to as *extended concatenations.* In this construction of concatenations, the extremals $u\,(0)$ and $u\,(T)$ remain unchanged to simplify the solution, as indicated in Figure 5.3.

In the construction of extremal paths for unidirectional Dubins cars, all points at which the extremal $u\,(t)$ switches between 1 and r^{-1} lie on a certain line, called

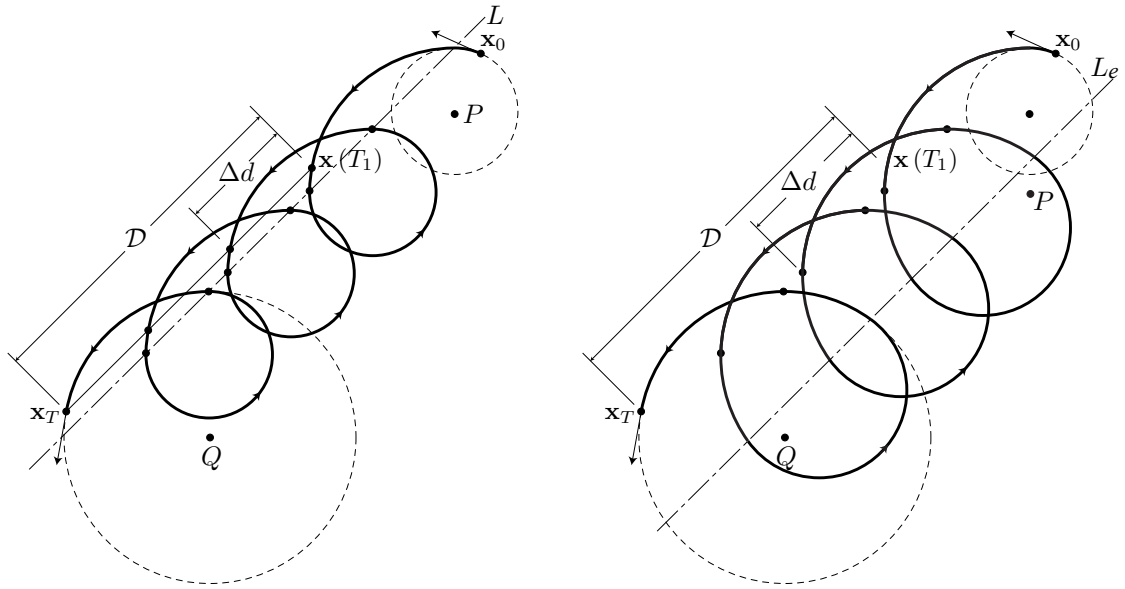

(a) The concatenation $\mathbf{C}$ for a combination $(u(0), u(T)) = (r^{-1}, 1)$

(b) The extended concatenation $\mathbf{C}2$ of $\mathbf{C}$

Figure 5.3: The extended concatenations.

the *switching line* and denoted L. This switching line L is uniquely characterized by $\Delta\phi$ in $[0, \pi]$ for each combination $(u(0), u(T))$. Since the construction of extended concatenations leaves the extremals $u(0)$ and $u(T)$ unchanged, the switching line for extended concatenations is also characterized by $\Delta\phi$ in $[0, 2\pi]$ for any combination $(u(0), u(T))$ and any radius r_e in $[r, 1]$. The switching line for extended concatenations contains all points at which the control $u(t)$ switches either between 1 and r_e^{-1} or between r_e^{-1} and r^{-1}. This switching line is denoted L_e and referred to as the *extended switching line.*

Let P and Q be two centers of the initial circular arc for $u(0) = u(T)$ (arc following the initial arc for $u(0) \neq u(T)$) and the final circular arc, respectively. It follows from the results in Chapter IV that the extended switching line L_e is a line obtained by translating the line passing through P and Q by a vector which has magnitude $u^{-1}(0)\,|\cos(\Delta\phi/2)|$ for $u(0) = u(T)$ (magnitude $u^{-1}(T)\,|\cos(\Delta\phi/2)|$ for $u(0) \neq u(T)$) and is formed by rotating $\overrightarrow{PQ}$ by $-\operatorname{sgn}(\cos(\Delta\phi/2)) \cdot \pi/2$ (Figure 5.4). For each combination $(u(0), u(T))$ with $u(0) \neq u(T)$, the first time where

$u(t)$ switches is unchanged by alterations of the radius r_e. Thus, the combination $(u(0), u(T))$ with $u(0) \neq u(T)$ can be regarded as the combination $(u(0), u(T))$ with $u(0) = u(T)$ by letting the arc following the initial arc be an initial arc and letting the first time where $u(t)$ switches be 0. Henceforth, only combinations with $u(0) = u(T)$ will be considered.

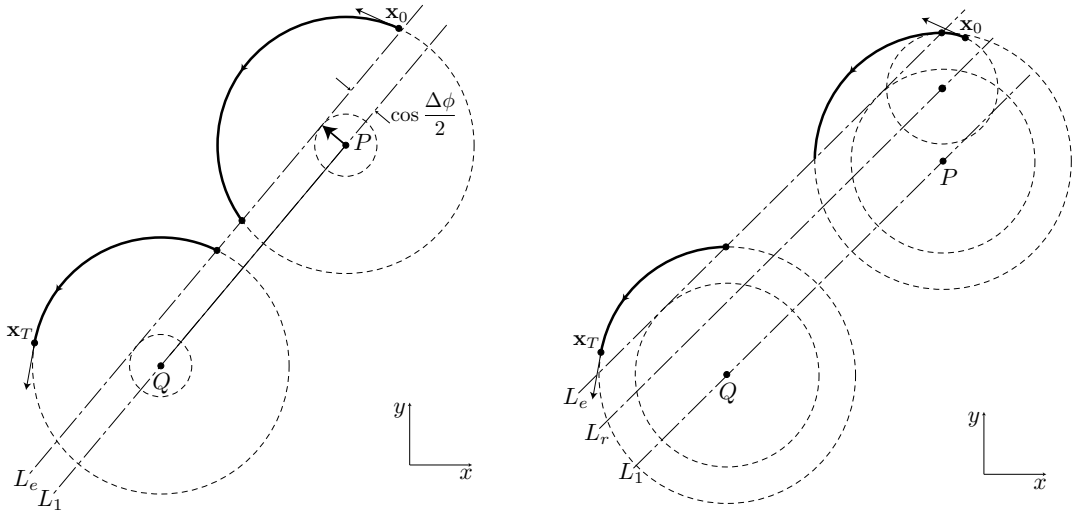

(a) A combination $(u(0), u(T)) = (1, 1)$. (b) A combination $(u(0), u(T)) = (r^{-1}, 1)$.

Figure 5.4: The construction of the extended switching line L_e.

We now define the radius r_e of extended concatenations for any combination $(u(0), u(T))$ with $u(0) = u(T)$. This construction allows extended basic pairs to join the initial state $\mathbf{x}_0$ with the final state $\mathbf{x}_T$. Let n^* be the number of basic pairs of the optimal path for unidirectional Dubins cars, and let $n \geq n^*$ be fixed. Then it follows from the results in Chapter IV that there is a closed interval in $[0, 2\pi]$ with end points satisfying $\left|\overline{PQ}\right| = 2(n-1)(1-r)\sin(\Delta\phi/2)$. This closed interval is denoted by I_n. If the radius r_e is given by

$$r_e = \begin{cases} 1 - \dfrac{\left|\overline{PQ}\right|}{2(n-1)\sin(\Delta\phi/2)} & \text{if } u(0) = 1, \\ \dfrac{\left|\overline{PQ}\right|}{2(n-1)\sin(\Delta\phi/2)} + r & \text{if } u(0) = r^{-1}, \end{cases} \tag{5.12}$$

which is defined for $\Delta\phi$ in I_n, then the extended concatenation with radius $u^{-1}(0)$ and r_e satisfies boundary conditions $\mathbf{x}(0) = \mathbf{x}_0$ and $\mathbf{x}(T) = \mathbf{x}_T$. In either case, by (5.11), (5.12) becomes

$$|PQ| = (n-1)\,\Delta d_e, \tag{5.13}$$

where $\Delta d_e = 2\,|u^{-1}(0) - r_e|\sin(\Delta\phi/2)$. Since Δd_e equals the distance between the centers of two adjacent circular arcs with the same radius, the $(n-1)$th extended basic pair and the final circular arc are smooth in the sense that at their juncture point lying on L_e they have a common tangent vector. Therefore, the extended concatenation with radius $u^{-1}(0)$ and r_e defined by (5.12) passes through two oriented points $\mathbf{x}_0$ and $\mathbf{x}_T$.

For each $n \geq n^*$, the radius r_e of extended concatenations is defined for $\Delta\phi$. It is straightforward to see that $r_e(\Delta\phi)$ is either strictly increasing or strictly decreasing on the closed interval I_n and there is a one-to-one correspondence between $\Delta\phi$ and r_e for all $\Delta\phi$ in I_n. Therefore, either of these variables can be used to characterize extended concatenations. For $u(0) = 1$, as r_e increases, $\Delta\phi$ first increases and then reaches π. For $u(0) = r^{-1}$, as r_e decreases, $\Delta\phi$ first increases and then reaches π. In either case, the extended switching line L_e approaches the line passing through P and Q as $\Delta\phi$ approaches π that is the endpoint of I_n.

We are now prepared to derive a condition for extended concatenations joining $\mathbf{x}_0$ and $\mathbf{x}_T$ to have length ranging from T^* to no less than $T^* + 2\pi r$. It follows from the results in Chapter IV that the optimal time (or length) T^* for the unidirectional Dubins car is given by

$$T^* = T_1 + (n^* - 1)\,\Delta T \tag{5.14}$$

where T_1 denotes the time at which the first basic pair has a point with ϕ_T and $\Delta T = (1-r)\,\Delta\phi^* + 2\pi r$. Since T_1 is unchanged by alterations of the radius r_e, it follows from (5.12) that the length T of the extended concatenation can be expressed

as

$$T = T_1 + (n-1)\,\Delta T_e = \begin{cases} T_1 + 2\,(n-1)\,\pi - \dfrac{\left|\overline{PQ}\right|\,(2\pi - \Delta\phi)}{2\sin\left(\Delta\phi/2\right)} & \text{if } u\,(0) = 1, \\ T_1 + 2\,(n-1)\,\pi r + \dfrac{\left|\overline{PQ}\right|\,\Delta\phi}{2\sin\left(\Delta\phi/2\right)} & \text{if } u\,(0) = r^{-1}, \end{cases} \tag{5.15}$$

where $n \geq n^*$. Note that $T^* = T_1 + 2\,(n^* - 1)\,\pi r + \left|\overline{PQ}\right|\,\Delta\phi^*/\left(2\sin\left(\Delta\phi^*/2\right)\right)$ where $\Delta\phi^*$

Since we are concerned with the variation of the length of extended concatenations, we need to deal with the difference $T - T^*$ given by

$$T - T^* = \begin{cases} \dfrac{\left|\overline{PQ}\right|\,(2\pi - \Delta\phi^*)}{2\sin\left(\Delta\phi^*/2\right)} - \dfrac{\left|\overline{PQ}\right|\,(2\pi - \Delta\phi)}{2\sin\left(\Delta\phi/2\right)} & \text{if } u\,(0) = 1, \\ \dfrac{\left|\overline{PQ}\right|\,\Delta\phi}{2\sin\left(\Delta\phi/2\right)} - \dfrac{\left|\overline{PQ}\right|\,\Delta\phi^*}{2\sin\left(\Delta\phi^*/2\right)} & \text{if } u\,(0) = r^{-1}. \end{cases}$$

The behavior of $T - T^*$, as a function of $\Delta\phi$, is the same in either case. For $\Delta\phi = \Delta\phi^*$, $T = T^*$. Then $T - T^*$ increases with an increase in $\Delta\phi$ and reaches a maximum value

$$\frac{\left|\overline{PQ}\right|\,(\pi - \Delta\phi^*)}{\sin\left(\Delta\phi^*/2\right)}$$

that occurs at $2\pi - \Delta\phi^*$. Thus, if the maximum of $T - T^*$ is greater than or equal to $2\pi r$, i.e.,

$$\frac{\left|\overline{PQ}\right|}{2\pi r}\,(\pi - \Delta\phi^*) \leq \sin\left(\Delta\phi^*/2\right) \tag{5.16}$$

then the extended concatenation has length T ranging from T^* to no less than $T^* + 2\pi r$.

5.4 Algorithm for Finding an Optimal Path for the Unidirectional Dubins Airplane

We now present an algorithm to determine an optimal path from an initial state $\mathbf{x}_0$ to a final state $\mathbf{x}_T$ for the unidirectional Dubins airplane. Let Δz be the altitude difference $z_T - z_0$ and let $T_{\Delta z} = |\Delta z| / v_{\max}$. The optimal path passes through $\mathbf{x}_T$ at either T^* or $T_{\Delta z}$ where T^* is the optimal time (or length) for the unidirectional Dubins car. If the optimal path has T^* as the transition time, then it follows from Pontryagin's minimum principle that the vertical rate $v(t)$ can have any value in V. In this case, $|\Delta z| \leq v_{\max} T^*$. If $v_{\max} T^* < |\Delta z|$, the optimal path cannot pass through $\mathbf{x}_T$ at T^* because of the altitude difference and climbing/descending constraints. In this case, the optimal path must have $T_{\Delta z}$ because $T_{\Delta z}$ is the least transition time. Thus, there are three cases to consider: (1) $T_{\Delta z} \leq T^*$, (2) $T^* < T_{\Delta z} < T^* + 2\pi r$ and (3) $T^* + 2\pi r \leq T_{\Delta z}$.

We consider first the case where $T_{\Delta z} \leq T^*$. The condition that $|\Delta z| / T^* \leq v_{\max}$ means that the optimal transition time T^* for the unidirectional Dubins car is sufficient to reach the final altitude z_T. In this case, the optimal control $v(t)$ is the constant function with value $\Delta z / T^*$ in V. Note that $v(t)$ can also be any function satisfying $\Delta z = \int_0^{T^*} v(t)\, dt$. Therefore, for $T_{\Delta z} \leq T^*$, the optimal path is a concatenation of alternating circular helices of radii 1 and r and of pitch[2] $2\pi |\Delta z| / T^*$ whose projection onto the xy plane is the optimal path for the unidirectional Dubins car from Chapter IV.

We next consider the case where $T^* + 2\pi r \leq T_{\Delta z}$. For this condition, the optimal time T^*, or any time less than $T_{\Delta z}$, is not sufficient to reach the final altitude z_T because $|v(t)| \leq v_{\max}$. In this case, the optimal control $v(t)$ is either $+v_{\max}$ or $-v_{\max}$, depending on the sign of Δz. It follows that the transition time from $\mathbf{x}_0$ to $\mathbf{x}_T$ is fixed

[2]The word "pitch" has a different meaning in aeronautics and in differential geometry. In this chapter, pitch refers to the change in height of a circular helix over one revolution of the helix.

and equal to $T_{\Delta z}$. Thus, for $T^* + 2\pi r \leq T_{\Delta z}$, the optimal path for the unidirectional Dubins airplane passes through the point $\mathbf{x}_T$ at time $T_{\Delta z}$. Since $(T_{\Delta z} - T^*) / (2\pi r) > 0$, there is exactly one positive integer m such that $m \leq (T_{\Delta z} - T^*) / (2\pi r) < m + 1$. It follows that

$$2\pi r \leq \frac{T_{\Delta z} - T^*}{m} < 4\pi r. \tag{5.17}$$

Therefore, if there is a planar path returning to the same oriented point of length ranging from $2\pi r$ to $4\pi r$, then this path with extremal control $v(t)$ can join two oriented points with the same x and y coordinates and the same direction ϕ, but with a difference of $\Delta z \pm v_{\max} T^*$ in altitude for any $T_{\Delta z}$ with $T_{\Delta z} \geq T^* + 2\pi r$.

Given any $T_{\Delta z}$ such that $T_{\Delta z} \geq T^* + 2\pi r$, there are two cases to consider: $m \geq r/(1-r)$ and $m < r/(1-r)$. For $m \geq r/(1-r)$, it follows that $2(m+1)\pi r \leq 2m\pi$. Thus, m circles of radius $(T_{\Delta z} - T^*) / (2m\pi)$ have length $T_{\Delta z} - T^*$ between $2m\pi r$ and $2(m+1)\pi r$. Note that the radius of these circles is in the closed interval $[r, 1]$. In that case, the optimal path for the unidirectional Dubins airplane is with a circular helix of radius $(T_{\Delta z} - T^*) / (2m\pi)$ and pitch $2\pi v_{\max}$ following a concatenation of alternating circular helices of radii 1 and r and of pitch $2\pi v_{\max}$ whose projection onto the xy plane is the optimal path for the unidirectional Dubins car. For example, if $r \leq 1/2$, then $m \geq r/(1-r)$ for all $m \in \mathbb{N}$, so there exists an optimal path with transition time $T_{\Delta z}$ for every time $T_{\Delta z}$ with $T_{\Delta z} \geq T^* + 2\pi r$.

For $m < r/(1-r)$, it follows that $2m\pi < 2(m+1)\pi r$. If $2m\pi r \leq T_{\Delta z} - T^* \leq 2m\pi$, then the optimal path for the unidirectional Dubins airplane can be defined in the same way as in the case where $m \geq r/(1-r)$. This argument does not apply, however, if $2m\pi < T_{\Delta z} - T^* < 2(m+1)\pi r$. This follows from unidirectional turning constraints restricting the radius of curvature to lie between r and 1. Note that since the Dubins airplane has no minimum absolute value of turn rate, its time-optimal path followed by a circular helix successfully connects any pair of $\mathbf{x}_0$ and $\mathbf{x}_T$ for the case in which $T^* + 2\pi r \leq T_{\Delta z}$ as stated in Chitsaz and LaValle (2007).

The case where $T^* + 2m\pi < T_{\Delta z} < T^* + 2(m+1)\pi r$ can be handled using the case where $T^* < T_{\Delta z} < T^* + 2\pi r$. If there exists a planar path, starting at $\mathbf{x}_0$, that passes through $\mathbf{x}_T$ at T ranging from T^* to $T^* + 2\pi r$, then this path followed by circles with radius in $[r, 1]$ passes through the oriented point $\mathbf{x}_T$ at any time $T_{\Delta z}$ with $T^* + 2m\pi < T_{\Delta z} < T^* + 2(m+1)\pi r$. This follows from the fact that $2(m+1)\pi r < 2m\pi + 2m\pi r$ for all m in $\mathbb{N}$. Therefore, the control $u(t)$ corresponding to the above path and the control $v(t) \equiv \operatorname{sgn}(\Delta z) \cdot v_{\max}$ are optimal for the unidirectional Dubins airplane. Henceforth only the case $T^* < T_{\Delta z} < T^* + 2\pi r$ will be considered.

For $T^* < T_{\Delta z} < T^* + 2\pi r$, $\psi_3(t)$ is a non-zero constant and the optimal control $v(t)$ equals $\operatorname{sgn}(\Delta z) \cdot v_{\max}$. The extended concatenation illustrated in the preceding section passes through $\mathbf{x}_T$ at any time T with $T^* \leq T \leq T^* + 2\pi r$ under the condition that the optimal path for the unidirectional Dubins car satisfies (5.16). The extended concatenation of the shortest unidirectional Dubins path with $|v(t)| \equiv v_{\max}$ followed by a circular helix of radius 1 and pitch $2\pi v_{\max}$ is the optimal path for the unidirectional Dubins airplane if $2m\pi < T_{\Delta z} - T^* < 2(m+1)\pi r$. This follows from the fact that $T^* \leq T_{\Delta z} - 2m\pi < T^* + 2\pi r$. This concatenation has length $|\Delta z| - 2m\pi v_{\max}$.

The extended concatenation has a maximum transition time $T^* + \left|\overline{PQ}\right|(\pi - \Delta\phi^*) \cdot \sin^{-1}(\Delta\phi^*/2)$, even though (5.16) does not hold for the shortest unidirectional Dubins path. This maximum length is denoted by $T_{\max}$. It follows that there is an optimal path for the unidirectional Dubins airplane if $T_{\Delta z} - 2m\pi \leq T_{\max}$. In this case, such a path is an extended concatenation with extremal control $v(t)$ followed by a circular helix of radius 1 and pitch $2\pi v_{\max}$. The optimal path has transition time $T_{\Delta z}$. When $T_{\max} < T_{\Delta z} - 2m\pi \leq T^* + 2(m+1)\pi r - 2m\pi$, a suboptimal path for the unidirectional Dubins airplane is used to join two oriented points $\mathbf{x}_0$ and $\mathbf{x}_T$. The shortest unidirectional Dubins path followed by m circles of radius r has length $T^* + 2m\pi r$. With extremal control $v(t)$, this path joins an initial oriented point $\mathbf{x}_0$ and a point with the same x and y coordinates and the same direction ϕ as

$\mathbf{x}_T$, but with a difference of $v_{\max} \cdot (T_{\Delta z} - T^* - 2m\pi r)$ in altitude. Since this altitude difference is less than or equal to $2\pi r$, an additional circle of radius r and with control $v(t) \equiv \operatorname{sgn}(\Delta z) \cdot v_{\max} ((T_{\Delta z} - T^*) / (2\pi r) - m)$ can connect such a point and the final oriented point $\mathbf{x}_T$.

The preceding results are compiled in Algorithm 5.1 defining a complete solution for the unidirectional Dubins airplane. Note that all cases return optimal solutions except Step III-5 which is included to ensure the algorithm is complete.

5.5 Algorithm Performance

We investigate the performance of our algorithm, stated in the preceding section over 10,000 test cases. Two performance metrics were considered: solution computation time and optimal (vs. suboptimal) path existence for each case. The initial and final states are constructed in a similar manner to algorithm analysis for the unidirectional Dubins car in Chapter IV. The initial state $\mathbf{x}_0 = (x_0, y_0, \phi_0)$ is uniformly distributed on $[-9, 9] \times [-9, 9] \times [0, 2\pi)$. For each $\mathbf{x}_0$, the values for the initial altitude z_0 vary over the set $\{0, 1/4, 1/2, 3/4, 1, 2, 3, 4, 5, 10\}$. Ten sample points on each axis (i.e., the x-axis, y-axis, z-axis and ϕ-axis) are considered as each component of $\mathbf{x}_0$. For every initial state $\mathbf{x}_0$, the final state $\mathbf{x}_T$ is given by $\mathbf{x}_T = (x_T, y_T, z_T, \phi_T) = (0, 0, 0, \pi/2)$. The turn rate u and the vertical rate v are bounded on $U = [1, 4]$ and $V = [-1/10, 1/10]$, respectively.

For every initial state $\mathbf{x}_0$, we evaluate the computation time of Algorithm 5.1, implemented in Matlab. Over 10,000 initial states, the average computation time of the algorithm is 3.33×10^{-3} seconds, on a 2.40 GHz Intel® Xeon® E5645 processor, running Linux Kernel 2.6.32. The average execution time of Algorithm 5.1 is of the same order of magnitude as that of the algorithm for the unidirectional Dubins car in Chapter IV because the algorithm for the unidirectional Dubins car is used in Step I and there is no recursive procedure through the remaining steps. The

Algorithm 5.1. Path-finding algorithm for the unidirectional Dubins airplane.

Given initial state $\mathbf{x}_0 = (x_0,\, y_0,\, z_0,\, \phi_0)$, final state $\mathbf{x}_T = (x_T,\, y_T,\, z_T,\, \phi_T)$, minimum radius of curvature r, and maximum rate of climb (or descent) $v_{\max}$, find an optimal path from $\mathbf{x}_0$ to $\mathbf{x}_T$ for the unidirectional Dubins airplane; if no optimal path exists, find a suboptimal path (Step III-5). Note that the maximum radius of curvature is assumed to be 1, and the vertical rate is bounded on $[-v_{\max},\, v_{\max}]$.

I. Compute the optimal time (or length) T^* for the unidirectional Dubins car using Algorithm 4.2 in Chapter IV.

II. Compute the altitude difference $\Delta z = z_T - z_0$ and $T_{\Delta z}$.

III. Find the optimal or suboptimal controls $u(t)$ and $v(t)$ corresponding to a transition from $\mathbf{x}_0$ to $\mathbf{x}_T$.

1. **If** $T_{\Delta z} \leq T^*$, **then** the optimal control $v\,(t)$ equals $\Delta z/T^*$, and the optimal control $u\,(t)$ is the same as the control corresponding to the optimal path for the unidirectional Dubins car from Chapter IV. Go to Step IV.
2. **If** $T^* < T_{\Delta z}$, **then** determine the number m of circles such that $m < (T_{\Delta z} - T^*)\,/\,(2\pi r) \leq m + 1$.
   - 2a. **If** $m \neq 0$ and $2m\pi r < T_{\Delta z} - T^* \leq 2m\pi$, **then** the optimal control $v\,(t)$ equals $\operatorname{sgn}(\Delta z) \cdot v_{\max}$, and the optimal control $u\,(t)$, $0 \leq t \leq T^*$, is the same as the optimal control for the unidirectional Dubins car and $u\,(t) \equiv 2m\pi/\,(T_{\Delta z} - T^*)$, $T^* \leq t \leq T_{\Delta z}$. Go to Step IV.
   - 2b. **Otherwise,** compute the maximum time $T_{\max}$ of the extended concatenation for the shortest unidirectional Dubins path and continue.
3. **If** $T_{\max} \geq T^* + 2\pi r$, **then** the optimal control $v\,(t)$ equals $\operatorname{sgn}(\Delta z) \cdot v_{\max}$, and the optimal control $u\,(t)$, $0 \leq t \leq T_{\Delta z} - 2m\pi r$, is the same as the control of the extended concatenation for the unidirectional Dubins car and $u\,(t) \equiv r^{-1}$, $T_{\Delta z} - 2m\pi r \leq t \leq T_{\Delta z}$. Go to Step IV.
4. **If** $T_{\max} < T^* + 2\pi r$ and $T^* < T_{\Delta z} - 2m\pi \leq T_{\max}$, **then** the optimal control $v\,(t)$ equals $\operatorname{sgn}(\Delta z) \cdot v_{\max}$, and the optimal control $u\,(t)$, $0 \leq t \leq T_{\Delta z} - 2m\pi$, is the same as the control of the extended concatenation for the unidirectional Dubins car and $u\,(t) \equiv 1$, $T_{\Delta z} - 2m\pi \leq t \leq T_{\Delta z}$. Go to Step IV.
5. **If** $T_{\max} < T^* + 2\pi r$ and $T_{\max} < T_{\Delta z} - 2m\pi \leq T^* + 2\,(m+1)\,\pi r - 2m\pi$, **then** find the suboptimal controls $u\,(t)$ and $v\,(t)$ during a time interval of length $T^* + 2\,(m+1)\,\pi r$.
   - 5a. For $0 \leq t \leq T^* + 2m\pi r$, the control $v\,(t)$ equals $\operatorname{sgn}(\Delta z) \cdot v_{\max}$ and the control $u\,(t)$, $0 \leq t \leq T^*$, is the same as the optimal control for the unidirectional Dubins car and $u\,(t) \equiv r^{-1}$, $T^* \leq t \leq T^* + 2m\pi r$.
   - 5b. For $T^* + 2m\pi r \leq t \leq T^* + 2\,(m+1)\,\pi r$, the control $v\,(t)$ equals $\operatorname{sgn}(\Delta z) \cdot v_{\max}\,((T_{\Delta z} - T^*)\,/\,(2\pi r) - m)$, and the control $u\,(t)$ equals r^{-1}. These controls generate an additional circular helix to compensate for the altitude difference $v_{\max} \cdot (T_{\Delta z} - T^* - 2m\pi r)$. Go to Step IV.

IV. Return $u\,(t)$ and $v\,(t)$ found in Step III.

computation times for the algorithm are nearly constant because the control region remains unchanged over 10,000 cases. This enables the algorithm to find an optimal or suboptimal path in real-time.

We examined the existence of optimal paths for the unidirectional Dubins airplane as percentages of the 10,000 test cases. In 99.9% of all cases, the algorithm found the time-optimal path from an initial oriented point $\mathbf{x}_0$ to a final oriented point $\mathbf{x}_T$. In 0.1% of all cases, the paths generated by the algorithm are suboptimal with transition times between $T_{\Delta z}$ and $T_{\Delta z} + 2\pi r$. Note that for all 10,000 test cases the algorithm successfully connected $\mathbf{x}_0$ and $\mathbf{x}_T$, demonstrating that the algorithm is complete. Figure 5.5 shows the number of cases in which optimal solutions were found. For each of the 100 initial points (x_0, y_0), there were 10 possible initial orientations ϕ_0. In Figure 5.5, a circled value of 10 implies all paths at that (x_0, y_0) were optimal. The initial (x_0, y_0) with suboptimal paths are indicated as circled numbers less than 10. For each altitude, as shown, cases with suboptimal solutions had relatively small distance between the initial oriented point $\mathbf{x}_0$ and final oriented point $\mathbf{x}_T$, therefore the optimal transition time T^* for each of them is less than $T_{\Delta z}$. Consequently, there is a higher probability that the algorithm will be required to find a suboptimal path from $\mathbf{x}_0$ to $\mathbf{x}_T$ in each of these cases. For each initial point (x_0, y_0, ϕ_0), the optimal transition time T^* is invariant with $|\Delta z|$, while the transition time $T_{\Delta z}$ increases with $|\Delta z|$. Therefore, more suboptimal solutions are found for lower $|\Delta z|$ because $m \geq r/(1-r)$ for all $m \in \mathbb{N}$ and all $r \leq 1/2$.

The likelihoods of selecting each of the five steps in Step III for each altitude difference Δz are shown in Table 1. For $|\Delta z| = 0$, there is no case in which a suboptimal path joins $\mathbf{x}_0$ with $\mathbf{x}_T$ because our problem is equivalent to the problem of finding the shortest paths for the unidirectional Dubins car. As $|\Delta z|$ increases from 0, the number of cases in which $T^* + 2\pi r \leq T_{\Delta z}$ increases and consequently the number of optimal paths corresponding to Step III-2a increases, as shown in Table 1.

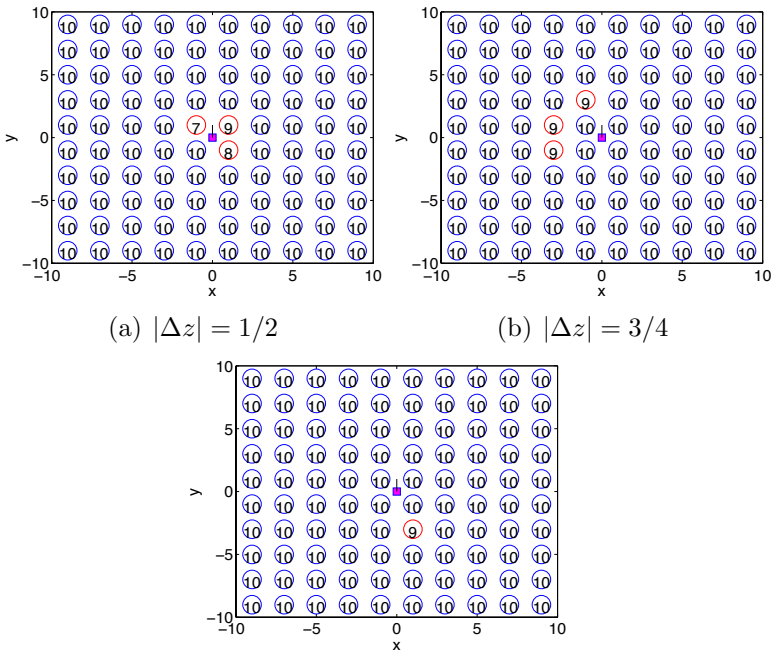

(a) $|\Delta z| = 1/2$ (b) $|\Delta z| = 3/4$

(c) $|\Delta z| = 1$

Figure 5.5: Uniformly distributed initial states for initial altitudes $z_0 = 1/2,\ 3/4,\ 1$. States resulting in optimal paths and suboptimal paths are indicated as the circled number 10 and numbers less than 10, respectively.

In particular, for $|\Delta z| \geq 4$, every optimal transition time T^* is less than $T_{\Delta z} - 2\pi r$, so the algorithm only generates an optimal path corresponding to Step III-2a. This follows from the fact that if $r \leq 1/2$, then $m \geq r/(1-r)$ for all $m \in \mathbb{N}$. By contrast, if $1/2 \leq |\Delta z| \leq 3$, then there are cases in which $T^* < T_{\Delta z} < T^* + 2\pi r$. In these cases, the algorithm determines whether or not there is an extended concatenation with transition time $T_{\Delta z}$.

Figure 5.6 illustrates the optimal or suboptimal path generated by the algorithm for different initial altitude cases when $(x_0,\ y_0,\ \phi_0) = (-1,\ 3,\ 6\pi/5)$. Since the optimal transition time T^* does not depend on z_0, it follows that $T^* = 6.4274$ for $z_0 = 1/2,\ 3/4,\ 1$. By comparing T^* with $T_{\Delta z}$ for each z_0, the optimal path for $z_0 = 1/2$ is a concatenation of alternating circular helices of radii 1 and r and of pitch $2\pi\,|\Delta z|\,/T^*$ whose projection onto the xy plane is the optimal path for the unidirectional Dubins car, as shown in Figure 5.6 (a). For $z_0 = 3/4$, the optimal time T^* is not sufficient

Table 5.1: The likelihoods of selecting each of the five steps in Step III over 10 initial altitudes for $r = 1/4$ and for $v_{\max} = 1/10$.

$\lvert\Delta z\rvert$	Step III-1	Step III-2a	Step III-2b		
			Step III-3	Step III-4	Step III-5
$\lvert\Delta z\rvert = 0$	100%	0%	0%	0%	0%
$\lvert\Delta z\rvert = 1/4$	99.6%	0%	0.4%	0%	0%
$\lvert\Delta z\rvert = 1/2$	97.0%	1.3%	1.1%	0%	0.6%
$\lvert\Delta z\rvert = 3/4$	93.6%	4.2%	1.8%	0.1%	0.3%
$\lvert\Delta z\rvert = 1$	86.6%	9.7%	3.3%	0.3%	0.1%
$\lvert\Delta z\rvert = 2$	46.8%	46.0%	7.2%	0%	0%
$\lvert\Delta z\rvert = 3$	3.0%	94.1%	2.9%	0%	0%
$\lvert\Delta z\rvert = 4$	0%	100%	0%	0%	0%
$\lvert\Delta z\rvert = 5$	0%	100%	0%	0%	0%
$\lvert\Delta z\rvert = 10$	0%	100%	0%	0%	0%

to reach final altitude z_T. To compensate for the increase in altitude difference $|\Delta z|$, it suffices to add one circle of radius r to the path. Since $T_{\max} < T_{\Delta z} < T^* + 2\pi r$, the algorithm generates a suboptimal path, as shown in Figure 5.6 (b). For $z_0 = 1$, $T^* + 2\pi r \leq T_{\Delta z}$, so the algorithm finds an optimal path with transition time $T_{\Delta z}$ corresponding to Step III-2a. As illustrated in Figure 5.6 (c), a circular helix of radius in $[r, 1]$ and pitch $2\pi v_{\max}$ is needed during a time interval of length $T_{\Delta z} - T^*$.

Figure 5.7 illustrates optimal paths generated by the algorithm for different initial orientations when $(x_0, y_0, z_0) = (-1, 3, 3/4)$. Since the optimal transition time T^* relies on ϕ_0, time T^* has different values for different orientations: $T^* = 7.0074$ for $\phi_0 = 4\pi/5$ and $T^* = 6.51$ for $\phi_0 = \pi$. Although $T^* < T_{\Delta z} < T^* + 2\pi r$ in either case, the maximum transition time $T_{\max}$ is greater than $T_{\Delta z}$. Thus, the extended concatenation with extremal control $v(t)$ passes through the final oriented point $\mathbf{x}_T$ at time $T_{\Delta z}$ by decreasing the maximum turning radius on the solution path to r_e, as shown in Figure 5.7.

As a final analysis, we examined the likelihoods of selecting each of the five steps in Step III over our 10,000 initial states for different minimum turning radii $r = 1/4, 1/2, 3/4$, as summarized in Table 2. As r increases, the optimal transition time

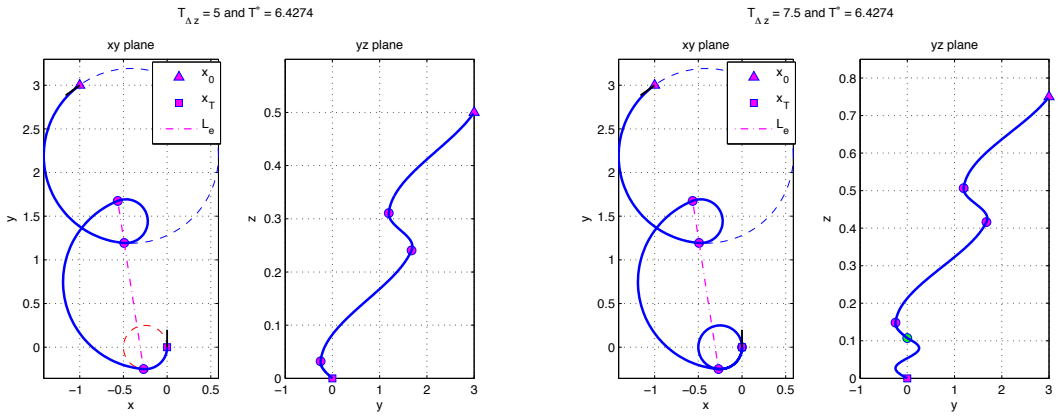

(a) An optimal solution path for $z_0 = 1/2$. (b) A suboptimal solution path for $z_0 = 3/4$.

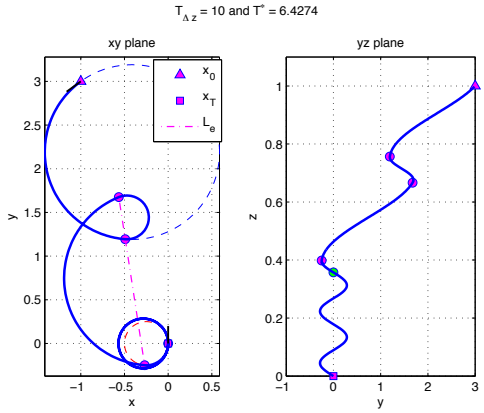

(c) An optimal solution path for $z_0 = 1$.

Figure 5.6: Example solution paths from $(x_0, y_0, \phi_0) = (-1, 3, 6\pi/5)$ with initial altitudes $z_0 = 1/2, 3/4, 1$ to $\mathbf{x}_T = (x_0, y_0, z_0, \phi_0) = (0, 0, 0, \pi/2)$.

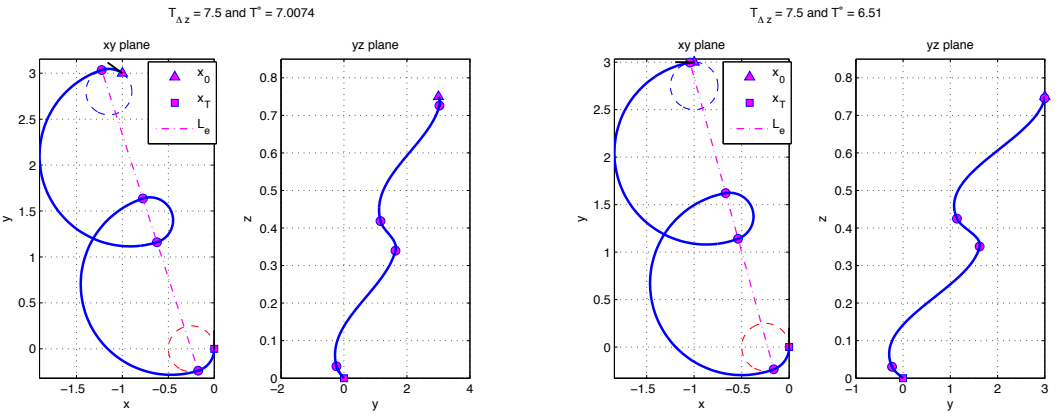

(a) An optimal solution path for $\phi_0 = 4\pi/5$. (b) An optimal solution path for $\phi_0 = \pi$.

Figure 5.7: Example solution paths from $(x_0, y_0, z_0) = (-1, 3, 3/4)$ with initial orientations $\phi_0 = 4\pi/5, \pi$ to $\mathbf{x}_T = (x_0, y_0, z_0, \phi_0) = (0, 0, 0, \pi/2)$.

T^* of the unidirectional Dubins path for each initial state increases. This follows from the fact that the number of basic pairs is inversely proportional to the difference $1-r$. Thus, the likelihood of choosing the case where $T_{\Delta z} \leq T^*$ is increased. However, the incidence of the suboptimal cases increases with r because the maximum transition time of extended concatenations decreases with r.

Table 5.2: The likelihoods of selecting each of the five steps in Step III over 10 initial altitudes for $v_{\max} = 1/10$.

r	Optimal path				Suboptimal path
	Step III-1	Step III-2a	Step III-3	Step III-4	Step III-5
$r = 1/4$	52.66%	45.53%	1.67%	0.04%	0.1%
$r = 1/2$	70.44%	26.54%	2.24%	0.41%	0.37%
$r = 3/4$	90.13%	7.15%	0.27%	1.57%	0.88%

5.6 Application: Emergency Landing for a Unidirectional Dubins airplane

In this section, we present application of Algorithm 5.1 to an aircraft emergency landing planning problem. For a damaged aircraft, the primary goal is to safely land on a runway. In an emergency, the pilot or autopilot first selects a runway (or landing site) within the local area that can safely accommodate the disabled aircraft (see Atkins et al. (2006)). The flight management system, with appropriate flight envelope knowledge, then constructs a landing trajectory to the selected runway.

Figure 5.8 recalls the discretized flight envelope for an F-16 aircraft flying at an altitude of 10,000 ft with an aileron jammed at +14 degrees (Stevens and Lewis (2003); Strube (2005)). In this case, the aircraft cannot fly straight at an airspeed of 250 ft/sec. Even though the aircraft can fly straight for airspeeds slower than 250 ft/sec, the aircraft may encounter stall near 200 ft/sec which is still too high for straight flight given even a slim margin from the envelope boundary. This follows from the fact that the stall speed for turning flight is typically higher than that for

straight and level flight. Since more feasible trim states are available at low altitudes than at high altitudes due to higher-magnitude aerodynamic forces and moments, the disabled F-16 aircraft retains the ability to follows a straight path at low altitudes ($<$ 10,000 ft). To enable a straight final approach, we assume that this ability is possible at an altitude of 2,000 ft or less, so we only need to apply a unidirectional turning constraint down to a final approach waypoint to allow a stabilized final segment to touchdown.

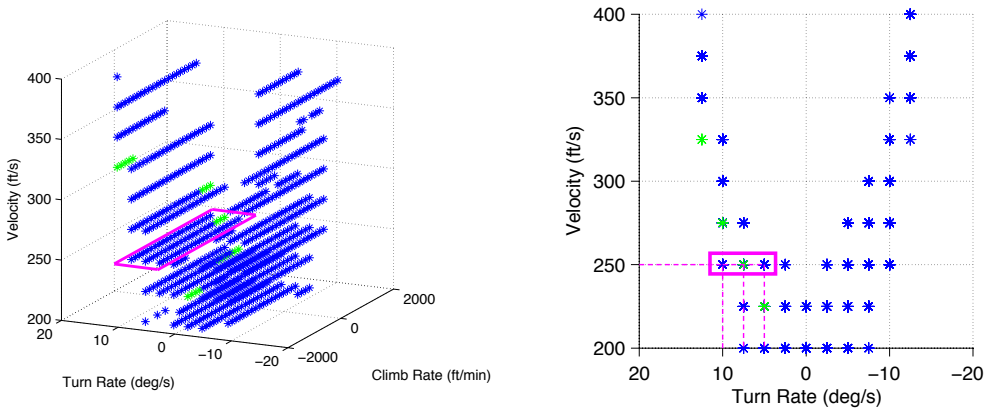

(a) $\left(V,\, \dot{\phi},\, \dot{z}\right)$-space (b) $\left(V,\, \dot{\phi}\right)$-space

Figure 5.8: Flight envelope for the F-16 aircraft flying at an altitude of 10,000 ft with an aileron jammed at 14 degrees.

We model the disabled F-16 aircraft at a speed of 250 ft/sec whose performance is shown in Figure 5.8. The aileron jam at 14° occurs at initial latitude 40.780°N and longitude 73.875°W, with full initial state $\mathbf{x}_0$ is given by $\mathbf{x}_0 = (x_0,\, y_0,\, z_0,\, \phi_0) = (73.875°\,\mathrm{W},\, 40.780°\,\mathrm{N},\, 10000\,\mathrm{ft},\, 210°)$. The F-16 has a range of turn rates varying from -10 deg/sec to -5 deg/sec and from $+5$ deg/sec to $+10$ deg/sec consistent with the discretized flight envelope shown in Fig. 5.8. Without loss of generality, we treat the F-16 capable of turning right (or clockwise). The F-16 is assumed to have a range of vertical rates varying from -25 ft/sec to 25 ft/sec; we are only interested in a descent to landing.

LaGuardia Airport (LGA) is closest to the location where the emergency occurs.

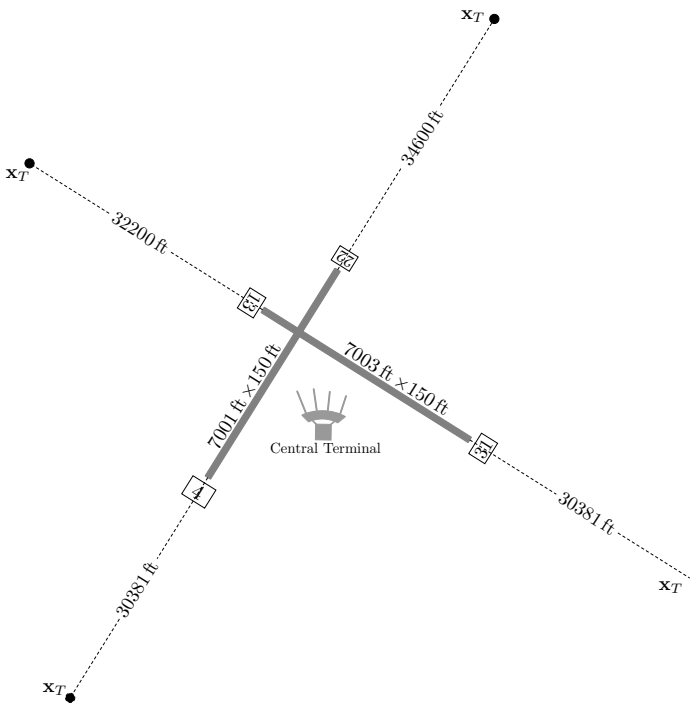

Figure 5.9: The final oriented point $\mathbf{x}_T$ near LGA.

We presume no wind for this case study thus no preferred landing direction. LGA has two runways, as shown in Figure 5.9. For each runway threshold, the final oriented point $\mathbf{x}_T$ is its final approach fix from which an aircraft executes a straight-in final approach presumed possible since the altitude of the fix is less than 2,000 ft. Thus, for the damaged F-16 aircraft, the algorithm can plan four possible landing trajectories, one for each runway end, i.e., runways 4-22 and 13-31. For this case study, every path generated by the algorithm is an optimal path corresponding to Step III-1 (i.e., the shortest unidirectional Dubins path with an unsaturated vertical rate), as illustrated in Figure 5.10 and summarized in Table 5.3.[3] The optimal path to LGA runway 22 has the minimum transition time because it has the minimum distance from $\mathbf{x}_0$ to $\mathbf{x}_T$ of the four solution paths. If the F-16 has the same aileron damage at altitudes less than 10,000 ft, the optimal time of the unidirectional Dubins car for each $\mathbf{x}_T$ remains unchanged. Therefore, at lower altitudes, the algorithm produces optimal paths with

[3]Coordinates of final approach fixes are based on an Area Naviation (RNAV) chart from http://flightaware.com

the same transition times as when $z_0 = 10,000$ ft, but with the smaller vertical rates than when $z_0 = 10,000$ ft because the absolute altitude difference $|\Delta z|$ decreases with z_0.

Table 5.3: Comparison of optimal paths to LGA final approach fixes.

Runway	$(x_T,\ y_T,\ z_T)$	$z_0 = 10,000$ ft		
		Step	T	dist $(\mathbf{x}_0, \mathbf{x}_T)$
LGA 04	(73.937° W, 40.705° N, 1700 ft)	III-1	959.008 s	50,837 ft
LGA 13	(73.958° W, 40.820° N, 1800 ft)	III-1	536.862 s	29,884 ft
LGA 22	(73.810° W, 40.859° N, 1900 ft)	III-1	499.373 s	28,689 ft
LGA 31	(73.882° W, 40.736° N, 1700 ft)	III-1	934.355 s	50,194 ft

In this case study, we assumed the disabled F-16 aircraft can fly straight at an altitude of 2,000 ft. However, with more severe damage or failure, e.g., higher angle jam, this ability might be impossible at any altitude. If the disabled F-16 loses the ability to fly straight throughout the landing, it is better for a turning landing trajectory to arrive at a runway threshold, not at its final approach fix. Figure 5.11 illustrates optimal paths to the four runway thresholds generated by the algorithm. The change of final oriented points decreases the distance between $\mathbf{x}_0$ and $\mathbf{x}_T$ decreasing the shortest time T^* for the unidirectional Dubins car, while it increases the absolute altitude difference $|\Delta z|$ increasing the time $T_{\Delta z}$. Therefore, for each threshold, the algorithm produces the optimal path corresponding to a different step in Algorithm 5.1, as summarized in Table 5.4.

For runways LGA 04 and LGA 31, the optimal paths are the shortest paths for the unidirectional Dubins car with unsaturated vertical rates, consequently they have transition time T^*. For runways LGA 13 and LGA 22, the shortest paths for the unidirectional Dubins car with saturated vertical rate are not sufficient to reach the final altitude z_T, consequently the optimal paths have transition time $T_{\Delta z}$. Of the four solution paths, the optimal path to LGA runway 13 has the minimum transition time. If the initial altitude is lower than 9740.58 ft, the optimal path to LGA runway 22 has the minimum transition time. This follows from the fact that the optimal

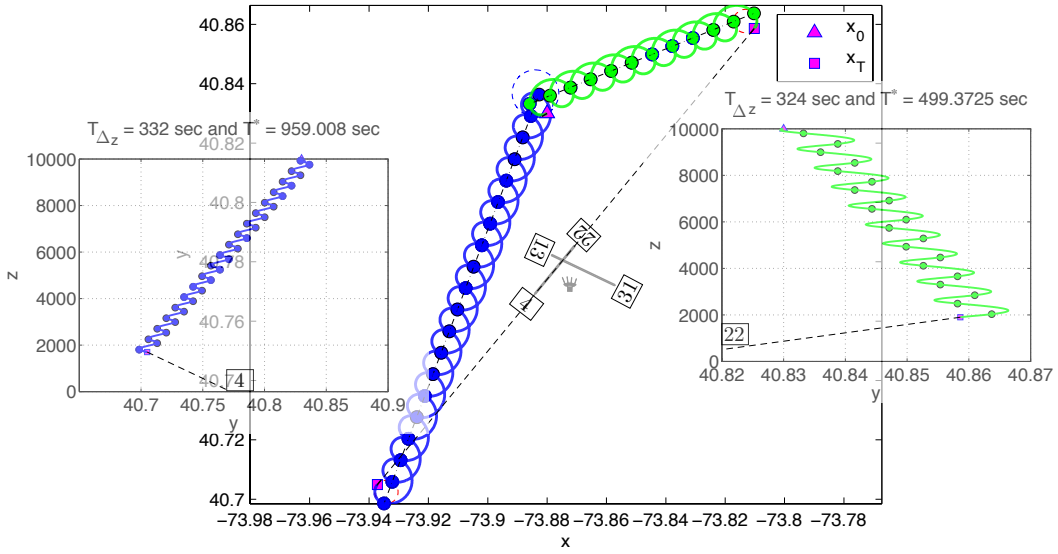

(a) Runway 4-22 final approach fixes.

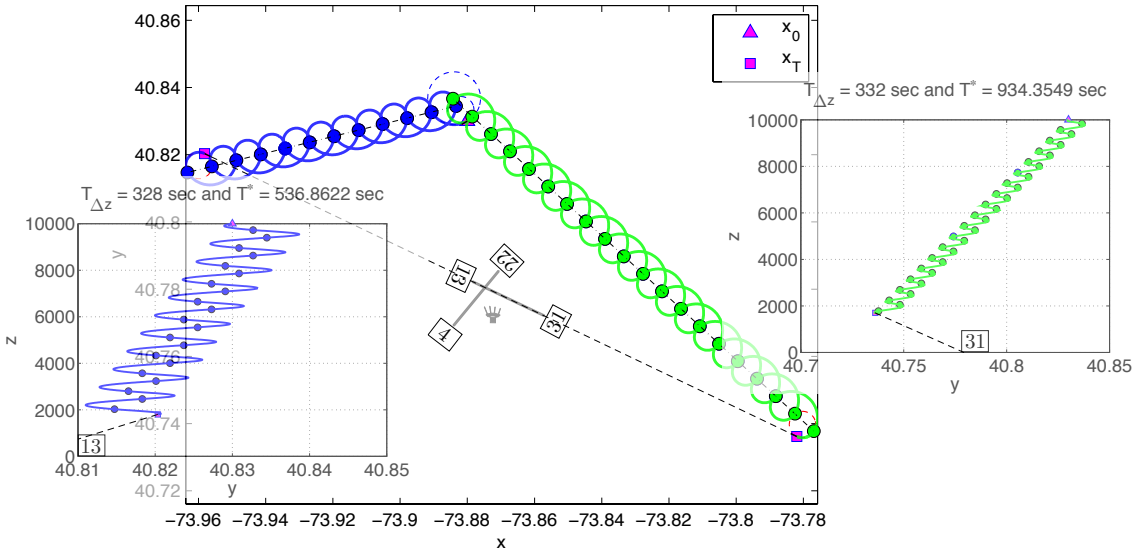

(b) Runway 13-31 final approach fixes.

Figure 5.10: Optimal paths to LGA final approach fixes for the F-16 aircraft with an aileron jammed at +14 degrees.

time of the unidirectional Dubins car for each $\mathbf{x}_T$ remains unchanged and the fact that time $T_{\Delta z}$ for each $\mathbf{x}_T$ decreases with z_0.

Table 5.4: Comparison of simulation results of optimal paths to LGA thresholds.

Runway	$(x_T,\, y_T,\, z_T)$	$h_0 = 10,000$ ft		
		Step	T	dist $(\mathbf{x}_0, \mathbf{x}_T)$
LGA 04	(73.884° W, 40.769° N, 20.6 ft)	III-1	467.175 s	24,380 ft
LGA 13	(73.879° W, 40.782° N, 11.6 ft)	III-4	399.536 s	20,073 ft
LGA 22	(73.871° W, 40.785° N, 11.5 ft)	III-2a	399.540 s	19,382 ft
LGA 31	(73.857° W, 40.772° N, 6.7 ft)	III-1	444.982 s	24,823 ft

5.7 Conclusions

This chapter has derived time-optimal paths for the unidirectional Dubins airplane as an extension of the unidirectional Dubins car. By Pontryagin's minimum principle, the optimal path is divided into two paths, one with transition time for the unidirectional Dubins car, and the other with transition time equal to the absolute altitude difference divided by the maximum vertical rate. The former has the same optimal control as the unidirectional Dubins car with unsaturated vertical rate. The latter has saturated vertical rate but the optimal or suboptimal turn rate depends on the altitude difference and the absolute maximum vertical rate. In the latter case, the shortest unidirectional Dubins path or its extended path with saturated vertical rate followed by a circular helix of radius in $[r,\, 1]$ is time-optimal if it exists. Otherwise, a suboptimal but feasible path is planned by considering an additional circle of radius r with saturated vertical rate.

The corresponding optimal path-finding algorithm was applied to a series of numerical examples. The algorithm was able to plan optimal paths for most cases, but there are some cases in which suboptimal paths are found. Moreover, an application of our results to an emergency landing problem verified that the severely disabled aircraft can generate landing trajectories to runways at a specific final position and

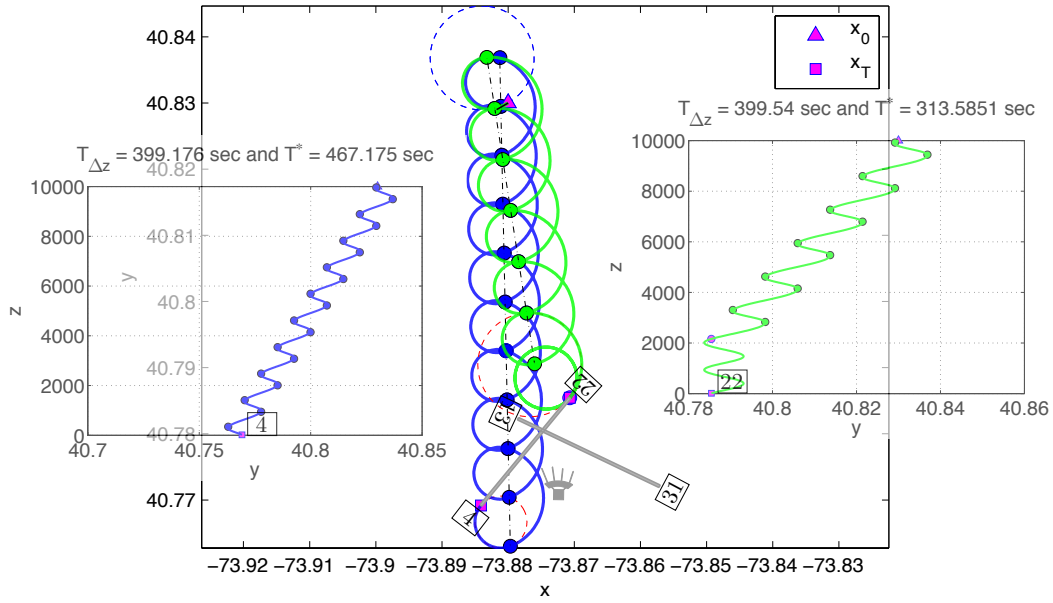

(a) Runway 4-22.

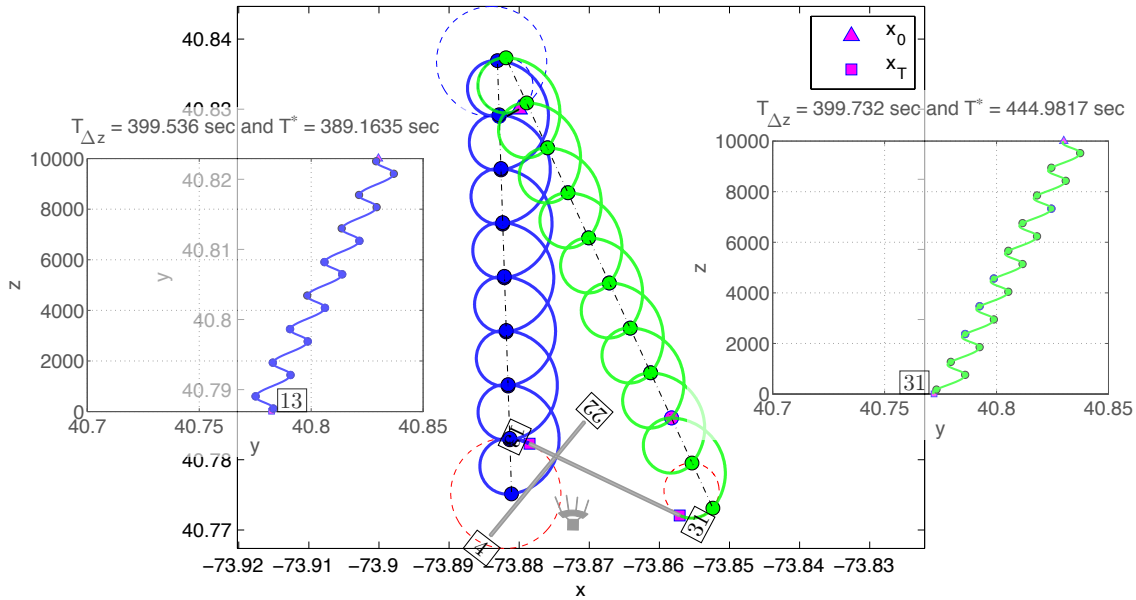

(b) Runway 13-31.

Figure 5.11: Optimal paths to LGA runway thresholds for the F-16 aircraft with an aileron jammed at +14 degrees.

orientation. Of all such landing paths, the optimal path with the minimum transition time does not necessarily translate to the minimum distance between two oriented points.

We have defined the optimal or suboptimal path for the unidirectional Dubins airplane in the unobstructed space. In future work, paths will be planned around fixed and moving obstacles in the environment. Furthermore, a control scheme will be developed to track optimal or suboptimal paths generated by the algorithm. Work remains to identify a complete algorithm for which all solutions are guaranteed to be optimal.

CHAPTER VI

Conclusions and Future Work

6.1 Conclusions

This dissertation has addressed the problem of finding time-optimal paths for vehicles constrained to forward and unidirectional (clockwise or counterclockwise) turning motion to travel from a given initial oriented point to a given final oriented point. While previous motion planning research has extensively dealt with finding time-optimal paths for vehicles with minimum turning radius constraints, this dissertation for the first time embarks on finding time-optimal paths for vehicles unable to travel straight due to extreme constraints imposed by damage and/or failure conditions. This research derives a complete and real-time path planning method for both Dubins cars (two-dimensional) and Dubins airplanes (three-dimensional) constrained to unidirectional turning motions.

The path-planning problem is posed as a variant of the Dubins car problem in which vehicles move forward in a plane with constant speed and with a given maximum turn rate (i.e., minimum turning radius). Unlike the Dubins car and variations previously derived, the rate of turn is allowed to vary within given lower and upper bounds that are of the same sign, representing the unidirectional turning constraint. In two-dimensional Euclidean space, we extend the Dubins car to a Dubins car with unidirectional turning constraints. In three-dimensional Euclidean space, we then

extend the Dubins car with unidirectional turning constraints to a Dubins airplane with unidirectional turning constraints.

For both unidirectional Dubins vehicle formulations, this dissertation demonstrates the existence of optimal paths connecting given initial and final oriented points. We first defined admissible controls which yield paths of the Dubins car and airplane with the unidirectional turning constraint to reach a given final oriented point. In addition, we constructed continuous (not piecewise-continuous) controls which transfer the unidirectional Dubins car to a specified final oriented point. We then employed Filippov's existence theorem for the time-optimal problem to show the existence of optimal solutions. This work formed an initial basis of the solutions derived in subsequent chapters.

Time-optimal paths for the unidirectional Dubins car

We applied the minimum principle of Pontryagin to characterize the optimal path for the unidirectional Dubins car. As a result, we were able to determine the following three possible candidates for the optimal path: the arc of a circle with normalized maximum radius 1, the arc of a circle with normalized minimum radius r, or the concatenation of alternating arcs of two tangent circles with radii r and 1 at every switching point. On the basis of the geometric properties of the concatenations, we showed that the time at which the concatenations passes through a given final oriented point only depends on the value of the Hamiltonian. This fact enables direct identification of the optimal path for the unidirectional Dubins car. We then presented algorithms for finding time-optimal Dubins paths with unidirectional turning constraints and verified that these algorithms are complete and run in real-time though Matlab simulations.

Time-optimal paths for the unidirectional Dubins airplane

Pontryagin's minimum principle was again applied to derive necessary conditions of time-optimal paths for the Dubins airplane problem given unidirectional turning constraints. Such optimal paths have one of two transition times: (1) the shortest time for the unidirectional Dubins car and (2) the time equal to the absolute altitude difference divided by the maximum vertical rate. The optimal path with the transition time given by case (1) has the same optimal control as the unidirectional Dubins car with an unsaturated vertical rate. The optimal path with the transition time given by case (2) has a saturated vertical rate, but the optimal or suboptimal turn rate depends on the altitude difference and the absolute maximum vertical rate. In case (2), the shortest unidirectional Dubins car path or its extended path with the saturated vertical rate followed by a circular helix of radius in $[r, 1]$ is time-optimal if it exists. Otherwise, to ensure the algorithm is complete, a suboptimal path is planned by considering an additional circle of radius r with the saturated vertical rate. Thus, we presented a complete algorithm for finding time-optimal paths for the unidirectional Dubins airplane. We validated the completeness and real-time performance of the Dubins airplane algorithm on a series of test cases. We also applied the algorithm to an aircraft emergency landing case study, showing that a severely disabled aircraft can successfully generate a family of landing trajectories to nearby runways, each defined by a final approach position and orientation.

6.2 Future work

The generation of motion plans involves two steps: path planning, the computation of controls achieving specified tasks; and path tracking, the execution of the motion following given paths. This dissertation has focused on path planning for vehicles with unidirectional turning constraints. To execute the motions that follow these

geometric paths, the trajectory tracking problem must also be considered, particularly given the challenge of unidirectional turning constraints. To this end, a controller might approximately linearize the error dynamics around a given geometric path, and switch between controllers as turning radius (or rate) changes are commanded. Guarantees of stability will likely require a hybrid system analysis (Souères et al. (2001)) to ensure switching as well as nominal tracking control is stable.

The weather, especially wind, also can have a significant effect on the ability of a vehicle to follow a given path. For example, an airplane flying even at its maximum speed can be substantially blown off course by the wind. The path-planning problem for the Dubins vehicles in steady uniform winds has been studied recently by McGee and Hedrick (2007), Rysdyk (2007) and Techy and Woolsey (2009). In these studies, time-optimal paths consist of straight and trochoidal segments. In future work, the model for the unidirectional Dubins vehicles must also be augmented to consider wind effects. To this end, we may again employ Pontryagin's minimum principle to find time-optimal paths in steady uniform winds.

Air Traffic Control (ATC) can provide emergency airspace and landing clearances to the disabled aircraft, but to do so quickly any path planner must be integrated via data link to the ATC system. New path planners must also be integrated with existing systems (capabilities) such as the Traffic Alert and Collision Avoidance Systems (TCAS) (Harman (1989)) and the Center-TRACON Automation System (CTAS) (Erzberger et al. (1993)). A key requirement for these technologies is the prediction and resolution of path conflicts. The conflict resolution problem has been widely studied in a number of papers, e.g., Krozel et al. (1996), Zhao and Schultz (1997), Tomlin et al. (1998), and Bicchi and Pallottino (2000). However, in these papers, all aircraft have been assumed to have nominal, or in some cases matching, performance. As a first step to integration, the disabled aircraft can be prioritized and all other aircraft asked to deconflict with the emergency aircraft's known path. In future work, conflict

resolution algorithms should more tightly integrate heterogeneous sets of performance constraints, including those present for a unidirectional Dubins airplane.

BIBLIOGRAPHY

BIBLIOGRAPHY

Atkins, E. M., I. A. Portillo, and M. J. Strube (2006), Emergency flight planning applied to total loss of thrust, *Journal of Aircraft*, *43*(4), 1205–1216, doi: 10.2514/1.18816.

Bailey, R., R. Hostetler, K. Barnes, C. Belcastro, and C. Belcastro (2005), Experimental validation: Subscale aircraft ground facilities and integrated test capability, in *AIAA Guidance, Navigation, and Control Conference and Exhibit*, American Institute of Aeronautics and Astronautics, doi:doi:10.2514/6.2005-6433.

Bakolas, E., and P. Tsiotras (2011), Optimal synthesis of the asymmetric sinistral/dextral Markov–Dubins problem, *Journal of Optimization Theory and Applications*, *150*(2), 233–250, doi:10.1007/s10957-011-9841-3.

Balachandran, S., and E. M. Atkins (2013), Flight safety assessment and management during takeoff, in *AIAA Infotech@Aerospace (I@A) Conference*, American Institute of Aeronautics and Astronautics, doi:doi:10.2514/6.2013-4805.

Balkcom, D. J., and M. T. Mason (2002), Time optimal trajectories for bounded velocity differential drive vehicles, *International Journal of Robotics Research*, *21*(3), 199–217,

Balkcom, D. J., P. A. Kavathekar, and M. T. Mason (2006), Time-optimal trajectories for an omni-directional vehicle, *International Journal of Robotics Research*, *25*(10), 985–999,

Belcastro, C., and S. Jacobson (2010), Future integrated systems concept for preventing aircraft loss-of-control accidents, in *AIAA Guidance, Navigation, and Control Conference*, American Institute of Aeronautics and Astronautics, doi: doi:10.2514/6.2010-8142.

Bellman, R., and R. E. Kalaba (1965), *Dynamic programming and modern control theory*, Academic Press, New York.

Betts, J. T. (1998), Survey of numerical methods for trajectory optimization, *Journal of Guidance, Control, and Dynamics*, *21*(2), 193–207, doi:10.2514/2.4231.

Betts, J. T. (2010), *Practical Methods for Optimal Control and Estimation Using Nonlinear Programming*, second ed., Society for Industrial and Applied Mathematics, doi:10.1137/1.9780898718577.

Bicchi, A., and L. Pallottino (2000), On optimal cooperative conflict resolution for air traffic management systems, *Intelligent Transportation Systems, IEEE Transactions on*, *1*(4), 221–231, doi:10.1109/6979.898228.

Boissonnat, J.-D., A. Cérézo, and J. Leblond (1994), Shortest paths of bounded curvature in the plane, *11*(1-2), 5–20, doi:10.1007/BF01258291.

Bosworth, J., and P. Williams-Hayes (2007), Flight test results from the nf-15b intelligent flight control system (ifcs) project with adaptation to a simulated stabilator failure, in *AIAA Infotech@Aerospace 2007 Conference and Exhibit*, American Institute of Aeronautics and Astronautics, doi:doi:10.2514/6.2007-2818.

Cesari, L. (1965), An existence theorem in problems of optimal control, *Journal of the Society for Industrial and Applied Mathematics Series A Control*, *3*(1), 7–22, doi:10.1137/0303002.

Cesari, L. (1966), Existence theorems for optimal solutions in pontryagin and lagrange problems, *Journal of the Society for Industrial and Applied Mathematics Series A Control*, *3*(3), 475–498, doi:10.1137/0303032.

Cesari, L. (1983), *Optimization-theory and applications: problems with ordinary differential equations*, vol. 17, Springer-Verlag, New York.

Chen, T. L., and A. R. Pritchett (2001), Development and evaluation of a cockpit decision-aid for emergency trajectory generation, *Journal of Aircraft*, *38*(5), 935–943, doi:10.2514/2.2856.

Chitsaz, H., and S. M. LaValle (2007), Time-optimal paths for a Dubins airplane, in *2007 46th IEEE Conference on Decision and Control*, pp. 2379–2384, doi:10.1109/CDC.2007.4434966.

Choi, H., E. M. Atkins, and G. Yi (2010), Flight envelope discovery for damage resilience with application to an F-16, in *AIAA Infotech@Aerospace 2010*, American Institute of Aeronautics and Astronautics, doi:10.2514/6.2010-3353.

Cormen, T. H., C. E. Leiserson, R. L. Rivest, and C. Stein (2001), *Introduction to Algorithms, Second Edition*, Cambridge, MA, The MIT Press and McGraw-Hill Book Company.

do Carmo, M. P. (1976), *Differential geometry of curves and surfaces*, Englewood Cliffs, NJ, Prentice-Hall.

Dolinskaya, I. S., and A. Maggiar (2012), Time-optimal trajectories with bounded curvature in anisotropic media, *International Journal of Robotics Research*, *31*(14), 1761–1793,

Dubins, L. E. (1957), On curves of minimal length with a constraint on average curvature, and with prescribed initial and terminal positions and tangents, *American Journal of Mathematics*, *79*(3), 497–516, doi:10.2307/2372560.

Erzberger, H., T. J. Davis, and S. Green (1993), Design of center-tracon automation system, in *AGARD Guidance and Control Sym. Machine Intelligence in Air Traffic Management*, pp. 11.1–11.12.

Filippov, A. (1962), On certain questions in the theory of optimal control, *Journal of the Society for Industrial and Applied Mathematics Series A Control*, *1*(1), 76–84, doi:10.1137/0301006.

Harman, W. (1989), Tcas- a system for preventing midair collisions, *The Lincoln Laboratory Journal*, *2*, 437–458.

Johnson, H. H. (1974), An application of the maximum principle to the geometry of plane curves, *Proceedings of the American Mathematical Society*, *44*(2), 432–435, doi:10.2307/2040451.

Jordan, T. L., W. M. Belcastro, M. Christine, J. M. Foster, G. H. Shah, G. Howland, and R. Kidd (2004), Development of a dynamically scaled generic transport model testbed for flight research experiments, in *AUVSI Unmanned Systems North America 2004*, AUVSI, Arlington, VA.

Krishnakumar, K., N. Nguyen, and J. Kaneshige (2010), *Integrated Resilient Aircraft Control*, John Wiley & Sons, Ltd, doi:10.1002/9780470686652.eae510.

Krozel, J., T. Mueller, and G. Hunter (1996), Free flight conflict detection and resolution analysis, in *Guidance, Navigation, and Control Conference*, American Institute of Aeronautics and Astronautics, doi:doi:10.2514/6.1996-3763.

McDonough, K., I. Kolmanovsky, and E. M. Atkins (2014), Recoverable sets of initial conditions and their use for aircraft flight planning after a loss of control event, in *AIAA Guidance, Navigation, and Control Conference*, American Institute of Aeronautics and Astronautics, doi:10.2514/6.2014-0786.

McGee, T. G., and J. K. Hedrick (2007), Optimal path planning with a kinematic airplane model, *Journal of Guidance, Control, and Dynamics*, *30*(2), 629–633, doi:10.2514/1.25042.

Meek, D. S., and D. J. Walton (1989), The use of cornu spirals in drawing planar curves of controlled curvature, *Journal of Computational and Applied Mathematics*, *25*(1), 69–78, doi:http://dx.doi.org/10.1016/0377-0427(89)90076-9.

Meuleau, N., C. Plaunt, D. E. Smith, and T. B. Smith (2009), An emergency landing planner for damaged aircraft, in *Twenty-First Innovative Applications of Artificial Intelligence*.

Nguyen, N., K. Krishnakumar, J. Kaneshige, and P. Nespeca (2006), Dynamics and adaptive control for stability recovery of damaged asymmetric aircraft, in *AIAA Guidance, Navigation, and Control Conference and Exhibit*, American Institute of Aeronautics and Astronautics, doi:10.2514/6.2006-6049.

Nguyen, N. T., K. S. Krishnakumar, J. T. Kaneshige, and P. P. Nespeca (2008), Flight dynamics and hybrid adaptive control of damaged aircraft, *Journal of Guidance, Control, and Dynamics*, *31*(3), 751–764, doi:10.2514/1.28142.

Pinelis, I. (2005), Cyclic polygons with given edge lengths: Existence and uniqueness, *Journal of Geometry*, *82*(1-2), 156–171, doi:10.1007/s00022-005-1752-8.

Pontryagin, L. S., V. G. Boltyanskii, R. V. Gamkrelidze, and E. F. Mishchenko (1962), *The mathematical theory of optimal processes*, New York, Interscience Publishers.

Reeds, J. A., and L. A. Shepp (1990), Optimal paths for a car that goes both forwards and backwards., *Pacific Journal of Mathematics*, *145*(2), 367–393.

Reister, D. B., and S. M. Lenhart (1995), Time-optimal paths for high-speed maneuvering, *International Journal of Robotics Research*, *14*(2), 184–194.

Rysdyk, R. (2007), Course and heading changes in significant wind, *Journal of Guidance, Control, and Dynamics*, *30*(4), 1168–1171, doi:10.2514/1.27359.

Rysdyk, R., and A. Calise (1998), Fault tolerant flight control via adaptive neural network augmentation, in *Guidance, Navigation, and Control Conference and Exhibit*, American Institute of Aeronautics and Astronautics, doi:doi:10.2514/6.1998-4483.

Salaris, P., D. Fontanelli, L. Pallottino, and A. Bicchi (2010), Shortest paths for a robot with nonholonomic and field-of-view constraints, *Robotics, IEEE Transactions on*, *26*(2), 269–281, doi:10.1109/TRO.2009.2039379.

Souères, P., A. Balluchi, and A. Bicchi (2001), Optimal feedback control for route tracking with a bounded-curvature vehicle, *International Journal of Control*, *74*(10), 1009–1019, doi:10.1080/00207170110052211.

Stevens, B. L., and F. L. Lewis (2003), *Aircraft control and simulation*, 2nd ed ed., J. Wiley, Hoboken, N.J.

Stoer, J. (1982), Curve fitting with clothoidal splines, *Journal of Research of the National Bureau of Standards*, *87*(4), 317–346.

Strube, M., R. Sanner, and E. M. Atkins (2004), Dynamic flight guidance recalibration after actuator failure, in *AIAA 1st Intelligent Systems Technical Conference*, American Institute of Aeronautics and Astronautics, doi:10.2514/6.2004-6255.

Strube, M. J. (2005), Post-failure trajectory planning from feasible trim state sequences, Master's thesis, Aerospace Engineering Dept., University of Maryland, College Park,.

Sussmann, H. (1995), Shortest 3-dimensional paths with a prescribed curvature bound, in *Decision and Control, 1995., Proceedings of the 34th IEEE Conference on*, vol. 4, pp. 3306–3312 vol.4, doi:10.1109/CDC.1995.478997.

Sussmann, H., and G. Tang (1991), Shortest paths for the Reeds-Shepp car: A worked out example of the use of geometric techniques in nonlinear optimal control., *Tech. rep.*, Rutgers Center for Systems and Control Technical Report.

Tang, Y., E. M. Atkins, and R. Sanner (2007), Emergency flight planning for a generalized transport aircraft with left wing damage, in *AIAA Guidance, Navigation and Control Conference and Exhibit*, American Institute of Aeronautics and Astronautics, doi:10.2514/6.2007-6873.

Techy, L., and C. A. Woolsey (2009), Minimum-time path planning for unmanned aerial vehicles in steady uniform winds, *Journal of Guidance, Control, and Dynamics*, *32*(6), 1736–1746, doi:10.2514/1.44580.

Tomlin, C., G. Pappas, and S. Sastry (1998), Conflict resolution for air traffic management: a study in multiagent hybrid systems, *Automatic Control, IEEE Transactions on*, *43*(4), 509–521, doi:10.1109/9.664154.

Walsh, G., R. Montgomery, and S. Sastry (1994), Optimal path planning on matrix lie groups, in *Decision and Control, 1994., Proceedings of the 33rd IEEE Conference on*, vol. 2, pp. 1258–1263 vol.2, doi:10.1109/CDC.1994.411151.

Yang, G., and V. Kapila (2002), Optimal path planning for unmanned air vehicles with kinematic and tactical constraints, in *Decision and Control, 2002, Proceedings of the 41st IEEE Conference on*, vol. 2, pp. 1301–1306 vol.2, doi:10.1109/CDC.2002.1184695.

Zhao, Y., and R. Schultz (1997), *Deterministic resolution of two aircraft conflict in free flight*, American Institute of Aeronautics and Astronautics, doi:doi:10.2514/6.1997-3547.

Zhong, J., J. Yan, Y. Rahman, C. Wang, and D. Bernstein (2013), Retrospective cost model refinement for on-line estimation of constant and time-varying flight parameters, in *AIAA Guidance, Navigation, and Control (GNC) Conference*, American Institute of Aeronautics and Astronautics, doi:doi:10.2514/6.2013-5193.